

**ASSESSMENT OF VOLUME CHANGE AND MICROSTRUCTURE OF
CALCAREOUS SOILS CONTAMINATED WITH SULFURIC AND
PHOSPHORIC ACIDS**

BY
AMMAR MOHAMMED ALSHAMMARI

A Thesis Presented to the
DEANSHIP OF GRADUATE STUDIES

KING FAHD UNIVERSITY OF PETROLEUM & MINERALS
DHAHRAN, SAUDI ARABIA

In Partial Fulfillment of the
Requirements for the Degree of

MASTER OF SCIENCE

In
CIVIL ENGINEERING

January 2017

KING FAHD UNIVERSITY OF PETROLEUM & MINERALS
DHAHRAN- 31261, SAUDI ARABIA
DEANSHIP OF GRADUATE STUDIES

This thesis, written by **Ammar Mohammed Alshammari** under the direction his thesis advisor and approved by his thesis committee, has been presented and accepted by the Dean of Graduate Studies, in partial fulfillment of the requirements for the degree of **MASTER OF SCIENCE IN CIVIL ENGINEERING**.



Dr. Salah U. Al-Dulaijan
Department Chairman

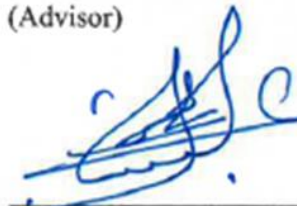


Prof. Salam A. Zummo
Dean of Graduate Studies

29/5/17
Date



Prof. Saad Ali Aiban
(Advisor)



Prof. Omar Saeed Baghabra Al-Amoudi
(Member)



Dr. Tawfik Abdo Saleh
(Member)

© Ammar Mohammed Alshammari

2017

*This Humble Achievement is
Dedicated to My Beloved Parents
and Wife and to All My Family
Members in Admiration and
Affection*

ACKNOWLEDGMENTS

All praises, glories and gratitude be to almighty ALLAH (Subhana Wa Ta'ala) for granting me health, power, guidance and patience to complete this research. After that, I wish to acknowledge King Fahd University of Petroleum and Minerals (KFUPM) for giving me this opportunity to conduct my master program.

Uncounted people have motivated and supported me during my study. I attributed the success of my work, after ALLAH, to them. First of all, I would like to thank my thesis advisor, Prof. Saad A. Aiban, for his guidance, comments and support. I am very thankful for his assistance throughout this work. I would like also to express my thanks to my committee member, Prof. Omar S. Baghabra Al-Amoudi for his persistent instructions and reviewing this thesis. My deep appreciation to Dr. Tawfik Abdo Saleh, my committee member, for his valuable suggestions and sustainable support during my work in this research.

I am very grateful to Eng. Abdulrahman Mohammed Hamid, the technician of the Geotechnical Engineering Lab, for his functional cooperation and feasible help to accomplish the experimental program in my thesis. I really enjoyed the work with him and I have learned a lot from him. Thanks and appreciations are extended to Eng. Tariq Mohammed, the technician of the Environmental Engineering Lab, for his assistance and support. Moreover, I would like to thank everybody helped me and encouraged me during my work. Last, but not the least, my sincere appreciation to my parents, siblings, wife, sons and friends for their emotional support, prayers, love, motivation and patience.

TABLE OF CONTENTS

ACKNOWLEDGMENTS.....	V
TABLE OF CONTENTS	VI
LIST OF TABLES.....	IX
LIST OF FIGURES.....	X
LIST OF ABBREVIATIONS.....	XIV
ABSTRACT	XV
ملخص الرسالة	XVII
CHAPTER 1 INTRODUCTION	1
1.1 General.....	1
1.2 Significance of This Investigation	2
1.3 Research Objectives	2
1.4 Research Methodology.....	3
CHAPTER 2 LITERATURE REVIEW	5
2.1 Calcareous Soil (Marl).....	5
2.2 Effect of Chemical Contamination on Soils	6
2.2.1 Soil Contaminated with Alkaline.....	6
2.2.2 Soil Contaminated with Acids	7
CHAPTER 3 EXPERIMENTAL PROGRAM.....	14
3.1 Research Stages.....	14
3.2 Materials Collocation.....	16

3.3	Characterization of Marl Samples	16
3.3.1	Specific Gravity (ASTM D 854)	16
3.3.2	Grain Size Analysis (ASTM D 422)	17
3.3.3	Atterberg Limits (ASTM D 4318)	17
3.3.4	Standard Proctor Compaction Test (ASTM D 698).....	17
3.4	Testing Program for Acid Contamination	17
3.4.1	Soil Samples Preparation	18
3.4.2	Acids Preparation	22
3.4.3	Samples Placement	24
3.4.4	Experiment Instrumentation and Operation.....	24
3.5	Strength Assessment	26
3.6	Scanning Electron Microscopy (SEM)	27
3.7	X-ray Diffraction (XRD)	27
	CHAPTER 4 RESULTS AND DISCUSSION	30
4.1	Soil Characteristics.....	30
4.1.1	Specific Gravity	30
4.1.2	Grain-Size Distribution.....	30
4.1.3	Atterberg Limits.....	32
4.1.4	Standard Proctor Compaction Test	32
4.2	Acid Contamination Consequences.....	34
4.2.1	First Round of Sulfuric Acid (20% Concentration).....	34
4.2.2	First Round for Phosphoric Acid (20% Concentration)	42
4.2.3	Second Round for Sulfuric Acid (32% Concentration).....	48
4.2.4	Second Round for Phosphoric Acid (48% Concentration)	56
4.2.5	Third Round for Sulfuric Acid (70% Concentration).....	63

4.2.6	Third Round for Phosphoric Acid (56% Concentration)	70
4.2.7	Summary of Expansion Resulted Due to Sulfuric Acid	77
4.2.8	Summary of Expansion Resulted Due to Phosphoric Acid	77
4.3	Soil Composition Alteration	79
4.3.1	M1 Compositional Analysis.....	80
4.3.2	M2 Compositional Analysis.....	83
4.4	Strength Variation Due to Acidification	85
4.4.1	Strength Alteration for the First Round	85
4.4.2	Strength Alteration for the Second Round	87
4.4.3	Strength Alteration for the Third Round	88
	CHAPTER 5 CONCLUSIONS AND RECOMMENDATIONS.....	90
5.1	Summary	90
5.2	Conclusions	91
5.3	Recommendations for Future Studies.....	93
	REFERENCES	94
	VITAE	98

LIST OF TABLES

Table 4-1: Soil characteristics.....	31
Table 4-2: XRD semi-quantitative analysis for uncontaminated and contaminated M1 with sulfuric acid.....	81
Table 4-3: XRD semi-quantitative analysis for uncontaminated and contaminated M1 with phosphoric acid	82
Table 4-4: XRD semi-quantitative analysis for uncontaminated and contaminated M2 with sulfuric acid.....	83
Table 4-5: XRD semi-quantitative analysis for uncontaminated and contaminated M2 with sulfuric acid.....	84
Table 4-6: Characteristics of all contaminated samples	86

LIST OF FIGURES

Figure 1-1: Research methodology	4
Figure 2-1: SEM of bentonite contaminated with chemicals (Singh and Prasad 2007)	9
Figure 2-2: Picture of the large mold. (Assa'ad 1998b)	11
Figure 2-3: A photo showing the differential movement of tank containment wall due to acid leak and interaction with carbonate foundation soils (Aiban, 2015).	12
Figure 2-4: A photo showing the solidification of carbonate soils due to leakage of sulfuric/phosphoric acid (Aiban, 2015).	13
Figure 3-1: Flow chart of the research program	15
Figure 3-2: Corrosion of stainless steel mold due to sulfuric acid	19
Figure 3-3: HDPE end cap used as a mold to host the samples during acid contamination	20
Figure 3-4: End cap (mold) dimensions.....	20
Figure 3-5: Drilling holes in the end cap (mold)	21
Figure 3-6: Leveling and fixing sample's mold in a CBR mold setup.....	23
Figure 3-7: Water bath for cooling	24
Figure 3-8: Molds containing marl samples inside the acid container	25
Figure 3-9: Glass plates on top of marl samples to house the LVDT rod and prevent it from acid reach.	26
Figure 3-10: CBR testing of acid contaminated soil.....	28
Figure 3-11: Scanning electron microscopy (SEM) model (JSM-6610LV).....	29
Figure 3-12: Sample holder for SEM.....	29
Figure 4-1: Grain size distribution curves for M1.	31
Figure 4-2: Grain size distribution curves for M2.	31
Figure 4-3: Compaction curve for M1 based on standard Proctor test	33
Figure 4-4: Compaction curve for M2 based on standard Proctor test	33
Figure 4-5: Free swell of M1 due to contamination with sulfuric acid of 20% concentration	36
Figure 4-6: SEM picture of uncontaminated uncompacted M1 sample	37
Figure 4-7: EDS analysis of uncontaminated M1	37
Figure 4-8: SEM picture for the top layer of M1 sample contaminated with 20% concentration sulfuric acid	38
Figure 4-9: SEM picture for the middle layer of M1 sample contaminated with 20% concentration sulfuric acid	38
Figure 4-10: SEM picture for the bottom layer of M1 sample contaminated with 20% concentration sulfuric acid	39
Figure 4-11: Free swell of M2 due to contamination with sulfuric acid of 20% concentration.....	40
Figure 4-12: SEM picture for the top layer of M2 sample contaminated with 20% concentration sulfuric acid.....	40

Figure 4-13: SEM picture for the middle layer of M2 sample contaminated with 20% concentration sulfuric acid	41
Figure 4-14: SEM picture for the bottom layer of M2 sample contaminated with 20% concentration sulfuric acid	41
Figure 4-15: Free swell of M1 due to contamination with phosphoric acid of 20% concentration.....	43
Figure 4-16: SEM picture for the top layer of M1 sample contaminated with 20% concentration phosphoric acid	44
Figure 4-17: SEM picture for the middle layer of M1 sample contaminated with 20% concentration phosphoric acid	44
Figure 4-18: SEM picture for the bottom layer of M1 sample contaminated with 20% concentration phosphoric acid	45
Figure 4-19: Free swell of M2 due to contamination with phosphoric acid of 20% concentration.....	46
Figure 4-20: SEM picture for the top layer of M2 sample contaminated with 20% concentration phosphoric acid	47
Figure 4-21: SEM picture for the middle layer of M2 sample contaminated with 20% concentration phosphoric acid	47
Figure 4-22: SEM picture for the bottom layer of M2 sample contaminated with 20% concentration phosphoric acid	48
Figure 4-23: Free swell of M1 due to contamination with sulfuric acid of 32% concentration.....	50
Figure 4-24: SEM picture for the top layer of M1 sample contaminated with 32% concentration sulfuric acid	51
Figure 4-25: SEM picture for the middle layer of M1 sample contaminated with 32% concentration sulfuric acid	52
Figure 4-26: SEM picture for the bottom layer of M1 sample contaminated with 32% concentration sulfuric acid	52
Figure 4-27: Free swell of M2 due to contamination with sulfuric acid of 32% concentration.....	53
Figure 4-28: SEM picture for the top layer of M2 sample contaminated with 32% concentration sulfuric acid	54
Figure 4-29: SEM picture for the middle layer of M2 sample contaminated with 32% concentration sulfuric acid	55
Figure 4-30: SEM picture for the bottom layer of M2 sample contaminated with 32% concentration sulfuric acid	55
Figure 4-31: Free swell of M1 due to contamination with phosphoric acid of 48% concentration.....	57
Figure 4-32: SEM picture for the top layer of M1 sample contaminated with 48% concentration phosphoric acid	58

Figure 4-33: SEM picture for the middle layer of M1 sample contaminated with 48% concentration phosphoric acid	59
Figure 4-34: SEM picture for the bottom layer of M1 sample contaminated with 48% concentration phosphoric acid	59
Figure 4-35: Free swell of M2 due to contamination with phosphoric acid of 48% concentration.....	60
Figure 4-36: SEM picture for the top layer of M2 sample contaminated with 48% concentration phosphoric acid	61
Figure 4-37: SEM picture for the middle layer of M2 sample contaminated with 48% concentration phosphoric acid	62
Figure 4-38: SEM picture for the bottom layer of M2 sample contaminated with 48% concentration phosphoric acid	62
Figure 4-39: Free swell of M1 due to contamination with sulfuric acid of 70% concentration.....	64
Figure 4-40: SEM picture for the top layer of M1 sample contaminated with 70% concentration sulfuric acid.....	65
Figure 4-41: SEM picture for the middle layer of M1 sample contaminated with 70% concentration sulfuric acid.....	65
Figure 4-42: SEM picture for the bottom layer of M1 sample contaminated with 70% concentration sulfuric acid.....	66
Figure 4-43: Free swell of M2 due to contamination with sulfuric acid of 70% concentration.....	67
Figure 4-44: SEM picture for the top layer of M2 sample contaminated with 70% concentration sulfuric acid.....	68
Figure 4-45: SEM picture for the middle layer of M2 sample contaminated with 70% concentration sulfuric acid.....	68
Figure 4-46: SEM picture for the bottom layer of M2 sample contaminated with 70% concentration sulfuric acid.....	69
Figure 4-47: Free swell of M1 due to contamination with phosphoric acid of 56% concentration.....	71
Figure 4-48: SEM picture for the top layer of M1 sample contaminated with 56% concentration phosphoric acid	72
Figure 4-49: SEM picture for the middle layer of M1 sample contaminated with 56% concentration phosphoric acid	73
Figure 4-50: SEM picture for the bottom layer of M1 sample contaminated with 56% concentration phosphoric acid	73
Figure 4-51: Free swell of M2 due to contamination with phosphoric acid of 56% concentration.....	74
Figure 4-52: SEM picture for the top layer of M2 sample contaminated with 56% concentration phosphoric acid	75

Figure 4-53: SEM picture for the middle layer of M2 sample contaminated with 56% concentration phosphoric acid	76
Figure 4-54: SEM picture for the bottom layer of M2 sample contaminated with 56% concentration phosphoric acid	76
Figure 4-55: The average free swell percentage of M1 and M2 due to sulfuric acid contamination.....	78
Figure 4-56: The average free swell percentage of M1 and M2 due to phosphoric acid contamination.....	79
Figure 4-57: Measurement profile of XRD for M1 contaminated with 20% concentration sulfuric acid.....	81
Figure 4-58: Strength curves for the first round	87
Figure 4-59: Strength curves for the second round.....	88
Figure 4-60: Strength curves for the third round	89

LIST OF ABBREVIATIONS

CBR:	California bearing ratio
EDS:	Energy-dispersive X-ray spectroscopy
G_s:	Specific gravity
HDPE:	High-density polyethylene
LVDT:	Linear variable differential transformer
PI:	Plasticity index
SEM:	Scanning electron microscope
w_{opt}:	Optimum moisture content
XRD:	X-ray diffraction
γ_d:	Dry unit weight, (kN/m³)
γ_{d(max)}:	Maximum dry unit weight, (kN/m³)

ABSTRACT

Full Name: Ammar Mohammed Alshammari
Thesis Title: Assessment of Volume Change and Microstructure of Calcareous Soils Contaminated with Sulfuric and Phosphoric Acids
Major Field: Civil Engineering (Geotechnical)
Date of Degree: Jan 2017

Soil contamination is a serious issue caused by faulty industrial activities such as chemical leakage and poor waste disposal. Acid contamination of soils is a common problem within fertilizer and petrochemical industries. The problem occurs when leaked or wrongly-disposed acids infiltrate to the ground and react with active materials like carbonate soils. The problem is aggravated when the leaking acids interact with carbonate soil causing swelling of the foundations of pumps and pipes handling such acids and thus leading to more leaks. All soil properties could be alerted due to acid contamination, especially the volume. Consequently, all structural facilities and infrastructures in the vicinity of the contaminated soils will experience unfavorable upheaval. On the other hand, when the leaked quantities are large, soil washouts may result in creating large voids and subsequent subsidence.

In eastern Saudi Arabia, most of the soils used for road bases and under pavement and walkways are calcareous in nature. These carbonate soils are susceptible to large volume change when attacked by acids. Moreover, there are huge petrochemical and fertilizer industries in the area that produce or utilize different acids. This research was intended to examine the volume and microstructural changes of calcareous soils due to interaction with sulfuric and phosphoric acids. Thus, the correlation between acid concentrations and

swelling is very important to investigate taking into account the changes in mineralogy and microstructure.

Sulfuric and phosphoric acid were utilized to react with two calcareous soils in the laboratory under controlled conditions. Soil samples were prepared in high-density polyethylene (HDPE) molds, which can resist aggressive acids. Then, these molds were placed in large containers and instrumented with linear variable differential transformer (LVDT) to measure volume change. After acidification, the contaminated samples were subjected to compositional analysis and strength assessment. Volume change and acid concentration were proportional except the case of sulfuric acid with the non-plastic marl. This happened because high concentration sulfuric acid reacted severely with carbonate minerals resulting in a blockage of the way for the acid to infiltrate into the whole sample. Moreover, all of expansion outcomes were interpreted with morphological and compositional analysis and strength assessment of contaminated samples.

ملخص الرسالة

الاسم الكامل: عمار محمد الشمري

عنوان الرسالة: تقييم تغير الحجم والبناء المجهري للتربة الجيرية الملوثة بحمض الكبريت وحمض الفوسفور

التخصص: الهندسة المدنية (جيوتقنية)

تاريخ الدرجة العلمية: يناير 2017

تلوث التربة هو قضية خطيرة ناجمة عن الأنشطة غير المرغوب فيها الصناعة مثل تسرب المواد الكيميائية وسوء التخلص من النفايات. يعتبر تلوث التربة بالأحماض تعتبر مشكلة شائعة في صناعات الأسمدة والبتر وكيمياويات، وتحدث هذه المشكلة عندما تتسرب الأحماض من المصانع أو يتم التخلص منها بطريقة خاطئة وتتفاعل مع المواد الفعالة مثل التربة الجيرية. وتتفاقم هذه المشكلة عندما تتفاعل الأحماض المتسربة مع التربة الجيرية وتتفكح أساسات المضخات والأنابيب التي تنقل مثل هذه الأحماض، وبالتالي تؤدي إلى المزيد من التسريبات. من الممكن أن تتغير كل خواص التربة بسبب التلوث بالأحماض وخاصة الحجم. ونتيجة لذلك، فإن جميع المنشآت والبنى التحتية في محيط التربة الملوثة سوف تعاني جیشان غير مرغوب. من ناحية أخرى عند ازدياد كميات الحمض المتسرب سوف تتحلل وتنجرف التربة وذلك قد يؤدي إلى خلق فراغات كبيرة وهبوطات في التربة.

معظم أنواع التربة المستخدمة لقواعد الطريق وتحت الأرصفة والممرات الخرسانية في المنطقة الشرقية من المملكة العربية السعودية هي من التربة الجيرية، والتي تعتبر عرضة لتغير الحجم عندما تتلوث بالأحماض. وعلاوة على ذلك، هناك مصانع بتر وكيميائية ومصانع أسمدة عديدة في هذه المنطقة تنتج وتستخدم أحماضاً مختلفة.

يهدف هذا البحث إلى دراسة تغير الحجم والبناء المجهري في التربة الجيرية بسبب التفاعل مع حمض الكبريت وحمض الفوسفور، حيث يتم اختبار تراكيز مختلفة من الأحماض مع نوعين من التربة الجيرية المستخدمة على نطاق واسع في شرق المملكة العربية السعودية. وبذلك يكون الربط بين تركيز الحامض ومقدار انتفاخ التربة هو النتيجة الرئيسية لهذا البحث، مع الأخذ بعين الاعتبار التغيرات في التركيب الكيميائي والمجهري للتربة.

تم استخدام حمض الكبريت وحمض الفوسفوريك للتفاعل مع اثنين من التربة الجيرية في المختبر تحت ظروف معينة وثابتة. تم تحضير عينات التربة في قوالب مصنوعة من البولي إيثيلين عالي الكثافة، والتي يمكن لها أن تتحمل الأحماض الشديدة. ثم بعد ذلك، تم وضع هذه القوالب في حاويات كبيرة و جُهزت بأدوات لقياس تغير الحجم. بعد تلويث العينات بالحمض، تم عمل التحليل التركيبي و تم أيضاً تقييم القوة. كان لتغير حجم العينات وتركيز الأحماض علاقة نسبية باستثناء حالة حمض الكبريت مع التربة الجيرية غير اللدنة. حدث هذا الأمر لأن تركيز حمض الكبريت العالي بشدة مع العناصر الكربونية في التربة أدى إلى انسداد الفتحات وعدم نفاذ الحمض لكامل العينة. وعلاوة على ذلك، فُسِّرَتْ جميع نتائج انتفاخ العينات مع التحليل المجهرى والتحليل التركيبي وتغير القوة للعينات.

CHAPTER 1

INTRODUCTION

1.1 General

Soil-acid contamination always results in numerous problems and most of them are environmental-based issues. The contamination of soil by acid could also lead to structural troubles such as upheaval of slabs and footings, which will lead to damage of the associated structural members and piping. Many damages could be associated with soil expansion or erosion (Sivapullaiah et al., 2004). In addition, acid is reactive with carbonate minerals and the results of their reactions are salt forming, carbon dioxide (CO_2) and water (H_2O). When carbonate minerals in calcareous soils react with acids, the physical and chemical properties of the soil will certainly be altered.

Acid leakage from fertilizer and petrochemical factories is a critical source of ground contamination (Assa'ad, 1998). Moreover, the problem will be more crucial if the type of soil is calcareous. Such a case is prevalent in eastern Saudi Arabia because it has enormous petrochemical and fertilizer industries. Furthermore, eastern Saudi Arabia has a semi-arid climate and the soils located in arid and semi-arid areas contain calcium carbonate (CaCO_3) due to the low precipitation and high evaporation (Mitchell and Soga, 1976).

As an attempt to assess the volume change caused by acid contamination in fertilizer factories, sulfuric and phosphoric acids were used to flood marl samples in the laboratory

under controlled conditions. Moreover, each acid has different concentrations to quantify the effect of acid concentration on carbonate soils heaving and microstructure.

1.2 Significance of This Investigation

Saudi Arabia, especially the Eastern Province, has numerous petrochemical and fertilizer industries. Some of them were built a few decades ago and some others are still under construction. Accordingly, concerns have been raised regarding maintenance, durability, and sustainability of those facilities. One of the biggest problems facing the petrochemical and fertilizer industries is the foundation upheaval due to the acid-carbonate reaction. When acid leakage occurs, which is an expected problem in the industry; it will react with the carbonates of the subsoil. As a result, chemical reaction will lead to compositional alteration followed by volumetric changes. Therefore, measuring volumetric and compositional changes of calcareous soil caused by acid contamination is a vital action to all the foundations and subsurface structures. Accordingly, this research was planned to assess this problem and work out some methodologies to solve it.

1.3 Research Objectives

The main objectives of this research were:

1. To measure the volume change of calcareous soils due to acid contamination. The intended acids for the research were sulfuric acid and phosphoric acid at different concentrations and two different calcareous soils.
2. Assess of the mineralogical and microstructural changes of the calcareous soils due to the interaction with these two acids.

1.4 Research Methodology

The research consists of several parts. The first part was devoted to the recent literature review, which was presented in Chapter 2. Few researchers, especially those from India, have reported some effects of chemical contaminations on different soils. However, the subject needs more exploration to suit our indigenous soil. The second part (Chapter 3) dealt with collecting two types of calcareous soils and homogenizing each type thoroughly to ensure consistency and homogeneity of the samples. Chapter 3 presented also the laboratory setup as well as securing enough quantities of sulfuric and phosphoric acids for the experimental work. High safety precautions are necessary for this experiment since the acids are very corrosive materials and harmful to the humans. This Chapter (Chapter 3) also described the experimental program to measure swelling of the contaminated calcareous soils and to quantify the mineralogical and microstructural changes. Last, but not the least, all laboratory results were analyzed and discussed in Chapter 4. At the end, recommendations and conclusions for the research were presented in Chapter 5. Figure 1-1 summarizes the research methodology.

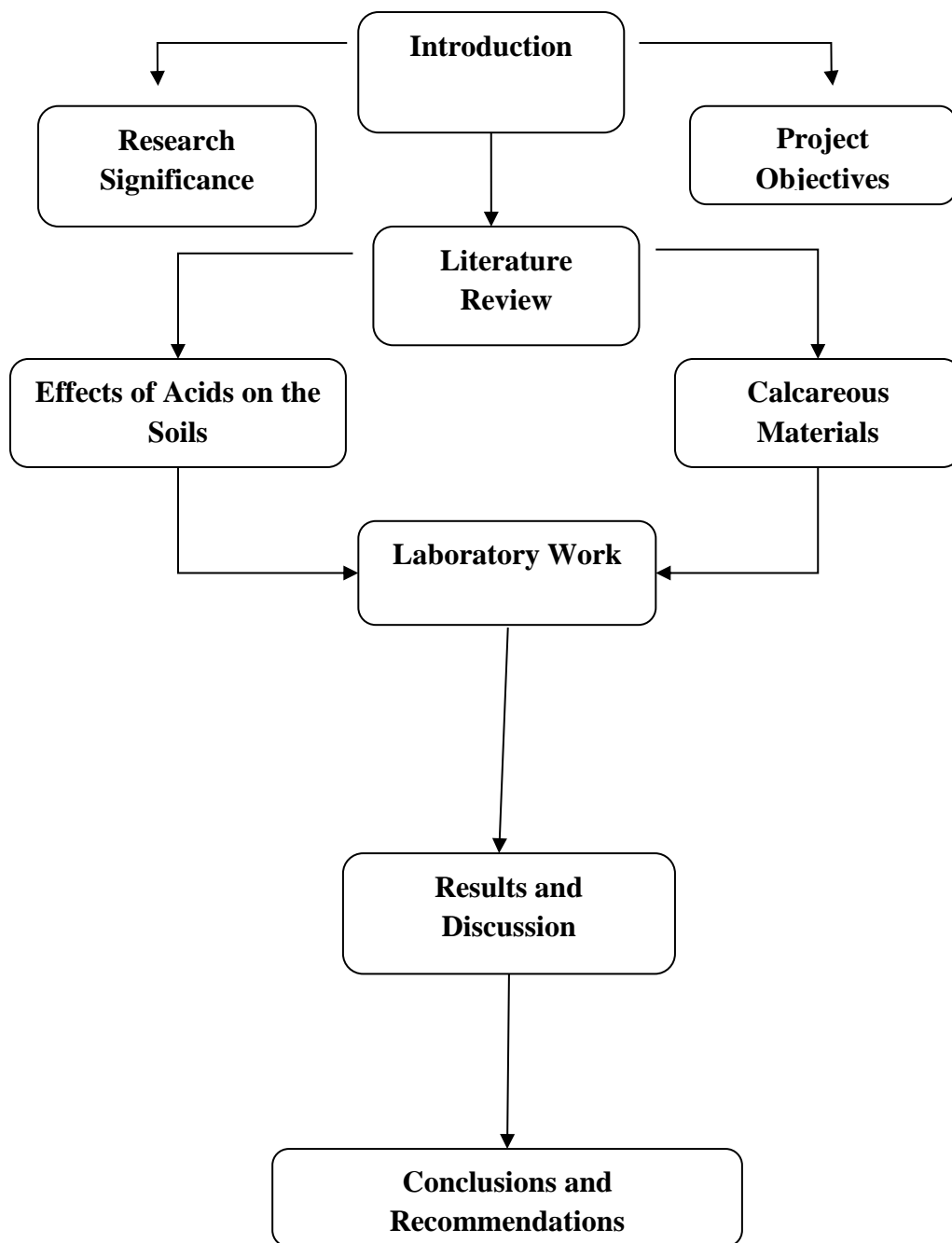


Figure 1-1: Research methodology

CHAPTER 2

LITERATURE REVIEW

2.1 Calcareous Soil (Marl)

The soils used in this research were calcareous marls that are predominant in the Eastern Province of Saudi Arabia. It is widely used in construction in the area (Aiban, 1995; Al-Amoudi et al., 2010). Several researchers defined marl as calcareous or carbonate soil. For example, Pettijohn et al. (1975) defined marl as a rock that contains 35% to 65% carbonate and some clay minerals. Furthermore, Sowers (1979) defined marl as a water deposit soil that has calcite in its composition and organic colloids. In Addition, marl is a dual blend of clay and calcium carbonate as defined by Akili (1980).

Marl soil is known to be calcareous in nature. Further, it is heterogeneous in terms of composition and features, and it is known to have significant reduction in strength upon exposure to water. For that, marl requires prior treatment without which a critical strength loss will occur upon water flooding (Aiban et al. 1998a; Aiban et al. 1998b). Marl soil is available in the Eastern Province of Saudi Arabia in several locations like Abqaiq, Dhahran, Dammam, Ras Alkair, Hofuf, Berri, Fadhli, Jubail, Abu Hadriyah and Safaniyah districts (Aiban et al. 1998a; Aiban et al. 1998b).

2.2 Effect of Chemical Contamination on Soils

2.2.1 Soil Contaminated with Alkaline

Alkalis and acids can affect soil properties as reported by several researchers. Sinha et al., (2003) reported 33% reduction in bearing capacity of a soil due to caustic soda contamination. They recommended naturalizing the soil with ferric chloride as a treatment action.

Rao and Rao (1994) have reported kaolinite heaving upon infiltration of caustic soda solution. The soil was originally non-swelling anhydrite type. Their investigations showed that the leakage of highly concentrated sodium hydroxide to the soil damaged the cementitious iron oxide coating in addition to the negative charges, which caused dispersion to the soil particles. They had simulated this phenomenon in the laboratory using odometer set up. At the end of their research, they recommended to prevent the leakage of caustic solution and treating the contaminated soil with 5% of ferric chloride.

High alkali solutions could produce unforeseen swelling for expansive soil and non-expansive soils as well (Sivapullaiah, 2005). The produced material from the reaction of sodium hydroxide and kaolinite mineral is sodium aluminum silicate hydroxide hydrate, as shown by X-ray diffraction (XRD) analysis. The result of the reaction is dependent on the following: time reaction, quantity of clay and caustic solution concentration. One of the main outcomes of this analysis is the effect of kaolinite crystalline structure that did occur after reacting with a high concentration of the caustic solution.

Sivapullaiah et al. (2004) recommended the use of geomembrane in order to protect the subsoil of an alumina extraction plant in Karnataka, India, from alkali contamination. Their investigations indicated that the long exposure of the soil to alkalis would create heave.

2.2.2 Soil Contaminated with Acids

The increase in industrial activities has resulted in environmental degradation of soils with unpredicted changes in their engineering behaviors (Umesha et al., 2012). The extent of this change depends on various parameters including both type and concentrations of the chemical compounds and the nature of the soils like particle size and specific surface area (Komnitsas et al., 1998).

There are different types of industrial contaminants including inorganic acids, alkalis, sulphates, organic contaminants, and metals that can change the behavior of soils to various extents. However, soil acidity is considered the most serious problem in regions where precipitation is enough to leach appreciable quantities of the exchangeable base-forming cations of calcium, potassium and magnesium from the soils that can result in geotechnical failures (Singh and Prasad, 2007). An experimental work has been conducted to study the effect of different industrial chemicals on bentonite that is considered a clay liner material. The intended chemical in the experiment was aluminum hydroxide and acetic acid that are very common in the industry. Many changes did happen to bentonite. The reaction of bentonite with aluminum hydroxide and acetic acid resulted in a reduction of free swell by 49% and 47%, respectively. In addition, the reductions of hydraulic conductivities were 17% for acetic acid and 12% for aluminum hydroxide. Figure 2-1 (a) shows the morphology of saturated bentonite, (b) shows the morphology of bentonite contaminated with aluminum hydroxide, and (c) shows the morphology of bentonite contaminated with

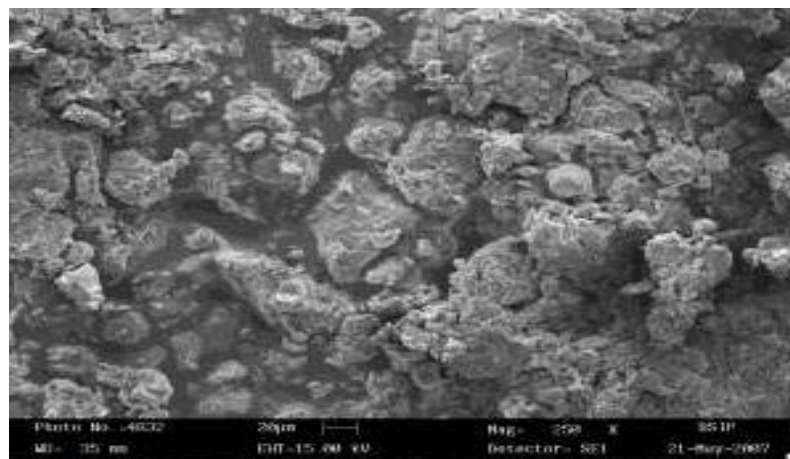
acetic acid. It was observed, using SEM, that flocks were formed due to acetic acid contamination. On the other hand, aluminum hydroxide contamination caused a formation of crystalline silicate hydrates due to partial degradation of $\text{Al}(\text{OH})_3$.

Varying concentrations (1–10 N) of sulfuric acid were reported to interact with montmorillonite clay forming catalytic active clay having Bronsted acid sites, which refers to proton donor (Tyagi et al., 2006). Their analysis was carried out by FT-IR spectroscopy.

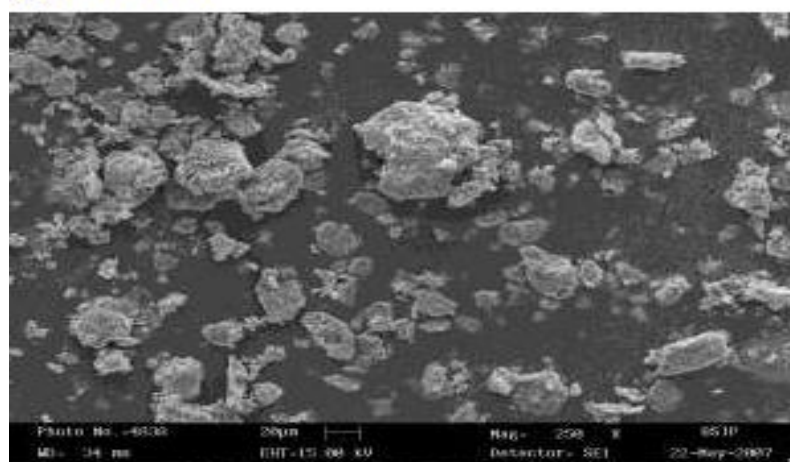
The effect of the acid attack on the aluminosilicate mineral soil was investigated and severe alteration of the crystal structures after acid treatment was reported (Jozefaciuk and Bowanko, 2002). The dissolution of Al was dominated over that of Si. However, in the case of alkali attack, the opposite happened.

The properties of different soils interacting with phosphoric and sulfuric acids were investigated by Ramesh et al., 2008. It was reported that the effect of low (1 N) concentration of phosphoric acid on the alkali-treated soils has a less negative effect than with that of sulfuric acid on the soil properties (Ramesh and Mohan, 2013).

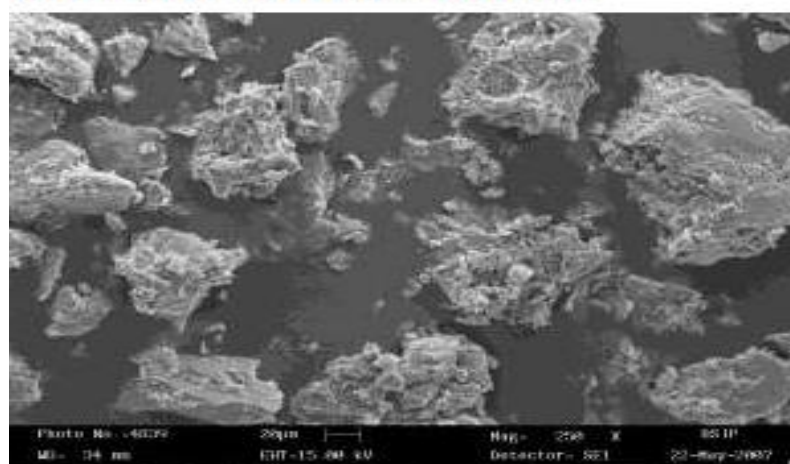
Sridharan et al. (1981) reported swelling of a non-expansive soil located in a fertilizer plant owing to the leakage of phosphoric acid into the soil mass. Acid leakage was coming from open drains and damaged joints. Primarily, the soil fabric has changed because of phosphate retention. Designing drains with good filter material and closed conduits were recommended as safety measures.



(a) Bentonite



(b) Bentonite + Aluminium Hydroxide



(c) Bentonite + Acetic Acid

Figure 2-1: SEM of bentonite contaminated with chemicals (Singh and Prasad 2007)

In the United States, Stephenson et al. (1989) reported that the formation of gypsum resulted from the reaction of calcite and sulfuric acid leading to more than 18 inches upward movement of portions of Kerr-McGee Electrolysis Plant in Henderson, Nevada.

Assa'ad (1998) reported the inclination of the phosphoric acid storage tank of fertilizer factory, Aqaba, Jordan. The inclination of this tank increased above the allowable limit and threatened to stop the operation of the plant. The inclination was due to the differential upheaval of the carbonate soil under the tank. Laboratory studies illustrated that the upheaval of soil was generated by the chemical reaction, which is taking place between the leaked phosphoric acid over the subgrade soil that is containing calcite. A large plastic mold (Figure 2-2) was used to perform his simulation. The mold had a height of 120 mm and an inside diameter of 180 mm. In addition, 16 holes, 10 mm diameter each, were drilled at two levels in the mold sides. Furthermore, flexible plastic pipes were connected to the holes to ensure high saturation of the soil with the phosphoric acid.

The output of the experimental program indicated that the inclination of storage tanks was due to the entrapped gas (Assa'ad, 1998). Finally, the author recommended the following:

- Restoration of the level of storage tanks by jacks.
- Using perforated plastic pipes of 4-inch (100 mm) diameter around the affected tanks to help releasing the generated gasses.
- Inspecting and maintaining the channels between the tanks to make sure that no further leakage of acid occurs.
- Monitoring the inclination of the tanks.

Studies have shown that swelling of up to 27% can be measured due to the reaction of carbonate minerals and sulfuric acid (Sivapullaiah et al., 2008). Their study has clearly indicated that the amount of swelling is increasing as the carbonate content increases. They have used oedometer test in their experimental program but the concentration of sulfuric acid was 1 N.

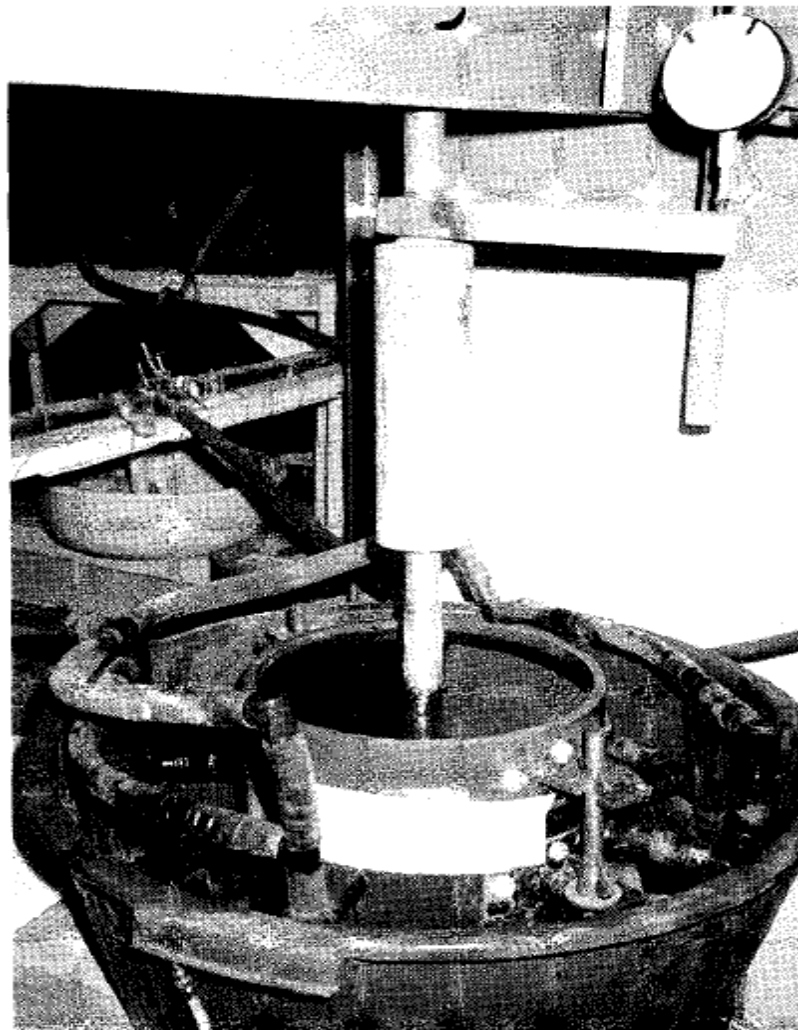


Figure 2-2: Picture of the large mold. (Assa'ad, 1998)

The upheaval of walkway slab and shallow containment walls of a tank can exceed 200 mm, as shown in the photograph, Figure 2.3 (Aiban, Personal communication, 2015). When the carbonate material interacts with sulfuric or phosphoric acid, it solidifies and swell, as shown in Figures 2-3 and 2-4. Such solidification reduces the permeability of the soil and most probably resulted in material's swelling or expansion leading to the upheaval of the slabs and containment walls.



Figure 2-3: A photo showing the differential movement of tank containment wall due to acid leak and interaction with carbonate foundation soils (Aiban, 2015).



Figure 2-4: A photo showing the solidification of carbonate soils due to leakage of sulfuric/phosphoric acid (Aiban, 2015).

CHAPTER 3

EXPERIMENTAL PROGRAM

This Chapter presents the research methodology that was conducted to assess the effect of acid contamination on calcareous soils. In order to fulfill the outlined objectives in Chapter 2, a set of experimental stages were accomplished. Figure 3-1 shows the flow chart of the research program with the main experimental stages.

3.1 Research Stages

All the stages of this research, which are reported in Figure 3-1, are summarized below:

1. Selecting the two soils and characterizing them in the laboratory.
2. Preparing the materials to be contaminated with acid and measuring the expansion due to acid contamination. This stage was executed with two acid types and three different concentrations for each acid.
3. The strength of the contaminated material was assessed and compared with the strength of the non-contaminated material.
4. X-ray diffraction and scanning electron microscopy (SEM) tests were conducted on the uncontaminated and contaminated soils to assess the chemical and microstructure changes.
5. Analyzing and evaluating the results.

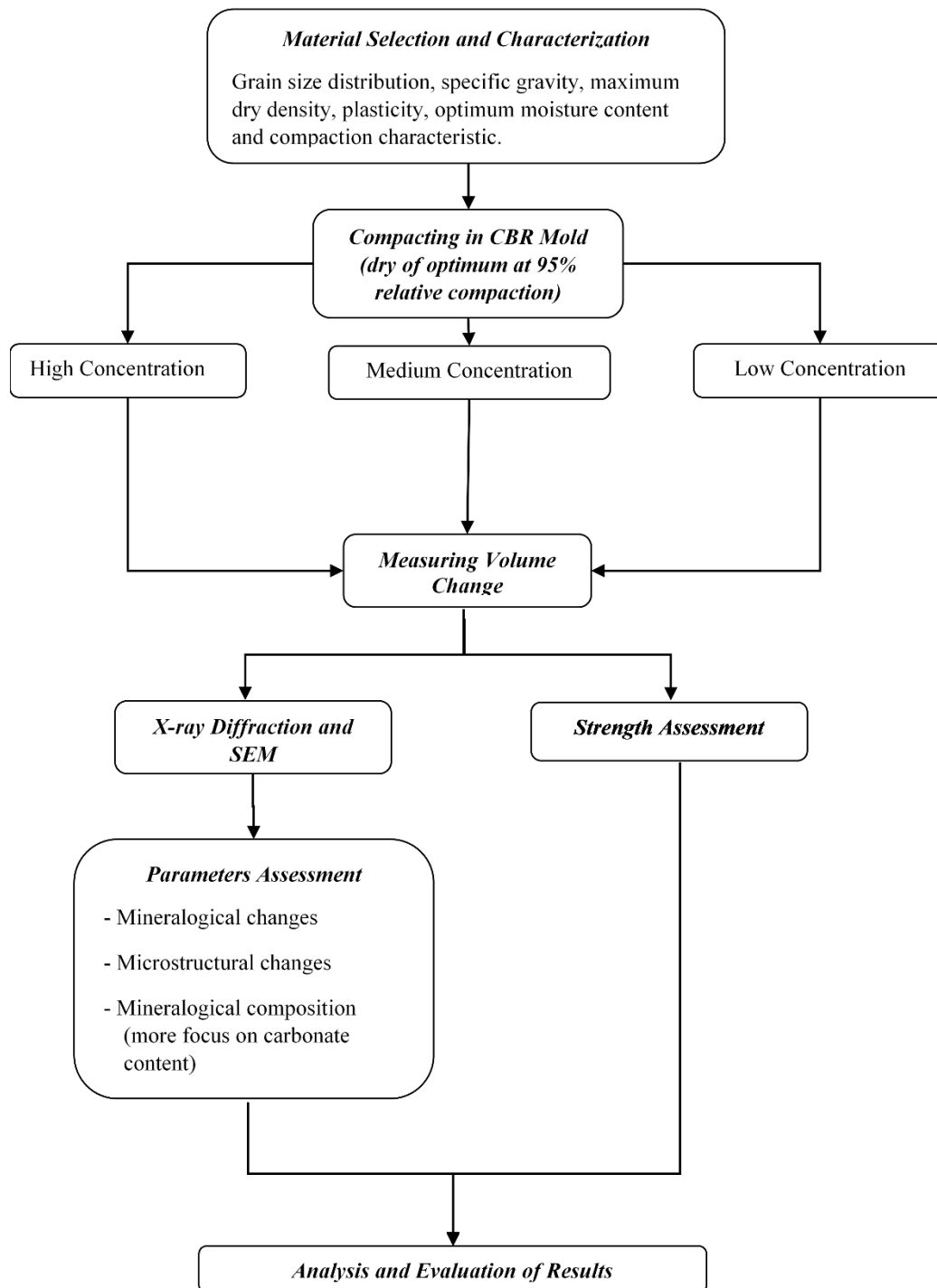


Figure 3-1: Flow chart of the research program

3.2 Materials Collocation

Samples from two marl types were collected from two different sources in the Eastern Province of Saudi Arabia in order to have various properties. Both of them are utilized for constructional purposes. The first sample was collected from a stockpile for road construction in Jubail Industrial City. The original source of this material is Al-Kkarsaniah. The second sample was brought from a stockpile belonging to Al-Osais Company. This material was proposed for embankment construction and it was originally brought from Abqaiq area.

Both marl samples were sieved through ASTM #4 sieve and kept in large bags for testing. These samples were then subjected to a set of ASTM tests for characterization. These tests included grain size analysis, specific gravity, consistency limits and standard Proctor compaction.

3.3 Characterization of Marl Samples

3.3.1 Specific Gravity (ASTM D 854)

The specific gravity of solid phase of soil is one of the fundamental physical properties of the soil. It helps in calculating the unit weight and voids ratio and it will help in soil classification. In this research, the specific gravity test was performed on both marl samples according to ASTM D 854. The average of three trials was considered as the specific gravity of the soil.

3.3.2 Grain Size Analysis (ASTM D 422)

The grain size analysis test was conducted on both marl samples using both the dry and the wet sieving methods, as per the ASTM D 422. Since the soil samples had a high proportion of particles passing through ASTM #200 sieve. The hydrometer test was utilized to get the grain size distribution of the fine material.

3.3.3 Atterberg Limits (ASTM D 4318)

Atterberg limits tests, which are used to determine liquid and plastic limits, were conducted based on ASTM D 4318. The plasticity tests for determining the liquid limit and the plastic limit were performed on the marl soil samples passing through No. 40 ASTM sieve in accordance with ASTM D 4318 standard. These tests indicate the moisture content limits to change the soil to plastic and liquid phases, respectively.

3.3.4 Standard Proctor Compaction Test (ASTM D 698)

The compaction test is implemented in the laboratory to determine the relationship between the moisture content and the dry density of the soil. The standard Proctor compaction test (ASTM D 698) was executed to determine the optimum moisture content (w_{opt}) and maximum dry unit weight (γ_d) of the proposed soils. The resulting compaction curves are showing the variations of dry unit weight with molding moisture content.

3.4 Testing Program for Acid Contamination

This section describes the experimental program set-up for volume and microstructural changes of calcareous soil upon acid contamination. In order to study the effect of acid on the calcareous material in the field, several steps were simulated in the laboratory. First, soil samples had to be prepared in suitable molds that can resist acid without any corrosion

or deterioration. After that, acids had to be diluted carefully and safely to the desirable concentrations. Then, the molds had to be placed and leveled in a proper container/bath. The bath was made of acid-resistant material that could take four soil specimens. After that, linear variable differential transformers (LVDTs) had to be mounted on the samples. Thereafter, the acid was poured gently in the bath. One bath was intended for sulfuric acid and the other one for phosphoric acid. Just before acid pouring, the data logger was initiated to measure the volume change of the soil before contamination and for the contaminated soil through the LVDT's. The soil baths were placed within a vacuum hood to prevent any fume or acid dispersion into the laboratory. The volume change testing was monitored for a period of two weeks from the starting time of contamination. This duration was selected base on the behavior of expansion in the first round of contamination where the swelling ceased after two weeks. Subsequently, the soil samples had to be assessed/analyzed in terms of strength, microstructure, and mineralogical changes.

3.4.1 Soil Samples Preparation

Metallic molds could not be used in this experiment because the metal will not resist aggressive acids. Figure 3-2 shows the effect of sulfuric acid with 50% concentration on the stainless steel mold. The color of the acid solution was changed to dark color, which is an indication of metallic corrosion. For that, a proper sample mold, made from high-density polyethylene (HDPE) was selected for this experimental program. The mold is the end cap of pipes (Figure 3-3). The dimensions for this sample mold are shown in Figure 3-4. The mold has a length (L) of 167.5 mm, 160 mm diameter (D) and 14.6 thickness (S). However, this mold has curvature at the bottom and the length from the opening to a point before the curvature (L2) is 123.5 mm.

In order to make the acid infiltrate inside the mold, 12 holes of 2.5 mm diameter were drilled in the bottom (Figure 3-5) in a direction parallel to the length of the mold. Moreover, to fit soil sample in a cylindrical shape without the end curvature, polypropylene pellets were filled inside the curvature of the mold and they were encapsulated by a geotextile made of polypropylene.



Figure 3-2: Corrosion of stainless steel mold due to sulfuric acid



Figure 3-3: HDPE end cap used as a mold to host the samples during acid contamination

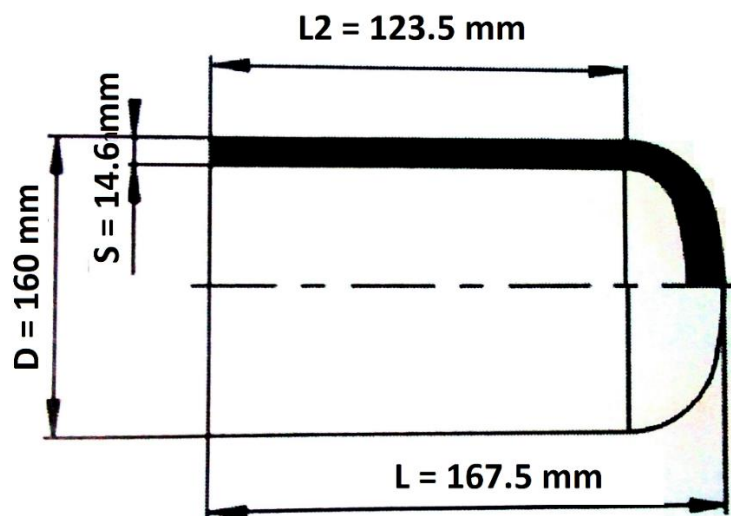


Figure 3-4: End cap (mold) dimensions

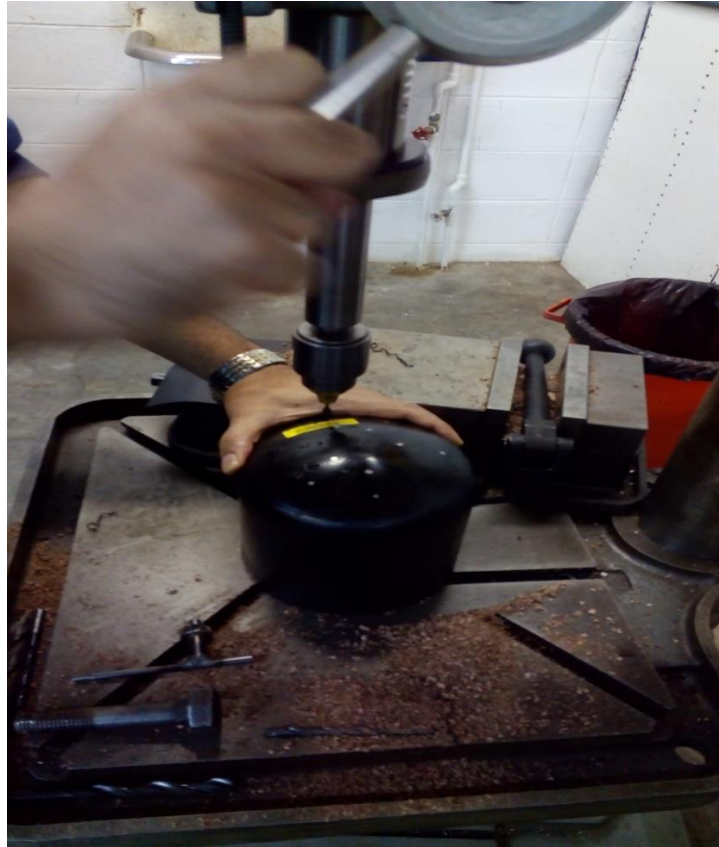


Figure 3-5: Drilling holes in the end cap (mold)

Each soil sample was compacted to 95% of the maximum dry unit weight on the dry side of optimum moisture content to enhance permeability of acid through the sample. Moreover, the compaction of the soil sample in the mold was similar to the standard Proctor compaction for 4-in mold but with different sample dimensions. The compaction procedure of the soil sample in the holder was as follows:

- An oven-dried soil was mixed with 95% dry of optimum moisture content.
- The mold was placed on a top of a CBR mold collar and held by the collar holders after being leveled, as shown in Figure 3-6.

- Polypropylene pellets were placed and leveled in the bottom of the holder to fill the curved portion of the mold. The pellets were encapsulated by a geotextile sheet.
- The weight of the soil sample, which had been compacted in the 4-in mold at 95% dry of optimum, was taken.
- One-third of the taken weight was laid in the mold then compacted by the standard rammer for 25 blows.
- The previous procedure was repeated two more times to get the three layers.

The dimension of the soil sample in the mold was 70 mm in height and 130.8 in diameter.

3.4.2 Acids Preparation

Sulfuric acid and phosphoric acid were secured from the Chemistry Department at KFUPM. The acids were delivered at the highest concentrations, which were 98% for sulfuric acid and 85% for phosphoric acid. Each one of these acids has an exothermic reaction with water. For that, the acid must be poured in water, and not the opposite, very slowly. If the temperature raised up severely, the dilution container should be directly emerged in a water bath for cooling, as shown in Figure 3-7. During the dilution process, all safety procedures, like gloves, goggles and protection coat, must be considered.



Figure 3-6: Leveling and fixing sample's mold in a CBR mold setup



Figure 3-7: Water bath for cooling

3.4.3 Samples Placement

In each experimental round, two samples of the first marl (M1) and two samples of the second marl (M2) were contaminated with sulfuric acid and similar samples were infiltrated with phosphoric acid. The contamination with each acid was done in a container that can resist aggressive chemical, as shown in Figure 3-8. This container takes four samples, two of each marl soil. Every sample mold was placed inside the container and leveled over an ash-tray. Glass bottles were placed inside the container to fill the space and reduce the quantity of acid for each test. Both sulfuric and phosphoric acid containers that were holding marl samples must be placed within a vacuum hood.

3.4.4 Experiment Instrumentation and Operation

After placing and leveling the marl samples in the container, a thin layer of sand was laid over each marl sample. This sand layer helped in leveling the marl sample and allowing the gas from acid reaction to escape. In addition, a glass plate housing the LVDT rod was

placed on top of the sand layer; the glass plate will prevent the LVDT rod from acid reach, as shown in Figure 3-9. The LVDT's were then attached to the samples, through specific holders, and connected to the data logger. At the end, the acid was poured gently into the container. Simultaneously, the data logger was started just before acid pouring to take the readings before and after acid pouring.



Figure 3-8: Molds containing marl samples inside the acid container



Figure 3-9: Glass plates on top of marl samples to house the LVDT rod and prevent it from acid reach.

3.5 Strength Assessment

The strength of soil is usually measured by conventional methods in the laboratory such as unconfined compressive strength, direct shear test, triaxial test and California bearing ratio (CBR) test that is an indirect method. However, the contaminated soil cannot be tested using the conventional methods because of two reasons. The first reason is the disturbance caused by extracting the sample from the mold. The second reason is the corrosion or damage of the testing equipment that would result from aggressive acids. For that, a modified way was developed to give an indication of the strength of the contaminated soil. It is basically utilizing the CBR plunger to penetrate inside the sample while it is in the HDPE mold at a constant rate (1.27 mm/min). The mold was fixed and leveled in the compression machine, as demonstrated in Figure 3-10. Before applying the compression load, the plunger was sealed by plastic bag to protect it from the acid in the sample. The results are in the form of stress versus penetration. Ultimately, the results of contaminated soil were compared with the corresponding values of uncontaminated samples.

3.6 Scanning Electron Microscopy (SEM)

Scanning electron microscopy (SEM) utilizing the JSM-6610LV model was used to assess the morphology and microstructure of the contaminated samples (Figure 3-11). Each sample was investigated by SEM from the top, middle and bottom layers. The analysis was carried out at high voltages (10 & 20 kV) and high vacuum. Samples preparation was a highly crucial process to achieve representative SEM results. To prepare the samples for this test, small pieces of undisturbed contaminated soil were placed on the samples holder (Figure 3-12). Then, the samples were gold coated for adequate conduction. Elemental compositional mapping was taken by the X-ray energy dispersive spectrometer (EDS) of the SEM to assess the level of acid elements in the samples. SEM images mapping of the contaminated soil were also taken at (x45) and (x1000) zooming.

3.7 X-ray Diffraction (XRD)

X-ray diffraction (XRD) was used to assess the contaminated soil samples to assess the mineralogical changes that took place. A small amount of the sample was needed for XRD analysis. The sample must also be ground in order to get representative results.



Figure 3-10: CBR testing of acid contaminated soil



Figure 3-11: Scanning electron microscopy (SEM) model (JSM-6610LV)



Figure 3-12: Sample holder for SEM

CHAPTER 4

RESULTS AND DISCUSSION

All the experimental work and the methods used to study the effect of sulfuric and phosphoric acids on calcareous soils were elucidated in the previous Chapter. Therefore, this Chapter presents the results and the outcomes of the experimental part. The main results are marl characteristics, the volume increase of marl due to acid contamination, SEM that gives the microstructural changes and XRD that offers the mineralogical alteration due to acid contamination.

4.1 Soil Characteristics

4.1.1 Specific Gravity

The specific gravity of the soil samples passing sieve No. 4, was determined in accordance with ASTM D 854. Specific gravities of M1 and M2 samples were found to be 2.69 and 2.67, respectively, as shown in Table 4-1.

4.1.2 Grain-Size Distribution

Before conducting sieve analysis test, as per the ASTM D 422, marl (M1) and marl (M2) soil samples were first sieved through No. 4 sieve (4.75 mm opening size) to make the soil suitable for compaction in small diameter mold. The samples were then dried in the oven at 110°C for 24 hours. The hydrometer test was also conducted for the particles passing through sieve No. 200 (75 µm opening size). The results of the sieve analysis (dry and wet) and hydrometer tests are plotted in Figures 4-1 and 4-2 for M1 and M2 soils, respectively.

Table 4-1: Soil characteristics

Property	Designation	M1			M2		
Specific Gravity	ASTM D 854	2.72	2.68	2.67	2.65	2.68	2.68
		2.69			2.67		
Liquid Limit	ASTM D 4318	Non Plastic			23		
Plastic Limit	ASTM D 4318	Non Plastic			18.4		
Classification	USCS	Silty clayey sand			Silty sand		

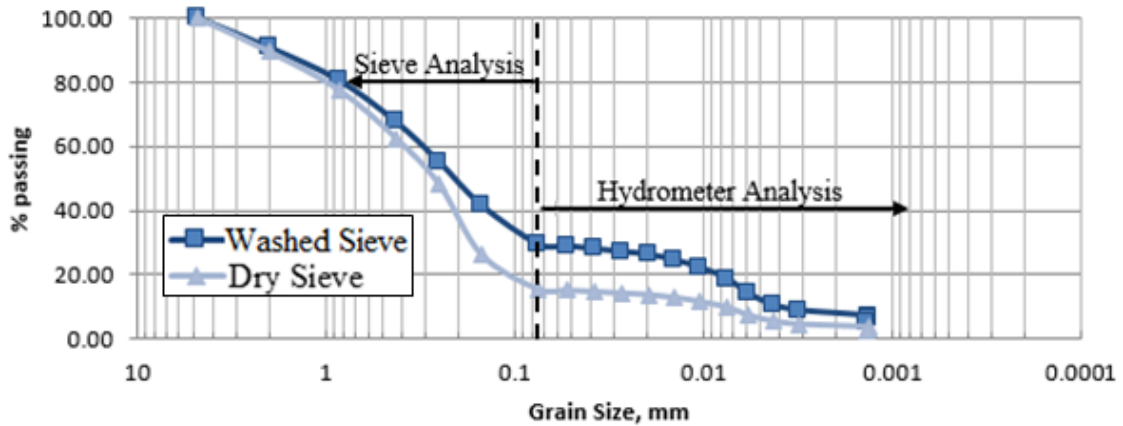


Figure 4-1: Grain size distribution curves for M1.

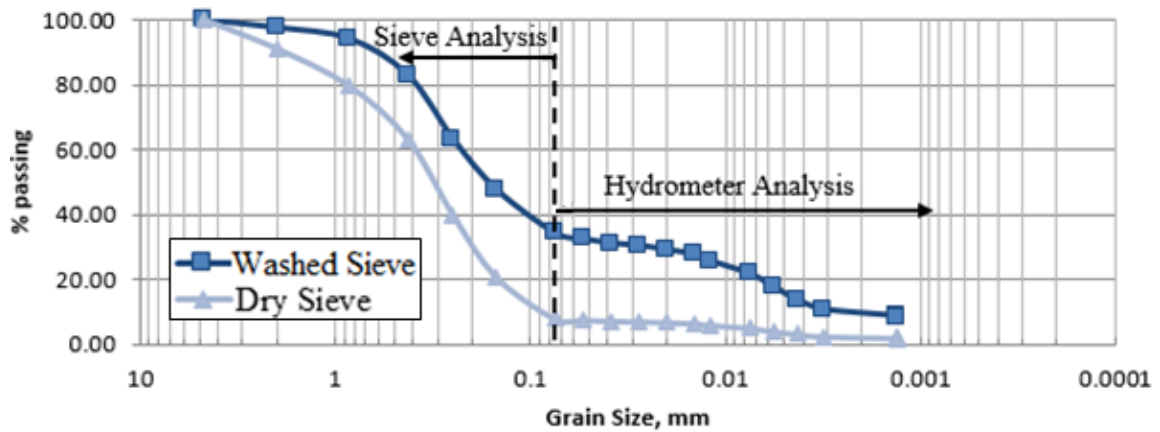


Figure 4-2: Grain size distribution curves for M2.

4.1.3 Atterberg Limits

The liquid limit and plastic limit tests were conducted on the two marl soil samples for material passing ASTM sieve No. 40, according to ASTM D 4318. For M1, it was not possible to get the number of blows for the liquid limit test, so the liquid limit is reported to be nil. In addition, the soil samples could not be rolled to a thread of 1/8 in (3.18 mm), therefore, the soil was classified as non-plastic soil, as shown in Table 4-1. On the other hand, M2 exhibited low plasticity having a plasticity index (PI) of 5. The plastic limit was 18% and the liquid limit was 23%. M1 and M2 were classified as silty clayey sand and silty sand, respectively, as per the Unified Soil Classification System (USCS).

4.1.4 Standard Proctor Compaction Test

Standard Proctor compaction test was conducted in the laboratory to determine maximum dry unit weight and optimum moisture content based on the relationship between the moisture content and the dry unit weight of the soil. Figures 4-3 and 4-4 are presenting the relationship between dry unit weight (γ_d) and moisture content (w) for M1 and M2, respectively.

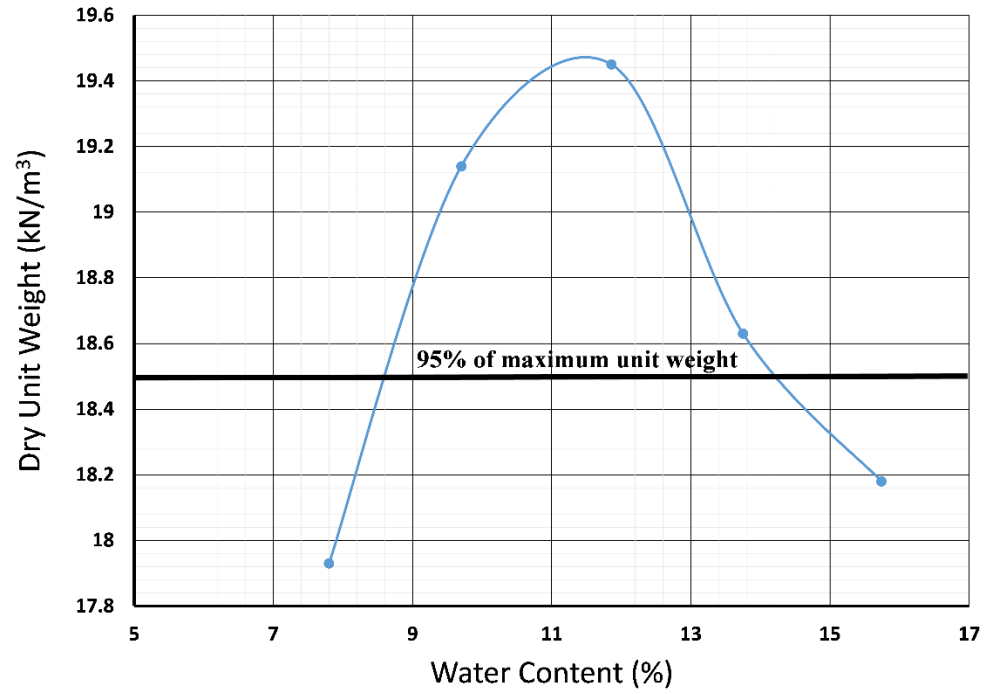


Figure 4-3: Compaction curve for M1 based on standard Proctor test

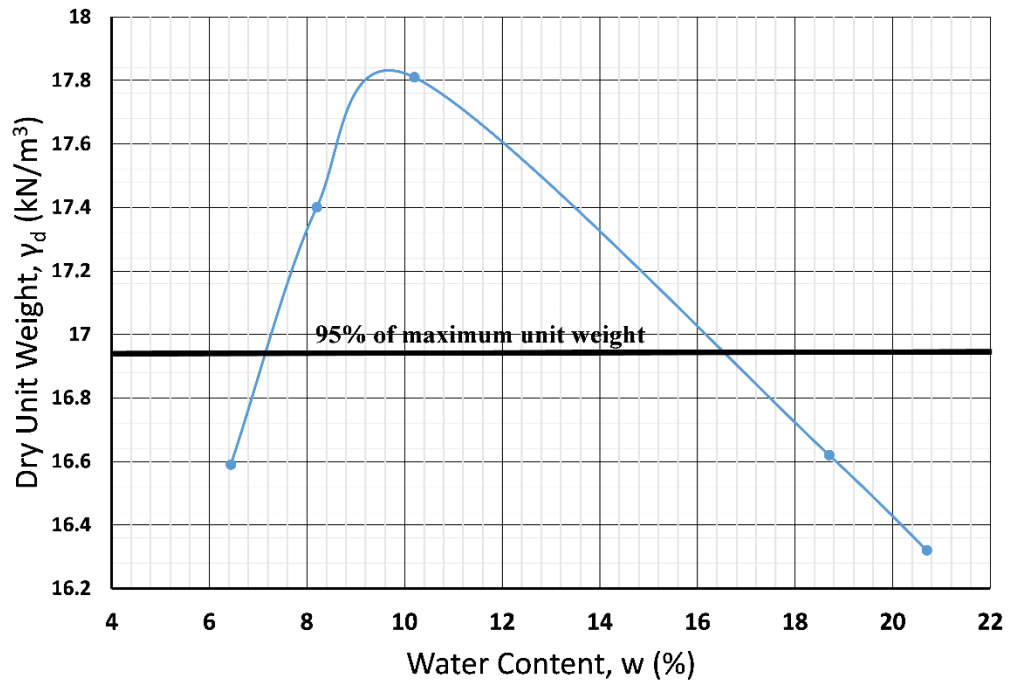


Figure 4-4: Compaction curve for M2 based on standard Proctor test

4.2 Acid Contamination Consequences

The contamination of marl soils was made with three different concentrations of both sulfuric and phosphoric acid, as presented in Chapter 3. The first run of the experiment was done with 20% concentration of both sulfuric acid and phosphoric acid. The second run was made with 32% concentration of sulfuric acid and 48% concentration of phosphoric acid. The last run was conducted with a relatively high concentration of sulfuric acid (70% concentration) and 56% for phosphoric acid. All of these percentages are commonly used in industry. The duration of each experimental run was two weeks. Moreover, the samples were prepared in duplicate for each acid concentration for both marls.

4.2.1 First Round of Sulfuric Acid (20% Concentration)

The effects of 20% concentration sulfuric acid on the non-plastic marl (M1) and low plastic marl (M2) are presented in this Section. First, the expansion pattern of M1 is shown in Figure 4-5. After one day, both M1 samples had a different rate of expansion. The rate of expansion decreased significantly after one week for both samples. At the end of testing, both identical samples exhibited asymptotic swelling curves with a difference of about 2 mm. The final result was 10 mm on average. The final swelling percentage is around 14%.

The morphological changes of M1 due to sulfuric acid interaction were investigated by SEM. High resolution pictures of 1000 time magnification were taken for uncontaminated and contaminated M1 samples. Figure 4-6 shows the microstructure of uncontaminated M1 sample. The purpose of this photo is to compare it with the contaminated samples. In addition, Figure 4-7 shows the spectrum of the elemental analysis for uncontaminated M1 using energy-dispersive EDS spectroscopy. One spot from SEM picture was selected and analyzed. This picture is presented for comparison purposes. Figure 4-8 shows the

microstructure of the top layer of the contaminated M1 sample. An obvious crystallization was displayed. This crystallization is a result of the acid-marl reaction. In addition, the microstructure shows a dense morphology, which resulted from crystallization of calcium phosphate. Figures 4-9 and 4-10 show the microstructure of the middle and bottom layers of contaminated M1 sample, respectively. The previous three figures show a clear crystallization that increases towards the bottom of the sample. This indicates that the acid reaction of the bottom layer of M1 sample is greater than the middle one and the middle one is greater than the top layer. Moreover, the SEM pictures of contaminated sample are showing a monoclinic crystal system, which is the shape of gypsum crystals. The gypsum was resulted from the reaction between sulfuric acid and carbonate.

On the other hand, M2 has also generated an expansion due to contamination with sulfuric acid of 20% concentration. Figure 4-11 shows the free swell of M2 as was effected by the sulfuric acid of 20% concentration. The two samples were swelling similarly for one day, then, the rate of swelling became different. After the fourth day, one sample experienced a significant change in the rate of expansion that produced a considerable variation in free-swelling between the two samples at the end of the experiment. Heterogeneity and the alteration of permeability in the bottom layer could lead to this outcome. The free swelling of one sample is 10 mm while it is 16 mm for the other sample. Further, the percent of free swelling for both samples are 14% and 23%, respectively. At the end of the experiments, both samples have small expansion rate and expected to give additional swell with time.

The changes in the microstructure of M2 due to infiltration of sulfuric acid were assessed by SEM. Figures 4-12, 4-13 and 4-14 are showing the morphology of the top, middle and bottom parts of M2 contaminated with 20% concentrated sulfuric acid. The pattern of

crystallization is similar to that of M1 where the crystallization increases towards the source of acid infiltration. However, the middle portion of M2 sample has some voids, that could have resulted from the pressurized carbon dioxide released from acid-base reaction, unlike the condensed matrix for M1 (Figure 4-9). This outcome had led to more permeability in M2, consequently, the rate of expansion in M2 is continuing after two weeks unlike the case of M1.

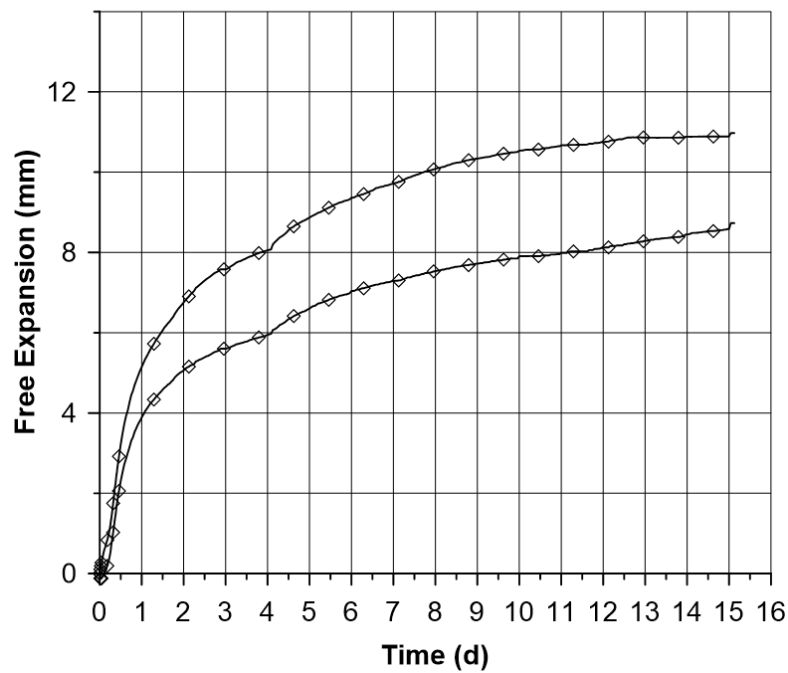


Figure 4-5: Free swell of M1 due to contamination with sulfuric acid of 20% concentration

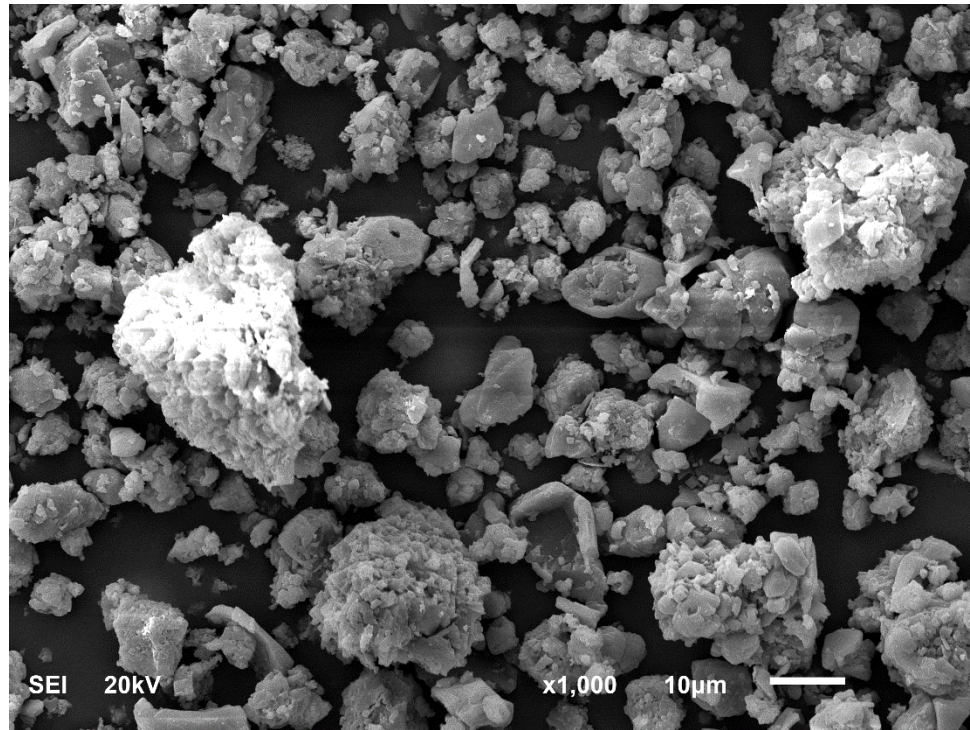


Figure 4-6: SEM picture of uncontaminated uncompacted M1 sample

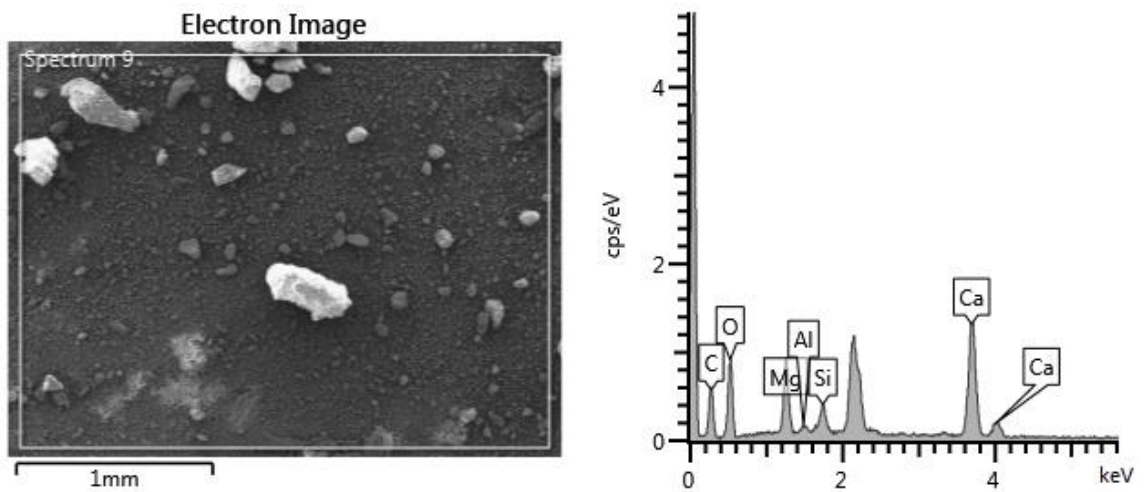


Figure 4-7: EDS analysis of uncontaminated M1

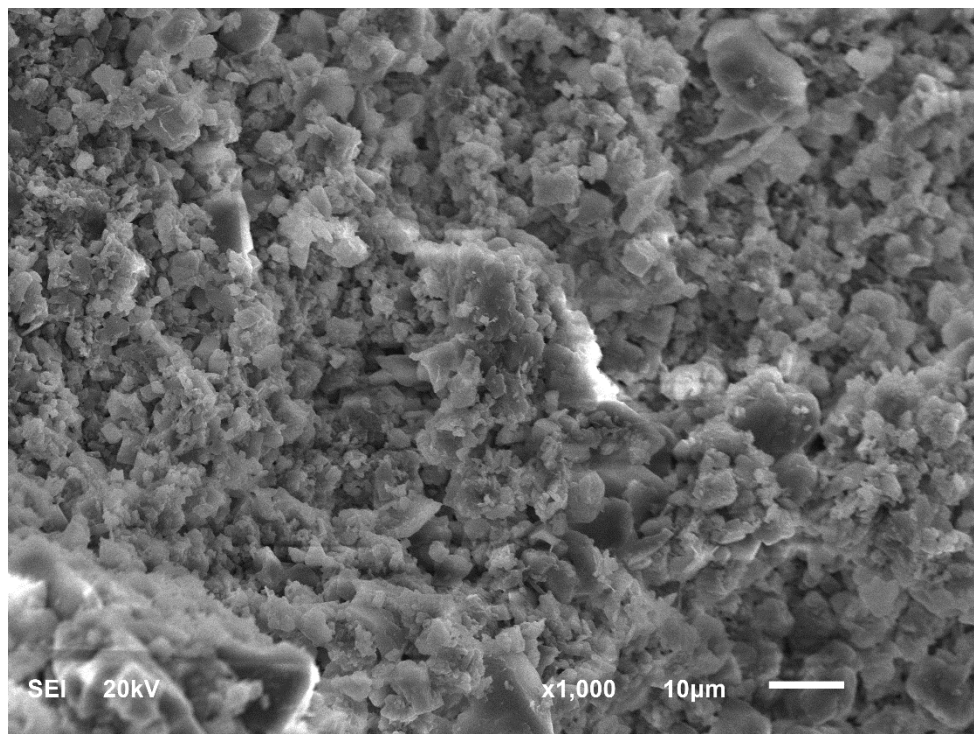


Figure 4-8: SEM picture for the top layer of M1 sample contaminated with 20% concentration sulfuric acid

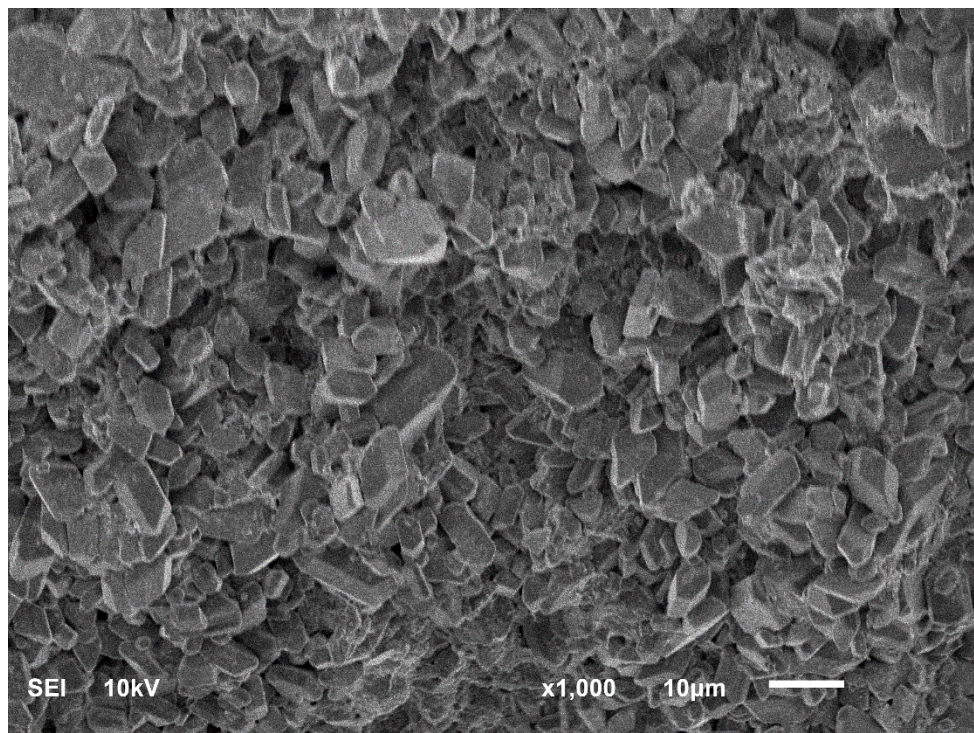


Figure 4-9: SEM picture for the middle layer of M1 sample contaminated with 20% concentration sulfuric acid

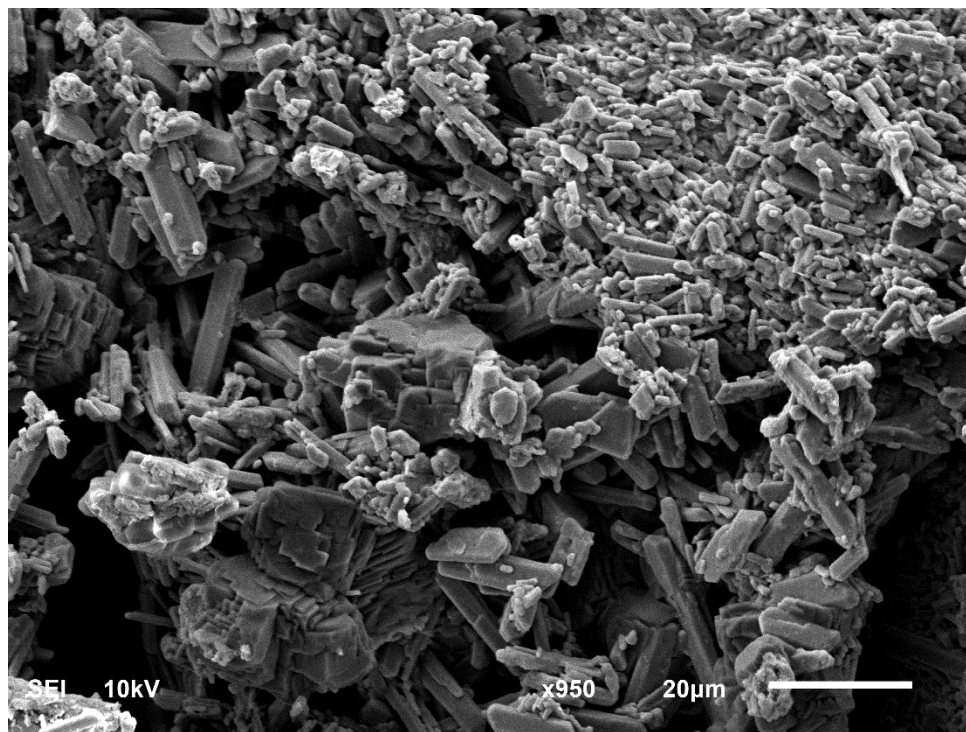


Figure 4-10: SEM picture for the bottom layer of M1 sample contaminated with 20% concentration sulfuric acid

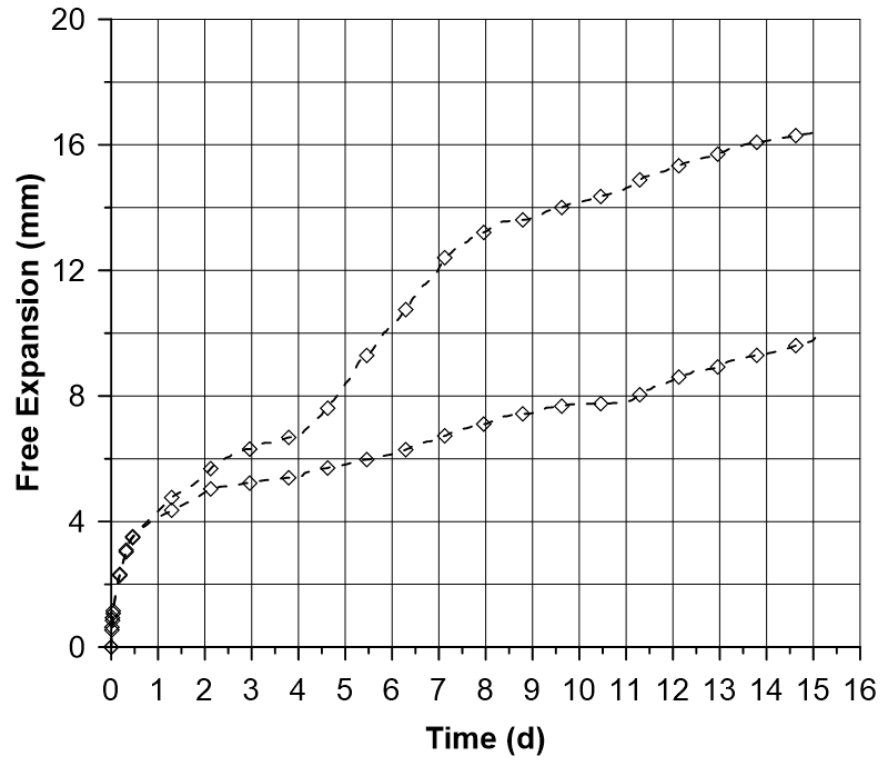


Figure 4-11: Free swell of M2 due to contamination with sulfuric acid of 20% concentration

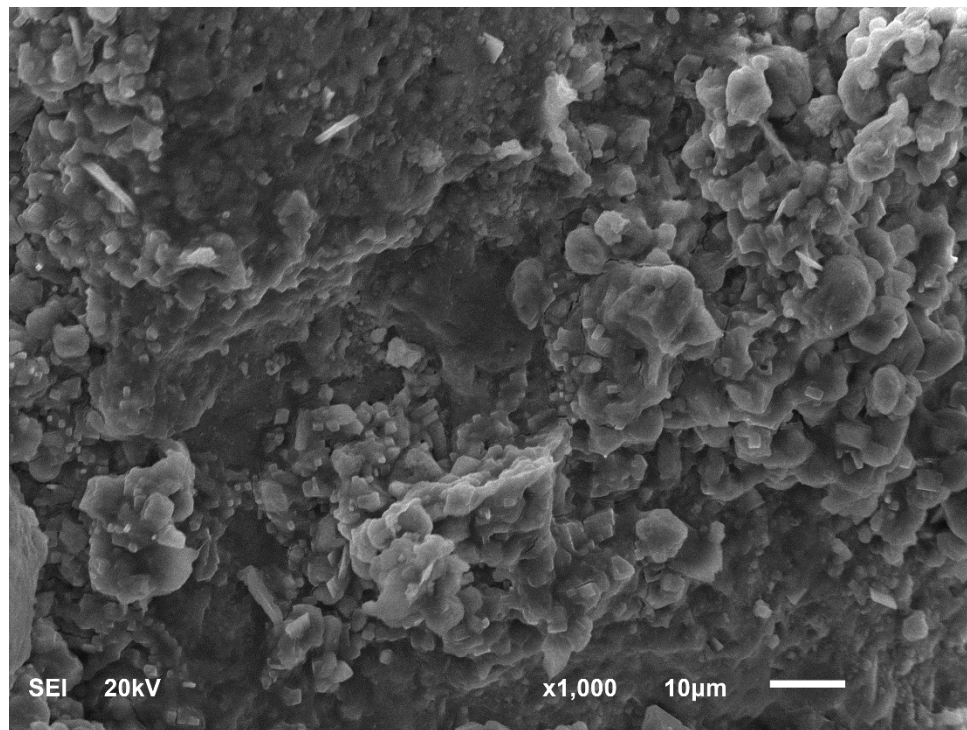


Figure 4-12: SEM picture for the top layer of M2 sample contaminated with 20% concentration sulfuric acid

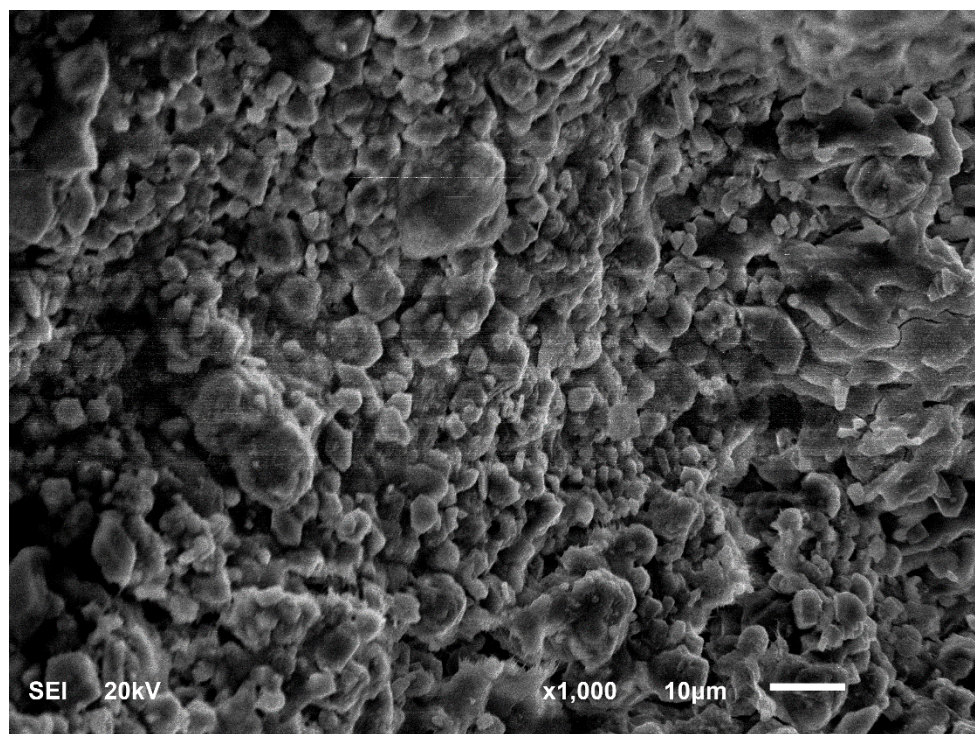


Figure 4-13: SEM picture for the middle layer of M2 sample contaminated with 20% concentration sulfuric acid

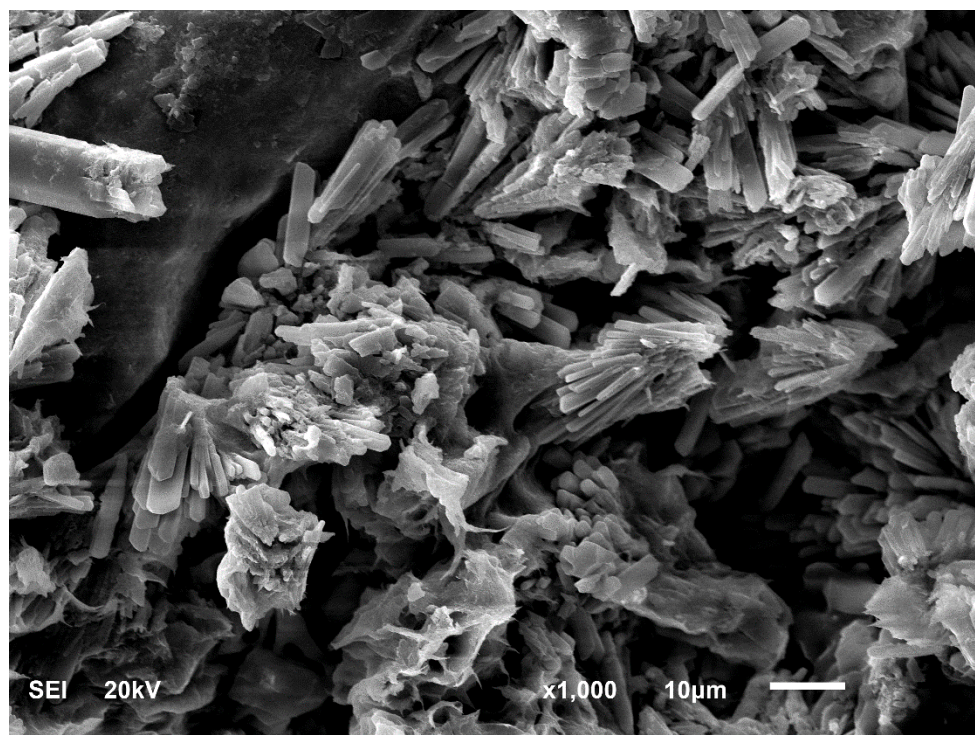


Figure 4-14: SEM picture for the bottom layer of M2 sample contaminated with 20% concentration sulfuric acid

4.2.2 First Round for Phosphoric Acid (20% Concentration)

Phosphoric acid of 20% concentration was used to assess the volume change characteristics of M1 and M2 soils. The free expansion of M1, which had been affected by the 20% concentration phosphoric acid, is presented in Figure 4-15. The expansion is extremely low while in one sample a minor reduction in sample height, around 1 mm, was surprisingly noted. The SEM photos, which are presented in Figures 4-16, 4-17 and 4-18 show similar microstructure for the top, middle and bottom layers of M1 sample. In addition, the crystallization of acid-calcareous reaction is barely found. This finding leads to the absence of phosphoric acid in the sample. The XRD and strength measurement were used to support this output.

On the other hand, a considerable expansion was noticed in the case of M2. The expansion pattern of M2 is shown in Figure 4-19. In the first day, both samples expanded together, after that, the rate of expansion became different. The rate of expansion diminished significantly after three days for one sample and after the fifth day for the other sample. This could be due to the fact that the acid had reached and reacted with the bottom layer of both samples at the same time and produced crystals that blocked further acid adsorption by these contaminated portions. The permeability and feature of the bottom layers had been altered and thus the infiltration of acid to the upper layers had been reduced or stopped completely for both samples. Ultimately, both samples showed similar swelling results of about 11 mm. The percentage of free swelling of M2 due to contamination with phosphoric acid of 20% concentration is around 15% for both samples.

The morphological shapes of the top, middle and bottom layers of M2 sample polluted by phosphoric acid are reported in Figures 4-20, 4-21 and 4-22, respectively. All layers in M2

sample had a noticeable formation of calcium phosphate due to the acid-calcareous soil reaction. The bottom layer of the sample had some voids, as shown in Figure 4-22. The possible reason for these voids is the entrapped pressurized carbon dioxide (CO₂) gas, which was produced as a result of acid-base reaction.

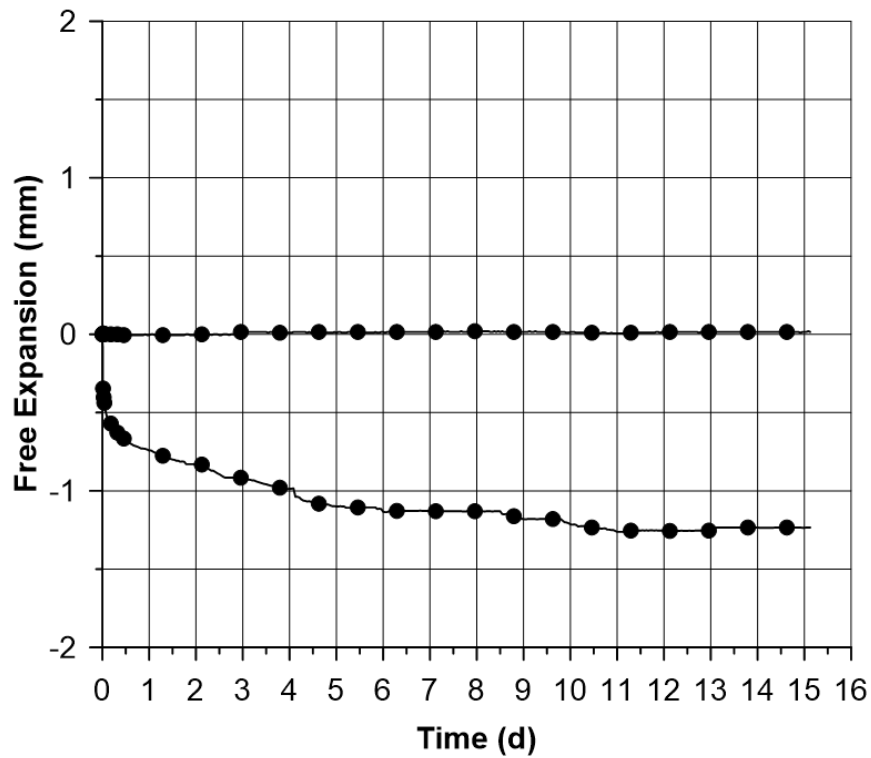


Figure 4-15: Free swell of M1 due to contamination with phosphoric acid of 20% concentration

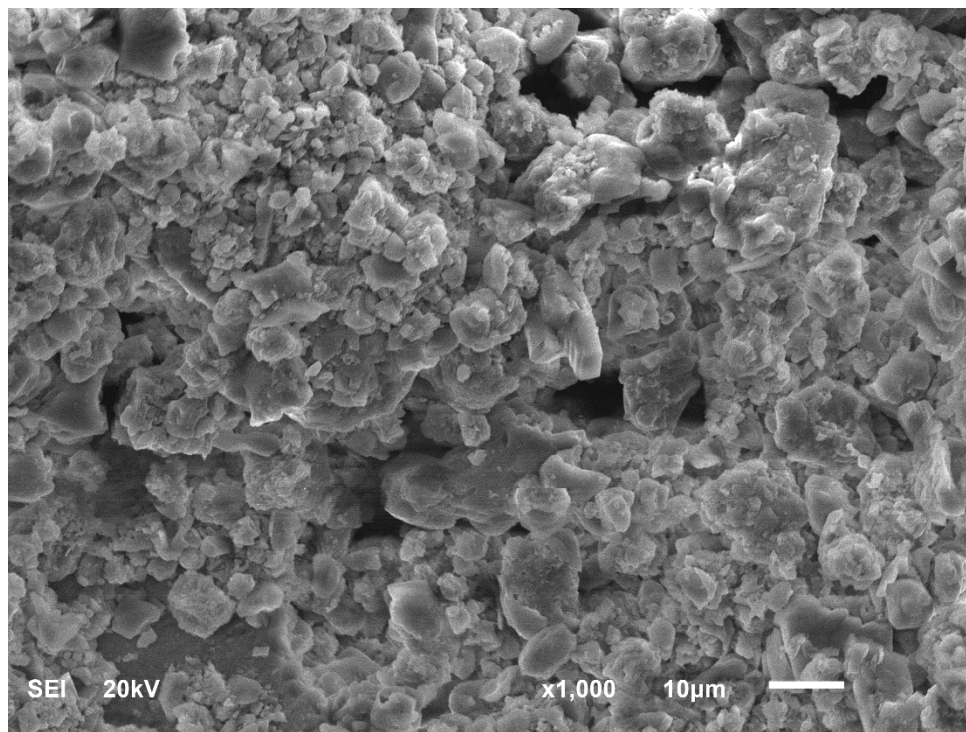


Figure 4-16: SEM picture for the top layer of M1 sample contaminated with 20% concentration phosphoric acid

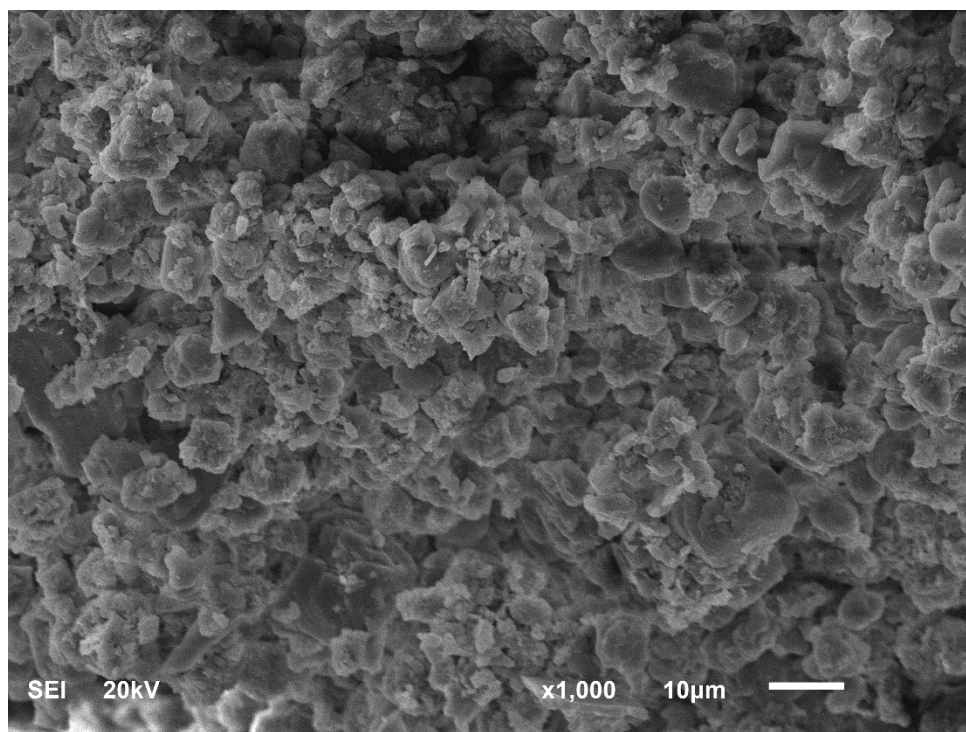


Figure 4-17: SEM picture for the middle layer of M1 sample contaminated with 20% concentration phosphoric acid

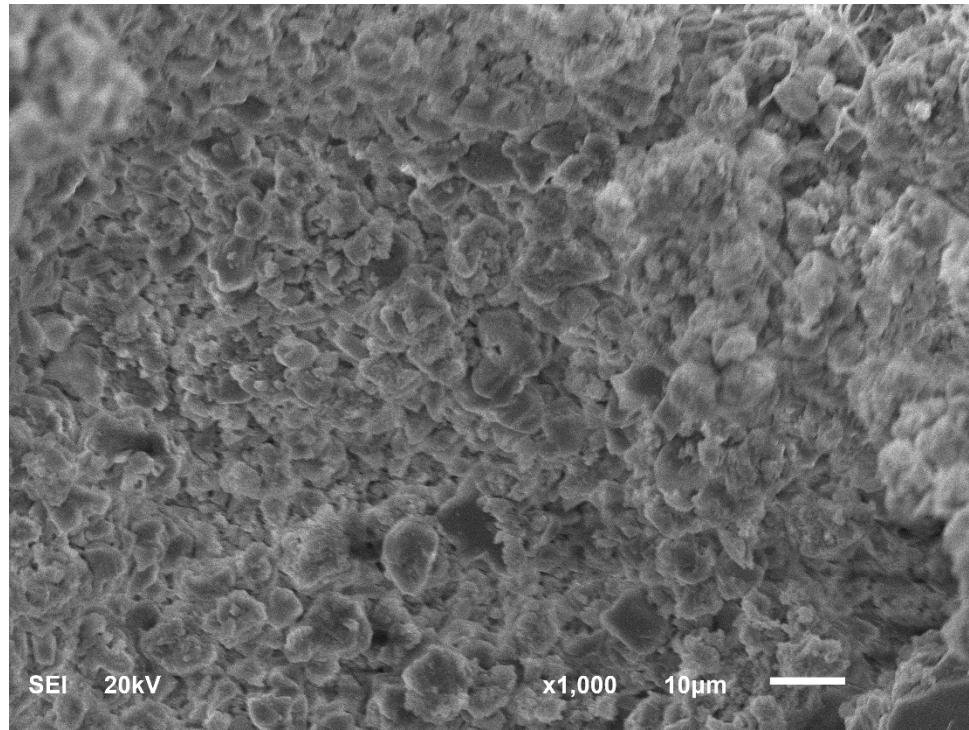


Figure 4-18: SEM picture for the bottom layer of M1 sample contaminated with 20% concentration phosphoric acid

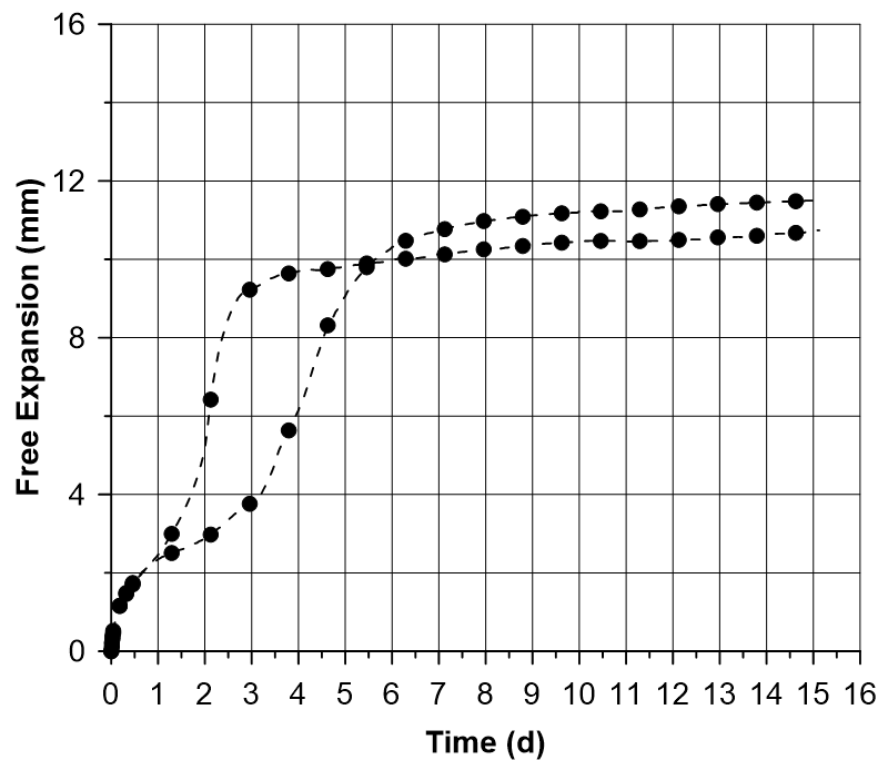


Figure 4-19: Free swell of M2 due to contamination with phosphoric acid of 20% concentration

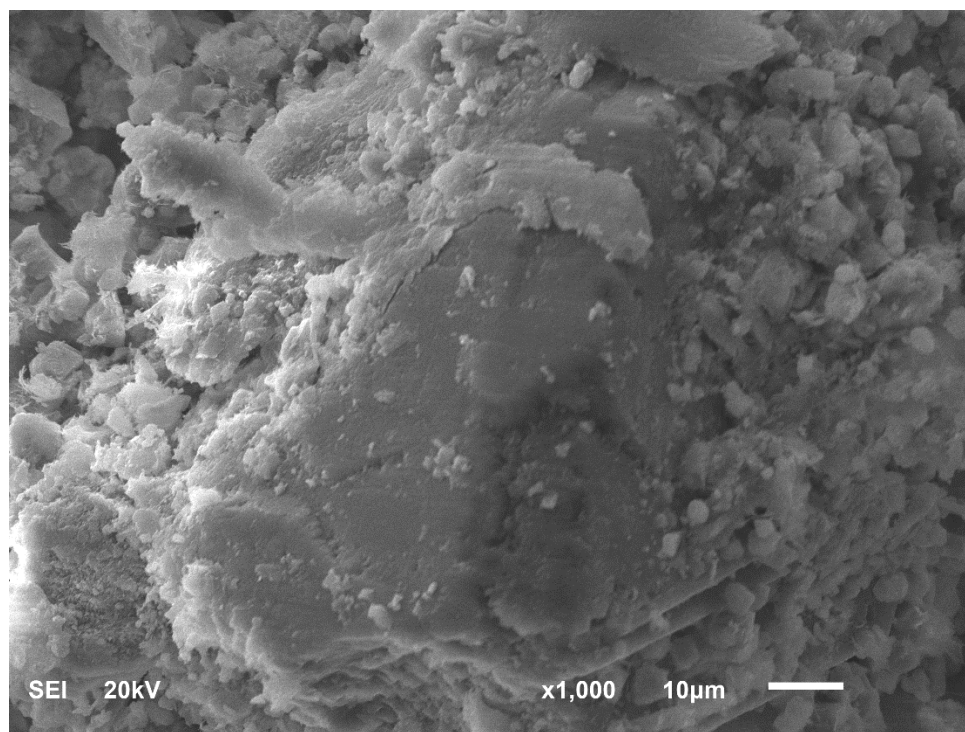


Figure 4-20: SEM picture for the top layer of M2 sample contaminated with 20% concentration phosphoric acid

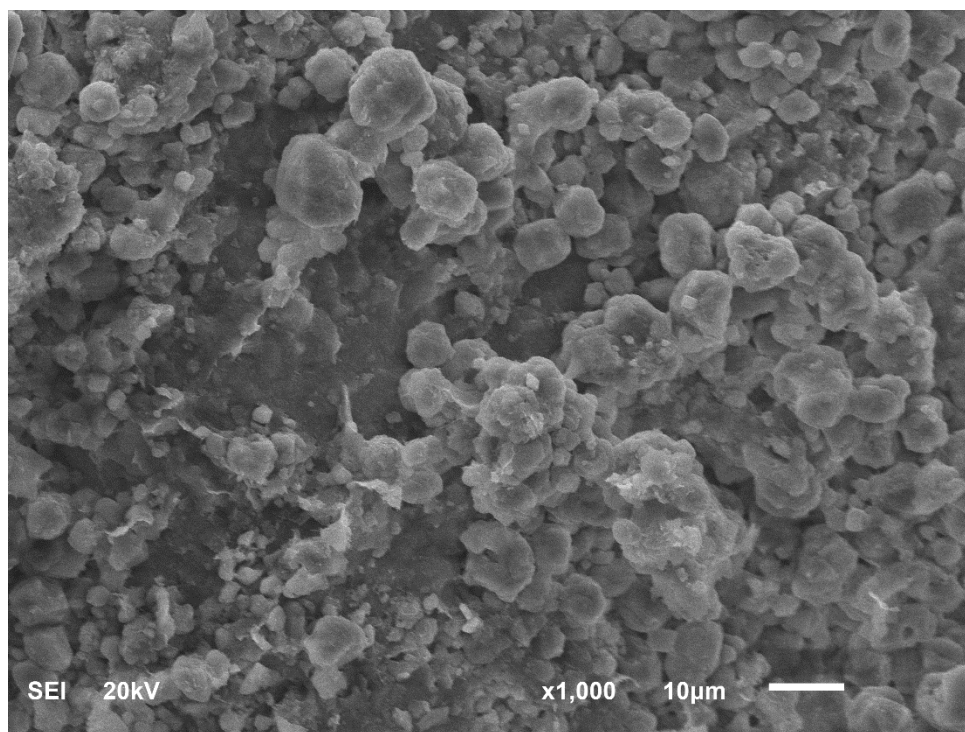


Figure 4-21: SEM picture for the middle layer of M2 sample contaminated with 20% concentration phosphoric acid

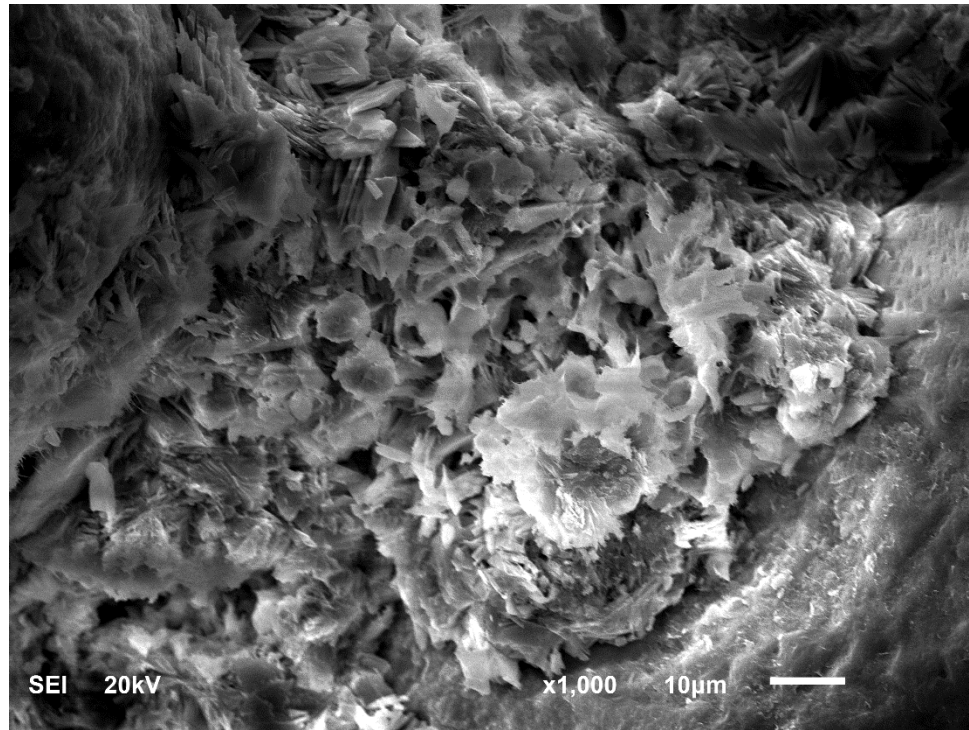


Figure 4-22: SEM picture for the bottom layer of M2 sample contaminated with 20% concentration phosphoric acid

4.2.3 Second Round for Sulfuric Acid (32% Concentration)

In this round, the concentration of sulfuric acid was increased to 32%. Two identical samples of each marl were contaminated in the same way as for the previous acid concentration. Figure 4-23 presented the free expansion of M1 samples when interacted with sulfuric acid of 32% concentration. M1 samples showed different expansion behavior for the two identical samples. The rate of swelling was similar for both samples in the first two days. After that, the expansion rate of one sample was small compared to the other sample, which continued to expand in noticeable rate. After the duration of contamination of two weeks, one sample has 7 mm change in height and the other had an expansion of 17 mm with a continuous increase in the rate of expansion. The percentage of free swell of M1 due to contamination with sulfuric acid of 32% concentration was close to 10% for the first sample and 23% for the second one. The expansion rate of both samples became different

due to alteration of acid penetration into the soil, which might have resulted from the noticed crystallization.

The morphological analysis has demonstrated an increase in the crystallization associated with the bottom of the sample. Figures 4-24, 4-25 and 4-26 show the microstructure of the top, middle and bottom layer of the contaminated M1 sample, respectively. These figures show a clear change in the microstructure of M1. For example, an obvious crystals of calcium sulphate are presented in the contaminated M1 sample, especially in the bottom layer.

The second marl M2 has also a diverse behavior of expansion due to contamination with sulfuric acid of 32% concentration. Figure 4-27 depicts the free swell of contaminated M2 by the sulfuric acid of 32% concentration. From the beginning of acid infiltration, both M2 samples were swelling in a different manner. After five days, one sample experienced a higher rate of expansion ending up with a greater value of swelling as compared with the other sample. This discrepancy of swelling values may be caused by the heterogeneity of M2 samples. The crystallization in M2 could affect the hydraulic conductivity of acid at different places in the sample. The maximum free swelling value is 29 mm with 41% swelling percent and the other one sample has 19 mm with 27% swelling expansion present.

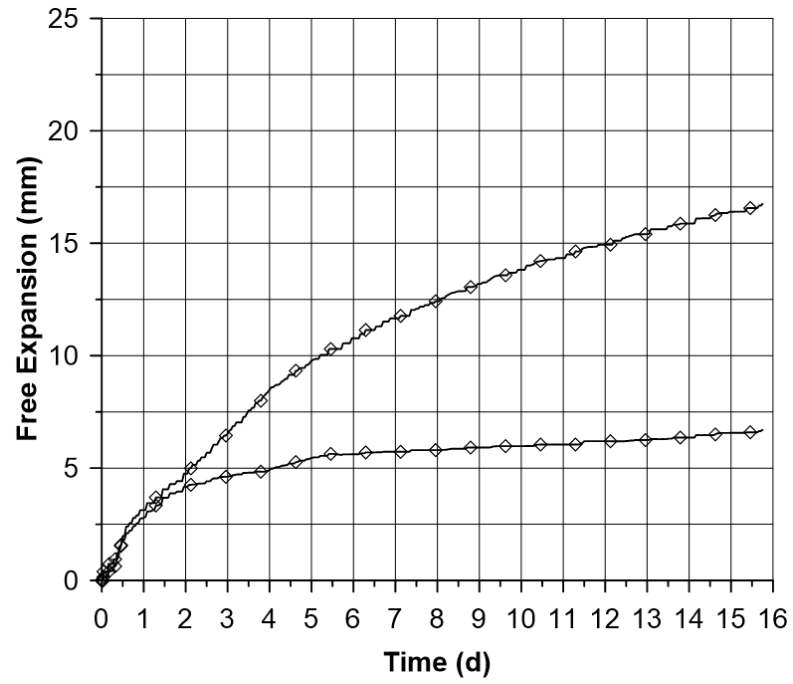


Figure 4-23: Free swell of M1 due to contamination with sulfuric acid of 32% concentration

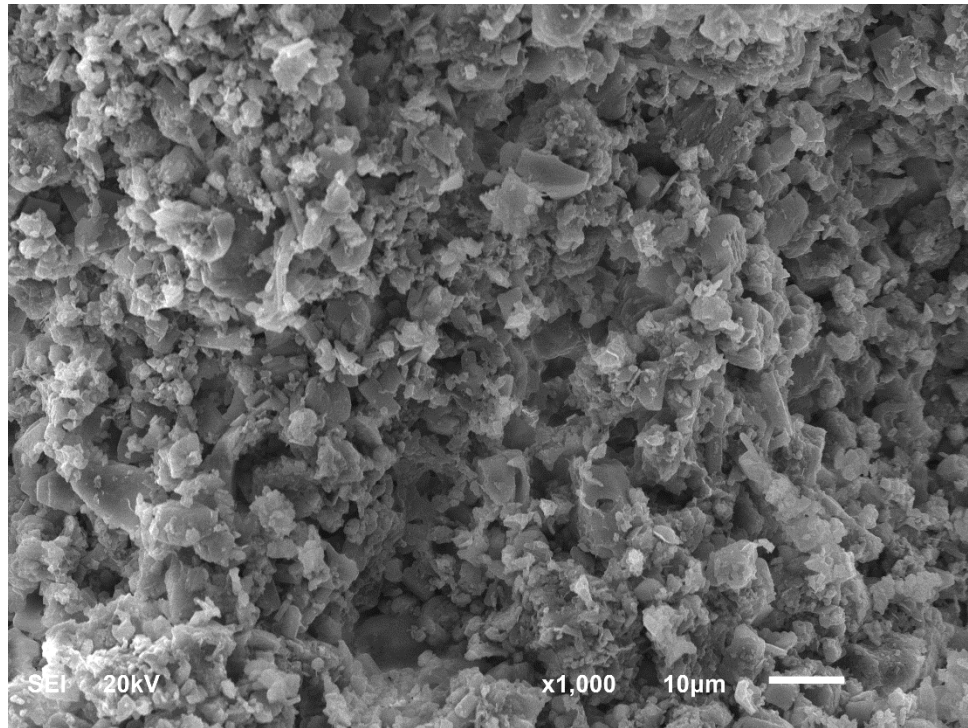


Figure 4-24: SEM picture for the top layer of M1 sample contaminated with 32% concentration sulfuric acid

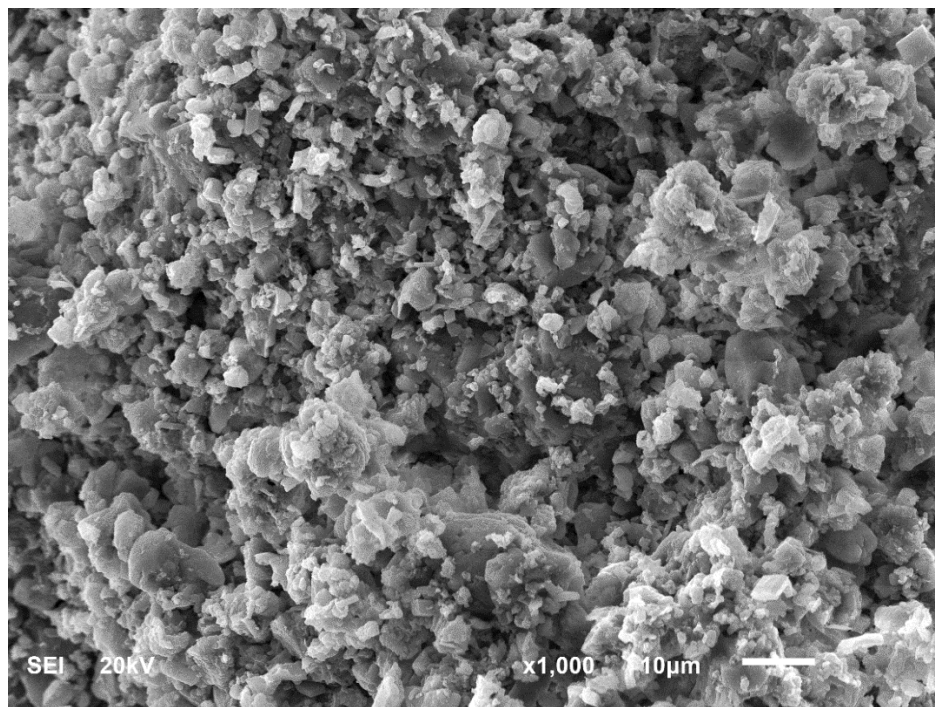


Figure 4-25: SEM picture for the middle layer of M1 sample contaminated with 32% concentration sulfuric acid

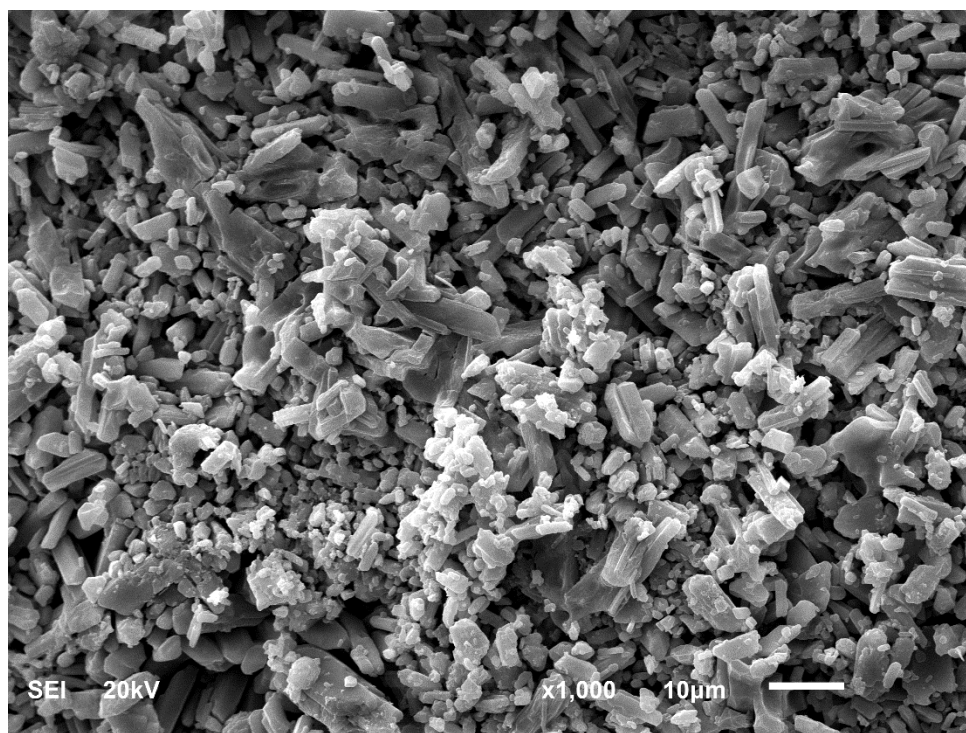


Figure 4-26: SEM picture for the bottom layer of M1 sample contaminated with 32% concentration sulfuric acid

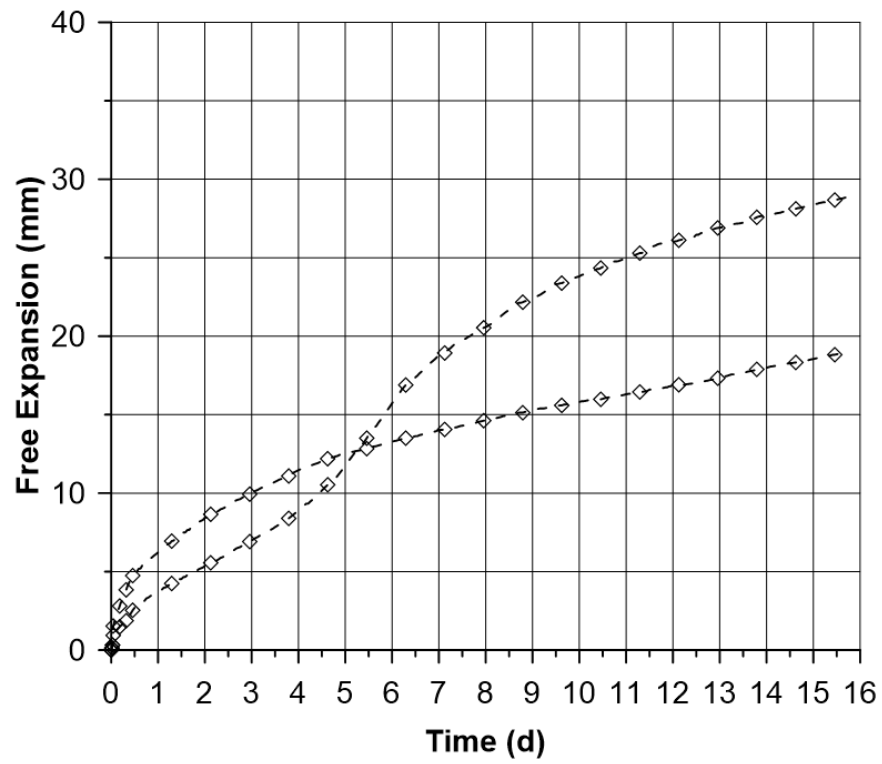


Figure 4-27: Free swell of M2 due to contamination with sulfuric acid of 32% concentration

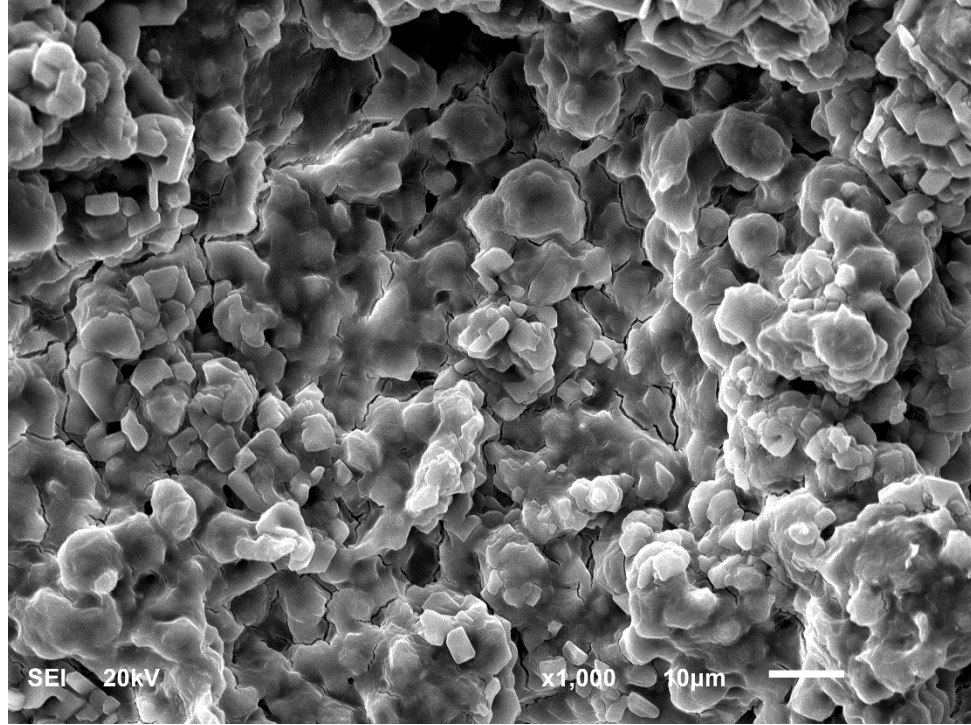


Figure 4-28: SEM picture for the top layer of M2 sample contaminated with 32% concentration sulfuric acid

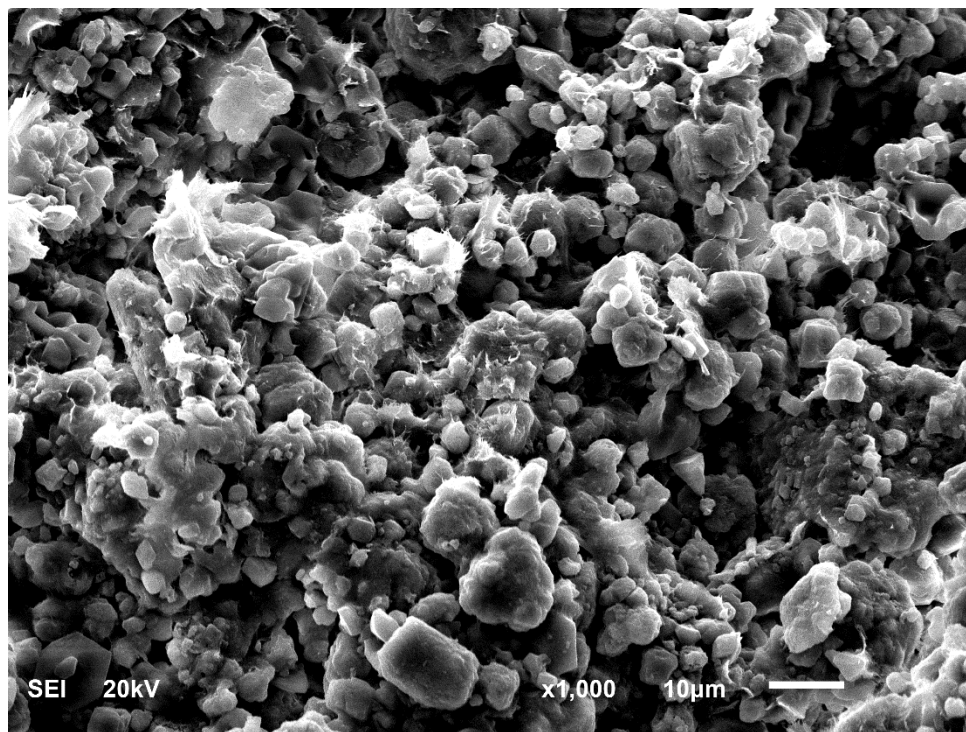


Figure 4-29: SEM picture for the middle layer of M2 sample contaminated with 32% concentration sulfuric acid

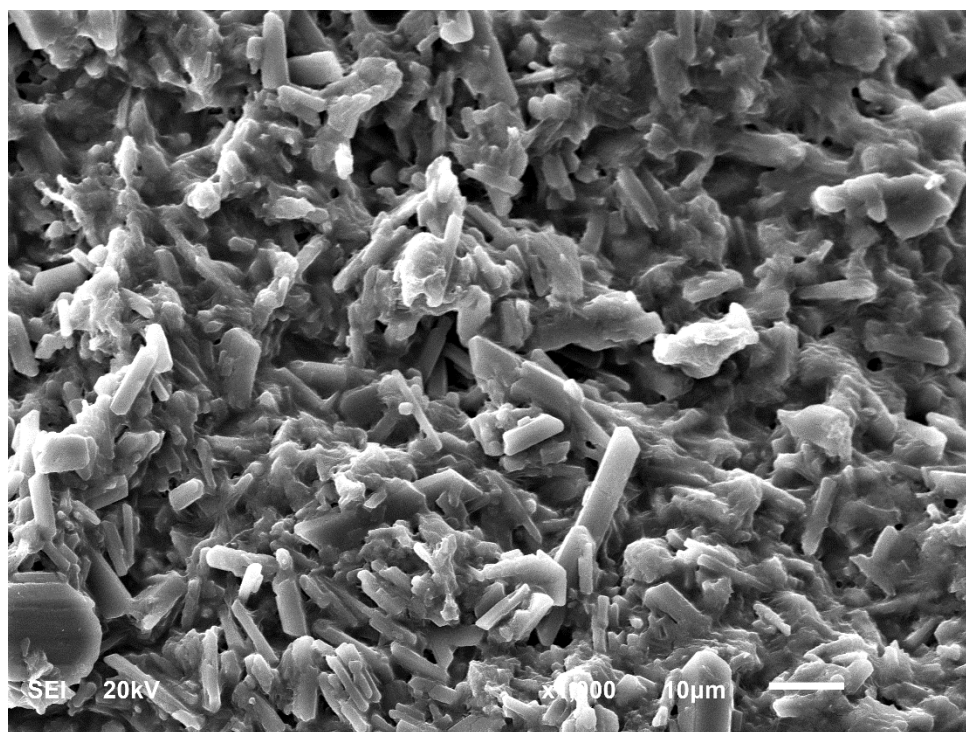


Figure 4-30: SEM picture for the bottom layer of M2 sample contaminated with 32% concentration sulfuric acid

4.2.4 Second Round for Phosphoric Acid (48% Concentration)

In this section, the effect of phosphoric acid of 48% concentration with M1 and M2 soils is presented. First, the free expansion of the contaminated M1 with phosphoric acid of 48% concentration is presented in Figure 4-31. Similar to the result of M1 with 20% concentration phosphoric acid, the amount of expansion is very little. The SEM pictures of M1 contaminated with 48% concentration phosphoric acid are presented in Figures 4-32 through 4-34 for the top, middle and bottom layers, respectively. In contrast to the result of M1 in the first round, this time M1 showed clear crystals of calcium phosphate for the bottom layer. Further, the middle layer is giving some crystallization as well. The XRD analysis will give more details on this finding, as will be reported in Section 4.3.

M2 has shown a remarkable free expansion with 48% concentration phosphoric acid. Figure 4-35 displays the free swell for M2 samples. Both samples were moving together for two days. After that, the rate of expansion of one sample started to diminish while the other one continued to expand until the 12th day. After two weeks, one sample experienced 21 mm free expansion with 31% of swelling and the other one has only 6 mm free expansion which is around 8% of the expansion. This great difference in the expansion for both samples could have resulted from the alteration of the acid permeability. Figures 4-36, 4-37 and 4-38 show the magnified pictures of the top, middle, and bottom, respectively, of the contaminated M2. Plate-like crystals of calcium phosphate are clearly shown in SEM pictures. Further, plate's size gets larger along with the direction of acid infiltration i.e. plates for the bottom part are larger than the middle and top parts. Unlike M1, M2 gave plate-like crystals because the quantity of carbonate minerals in M1 is more

than the quantity in M2. In other word, rod shape crystals, which are for M1, have higher crystallization than plate-like shape crystals.

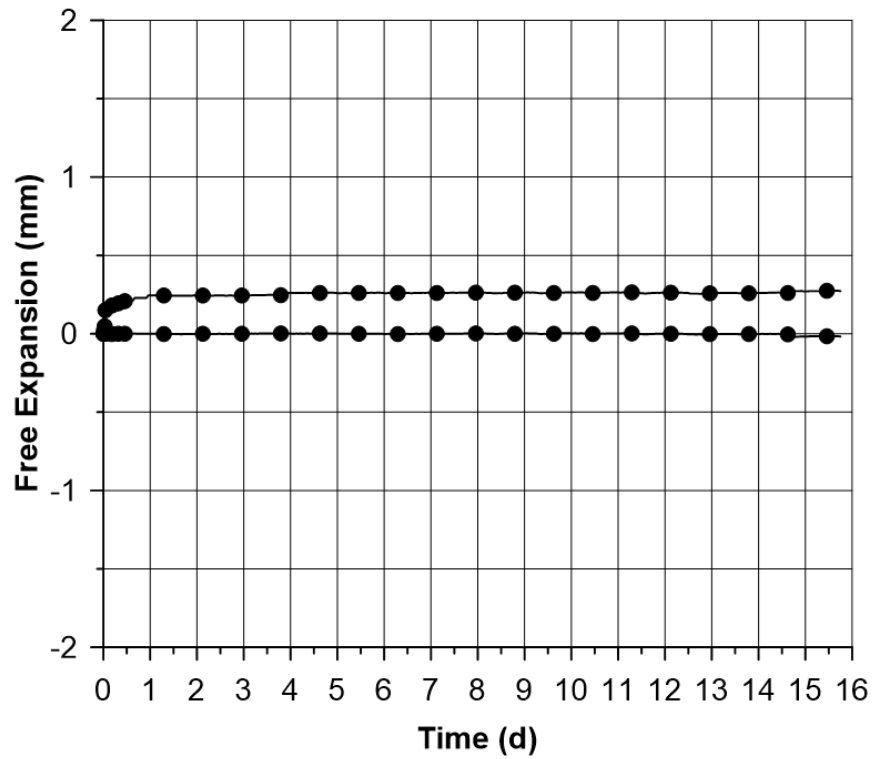


Figure 4-31: Free swell of M1 due to contamination with phosphoric acid of 48% concentration

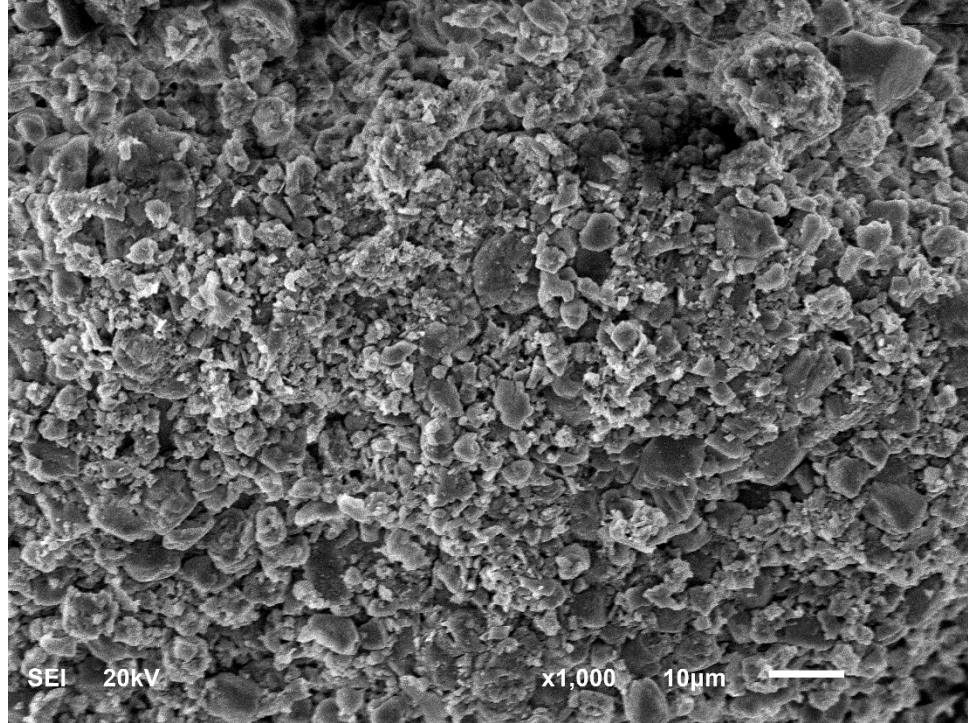


Figure 4-32: SEM picture for the top layer of M1 sample contaminated with 48% concentration phosphoric acid

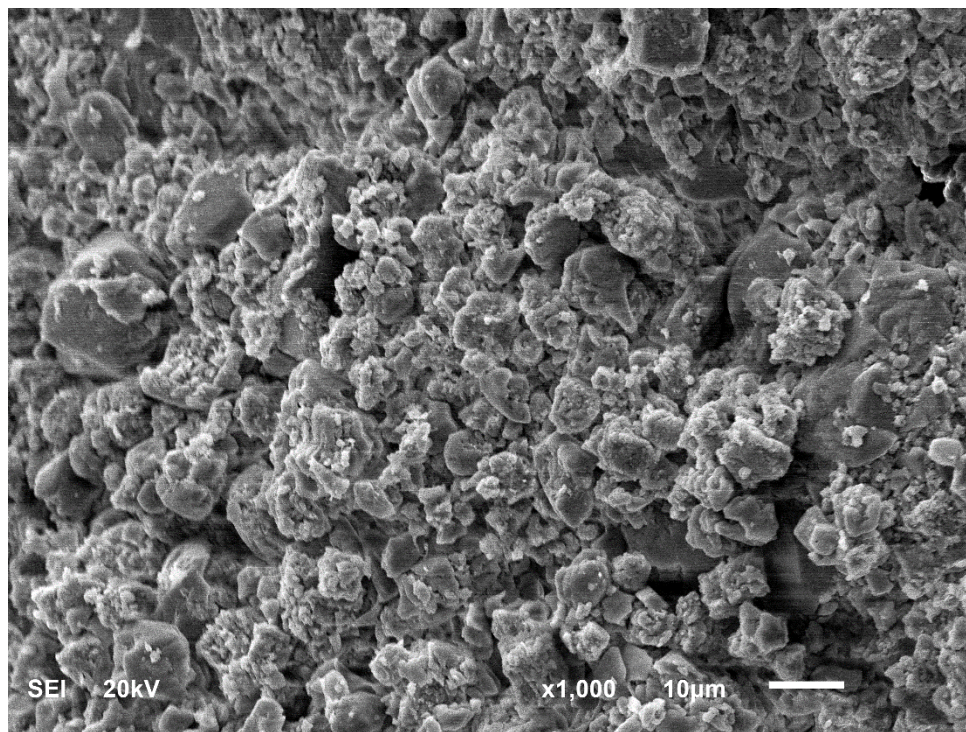


Figure 4-33: SEM picture for the middle layer of M1 sample contaminated with 48% concentration phosphoric acid

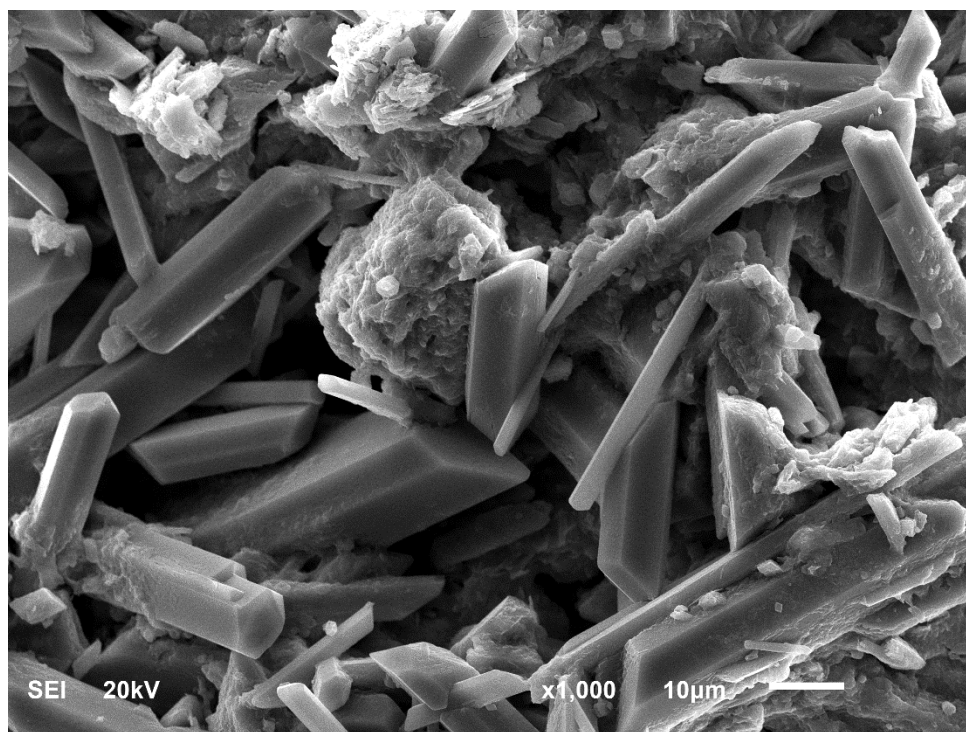


Figure 4-34: SEM picture for the bottom layer of M1 sample contaminated with 48% concentration phosphoric acid

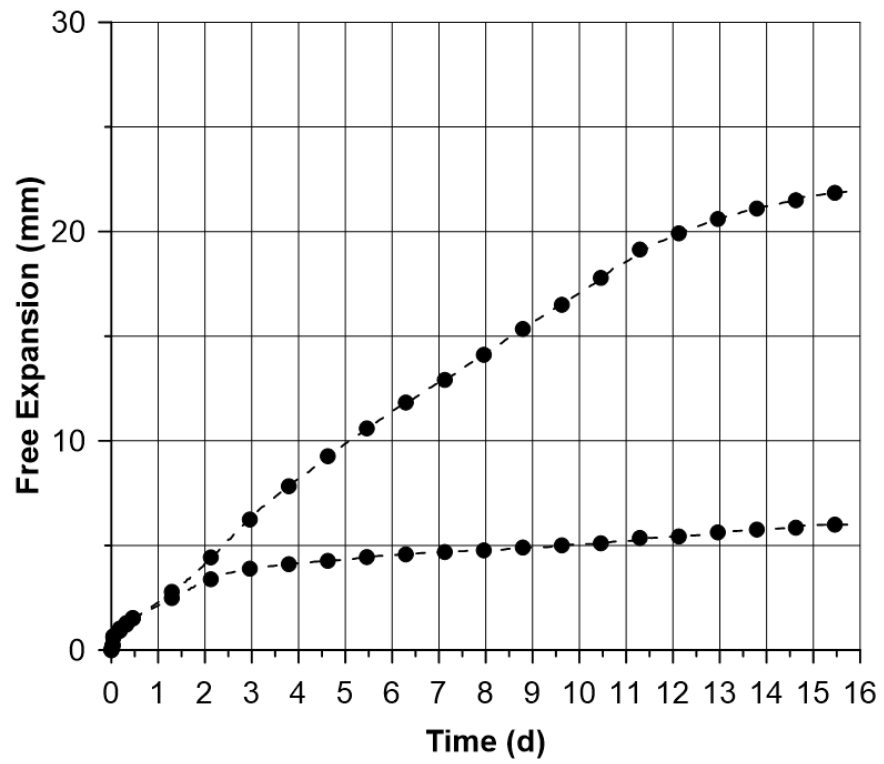


Figure 4-35: Free swell of M2 due to contamination with phosphoric acid of 48% concentration

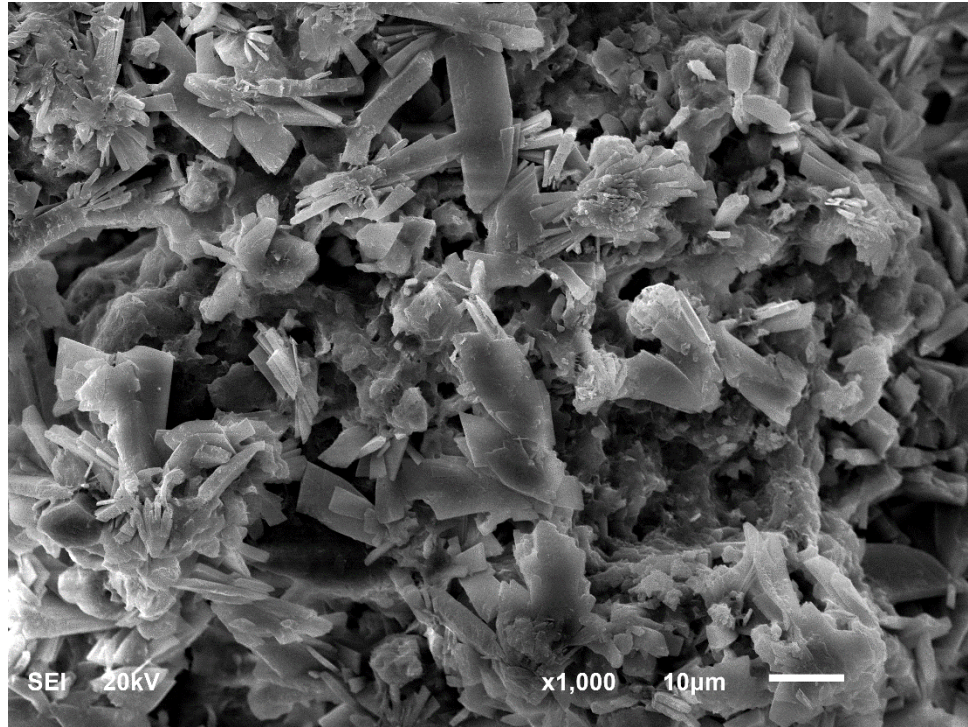


Figure 4-36: SEM picture for the top layer of M2 sample contaminated with 48% concentration phosphoric acid

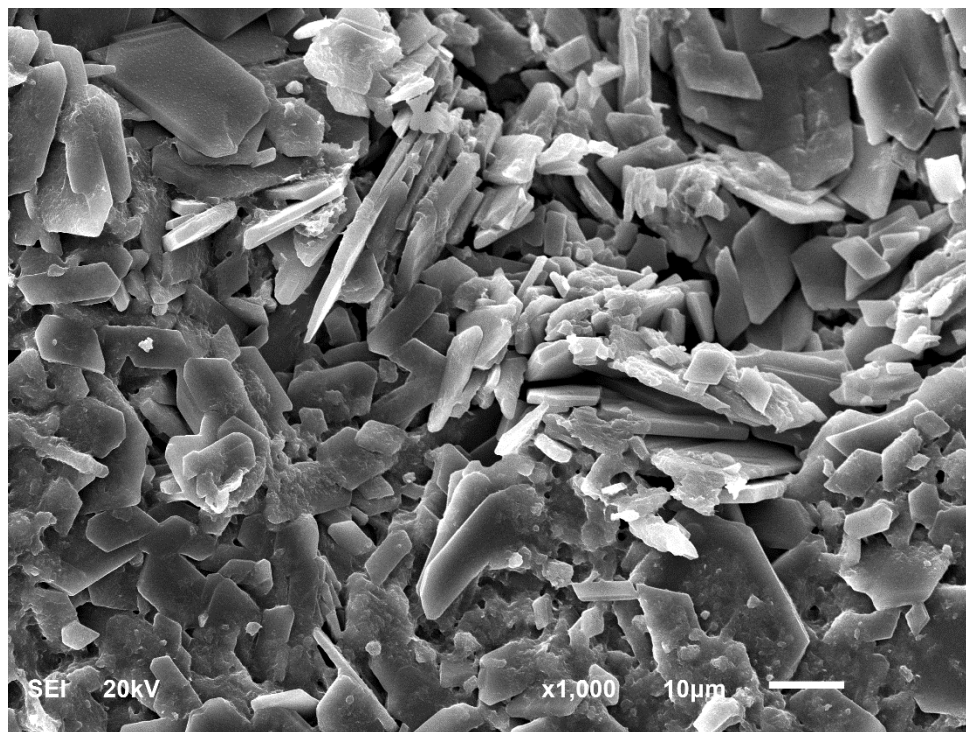


Figure 4-37: SEM picture for the middle layer of M2 sample contaminated with 48% concentration phosphoric acid

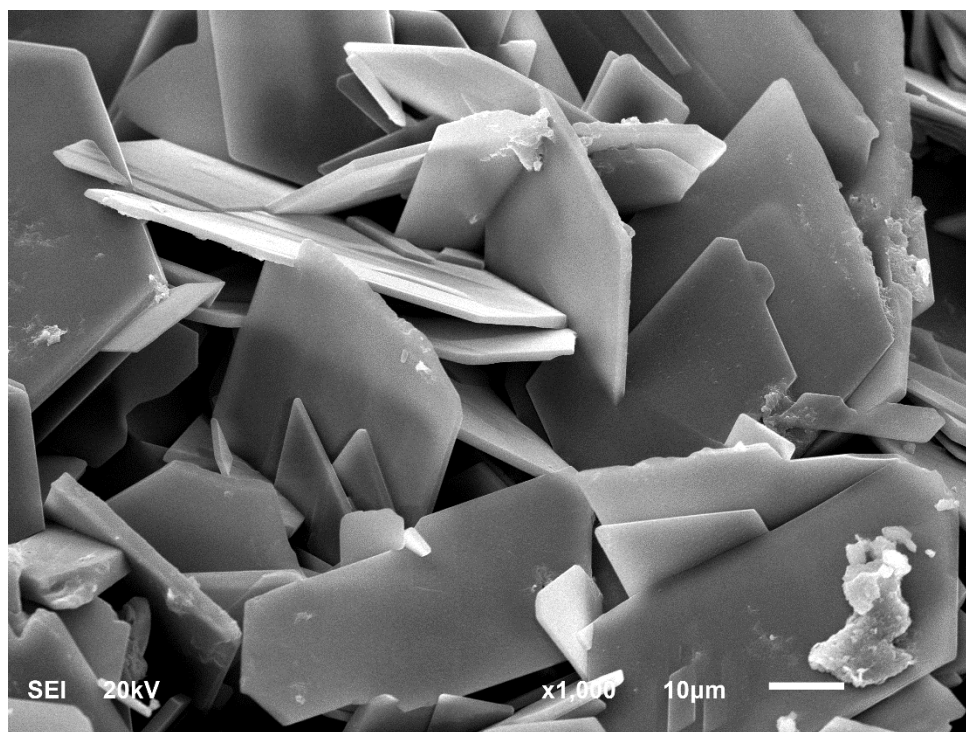


Figure 4-38: SEM picture for the bottom layer of M2 sample contaminated with 48% concentration phosphoric acid

4.2.5 Third Round for Sulfuric Acid (70% Concentration)

The third round of acid contamination consisted of using a high concentration (70%) of sulfuric acid to contaminate both marl types. The first marl (M1) showed an unexpected very low expansion behavior (Figure 4-39). Unlike the expansion with lower concentrations, 70% sulfuric acid has extremely small expansion for both samples. It is clear from the data in Figure 4-39 that there is marginal expansion rate after two weeks. SEM micrographs from the top, middle, and bottom of M1 contaminated with 70% sulfuric acid are presented in Figures 4-40, 4-41 and 4-42, respectively. All photos showed the tiny formation of crystals of calcium phosphate.

On the other hand, M2 samples showed approximately identical expansion behavior due to the contamination with 70% sulfuric acid. Figure 4-43 presents the free expansion of M2 samples polluted by the sulfuric acid of 70% concentration. The expansion rates for the two samples were similar for the first three days, after that, they got little divergence. Eventually, both expansion curves converged to have similar swelling results of about 40 mm and approximately 60% of expansion percentage. This was resulted because the permeability of 70% sulfuric acid through M2 is higher than the permeability in M1 and that was prove in Section 4.3.

The SEM outcomes of the top, the middle and the bottom part of M2 sample reacted with 70% sulfuric acid as shown in Figures 4-44, 4-45 and 4-46, respectively. The top, middle and bottom layers are having crystals showing an orthorhombic system, which is the crystal system of anhydrite. The size of these crystals in the bottom was higher than the middle. In addition, some gaps are located between crystals and those gaps are caused primarily by pressurized carbon dioxide.

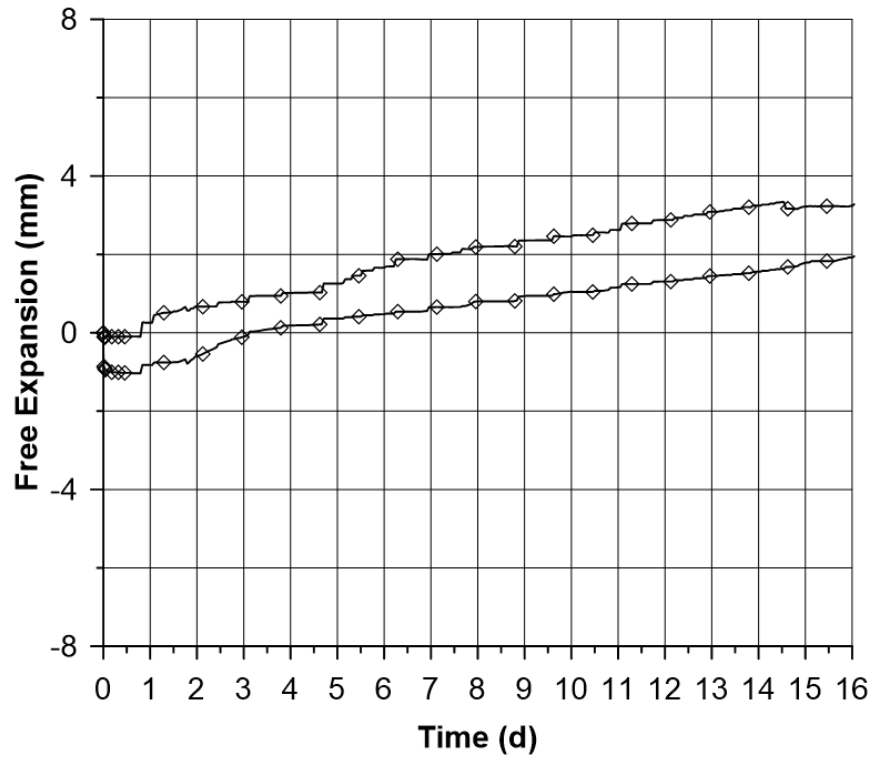


Figure 4-39: Free swell of M1 due to contamination with sulfuric acid of 70% concentration

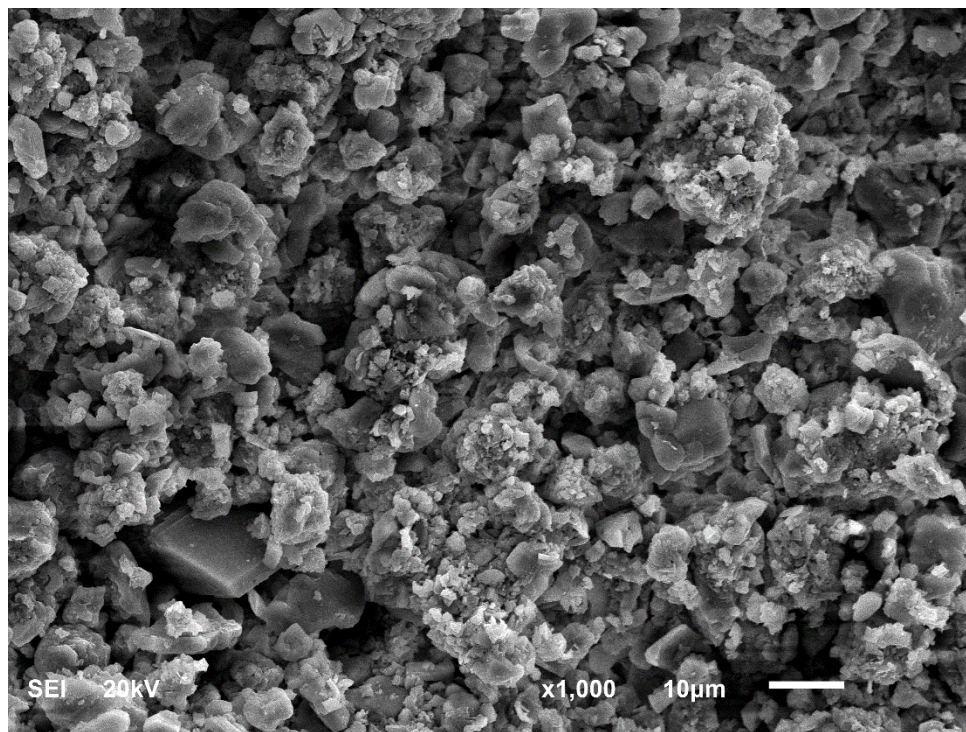


Figure 4-40: SEM picture for the top layer of M1 sample contaminated with 70% concentration sulfuric acid

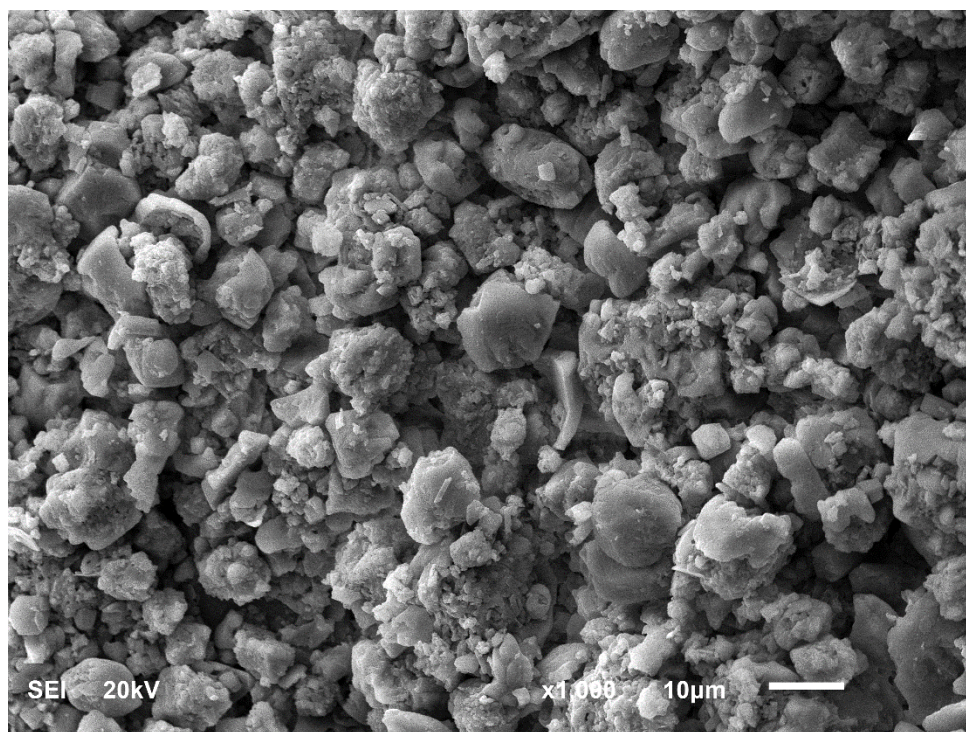


Figure 4-41: SEM picture for the middle layer of M1 sample contaminated with 70% concentration sulfuric acid

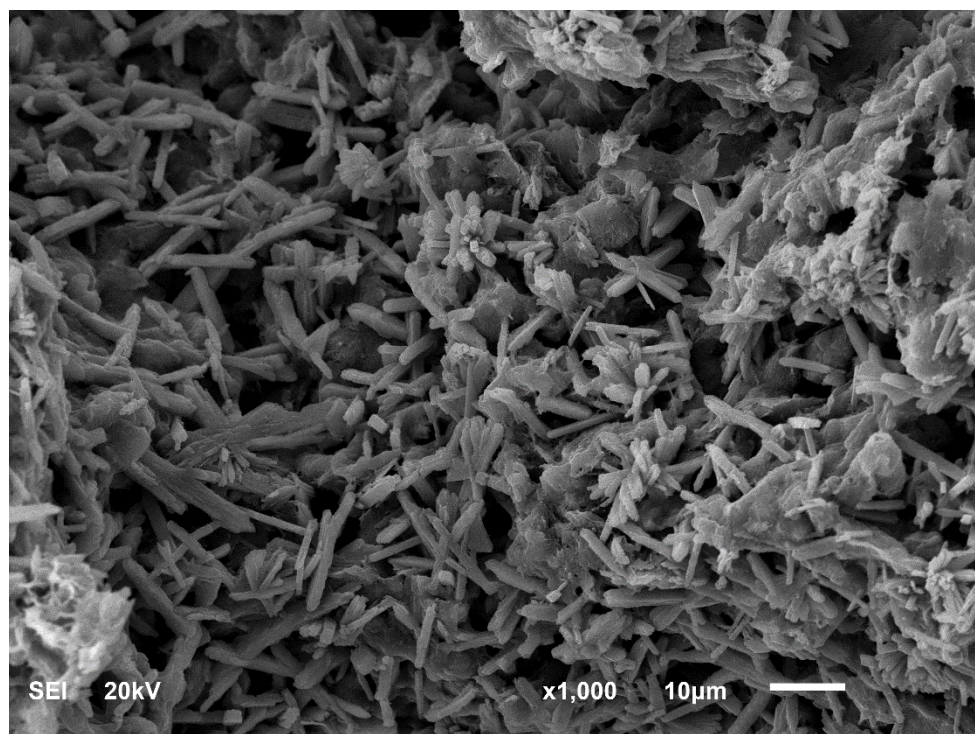


Figure 4-42: SEM picture for the bottom layer of M1 sample contaminated with 70% concentration sulfuric acid

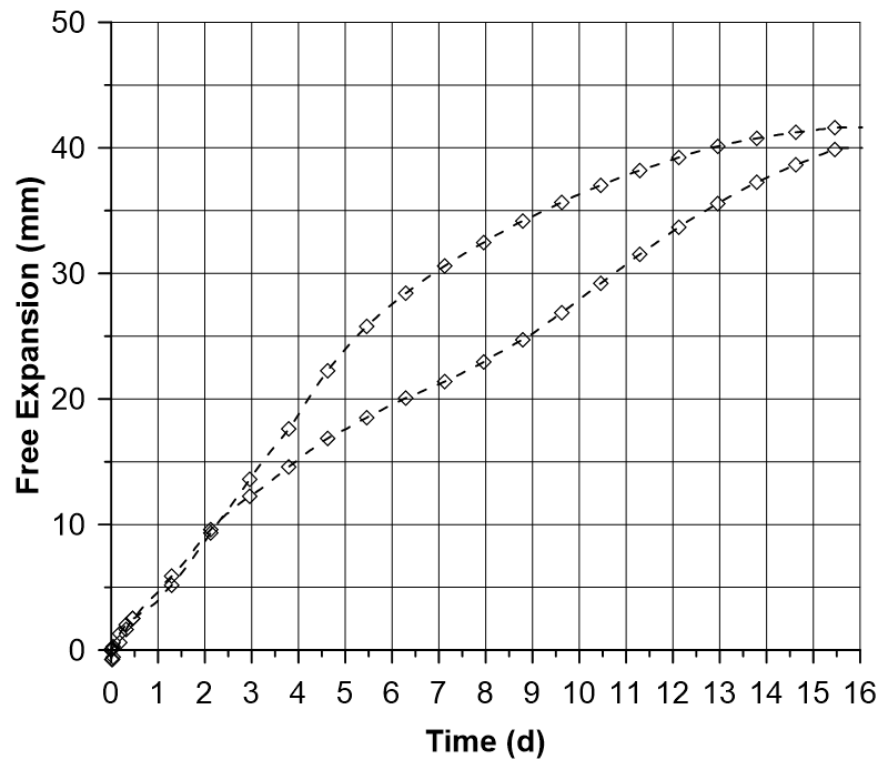


Figure 4-43: Free swell of M2 due to contamination with sulfuric acid of 70% concentration

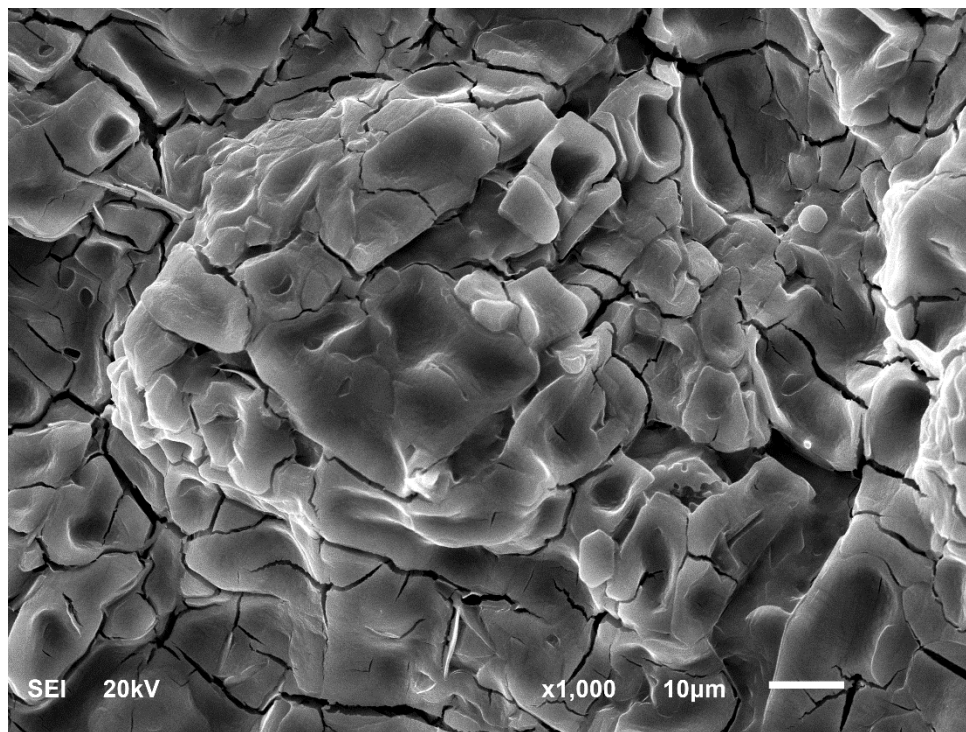


Figure 4-44: SEM picture for the top layer of M2 sample contaminated with 70% concentration sulfuric acid

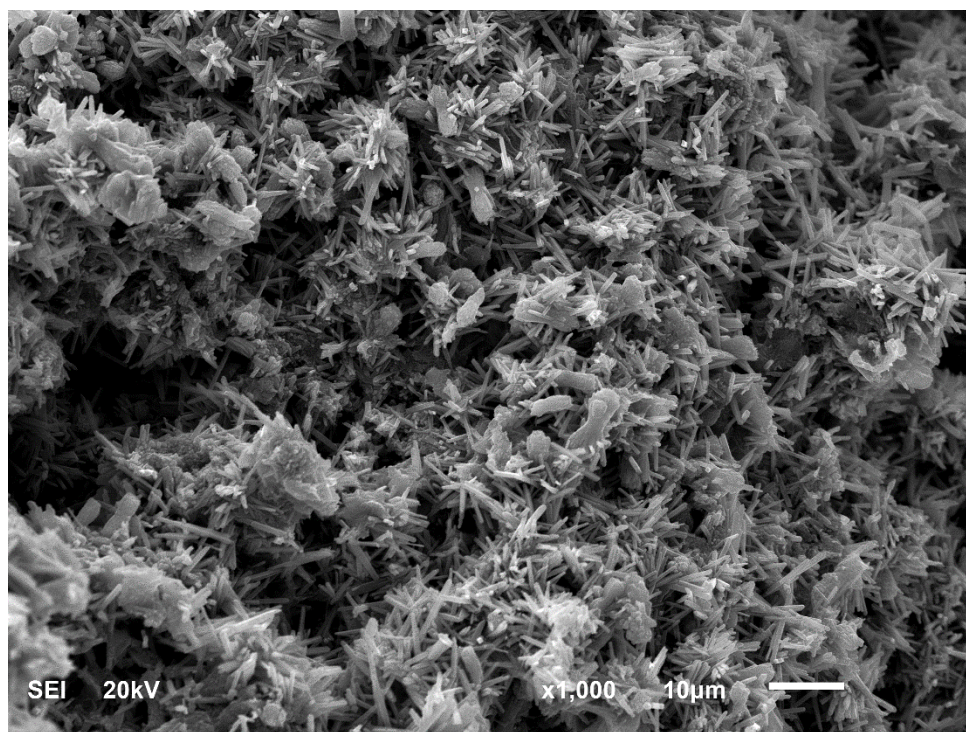


Figure 4-45: SEM picture for the middle layer of M2 sample contaminated with 70% concentration sulfuric acid

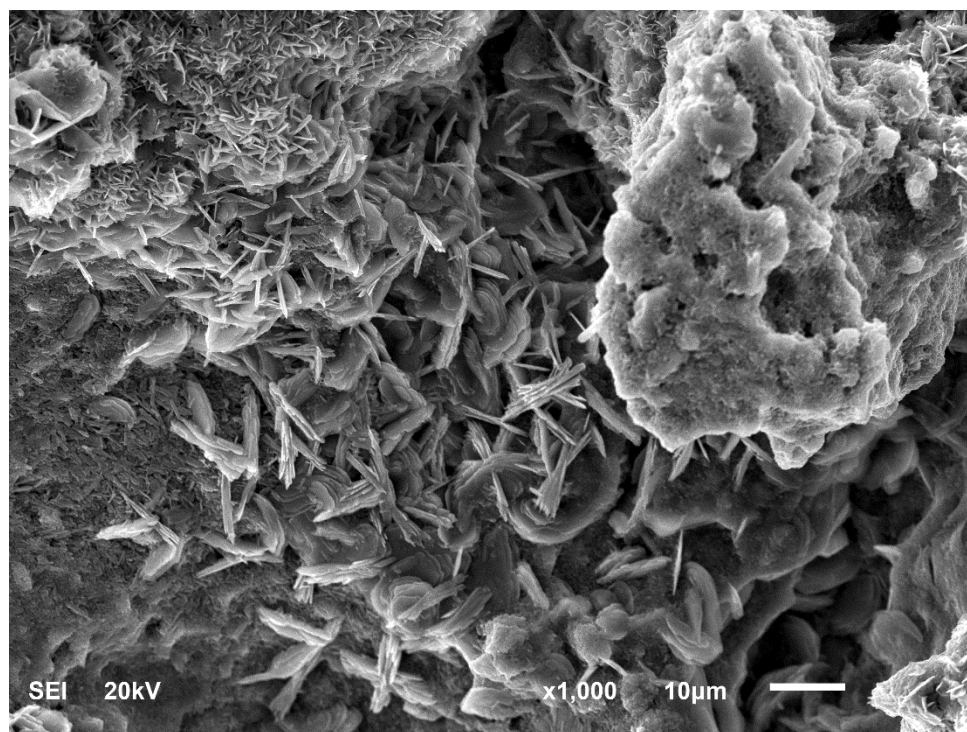


Figure 4-46: SEM picture for the bottom layer of M2 sample contaminated with 70% concentration sulfuric acid

4.2.6 Third Round for Phosphoric Acid (56% Concentration)

Phosphoric acid in the third round has 56% concentration. As the previous rounds, duplicate samples of each marl were tested. At first, M1 expansion results are shown in Figure 4-47. Similar to the results of M1 samples with 20% and 48% phosphoric acids, M1 samples with 56% phosphoric acid displayed marginal swelling. In addition, it is clear from Figures 4-48, 4-49 and 4-50 calcium phosphate crystals are barely found in the top, middle and bottom layers of M1 resulting from the interaction with the phosphoric acid of 56% concentration.

On the other hand, M2 reaction with 56% phosphoric acid produced a uniform swelling pattern for both samples. Figure 4-51 shows the free swelling of M2 samples contaminated by 56% phosphoric acid. After two weeks, both samples reached around 20 mm of free expansion, which is equivalent to approximately 30% expansion.

Figures 4-52, 4-53 and 4-54 present the enlarged SEM photos of the top, middle and bottom, respectively, of the affected M2. An accumulated plate-like crystals for calcium phosphate are observed. As usual, crystal's size gets more in the direction of the acid source.

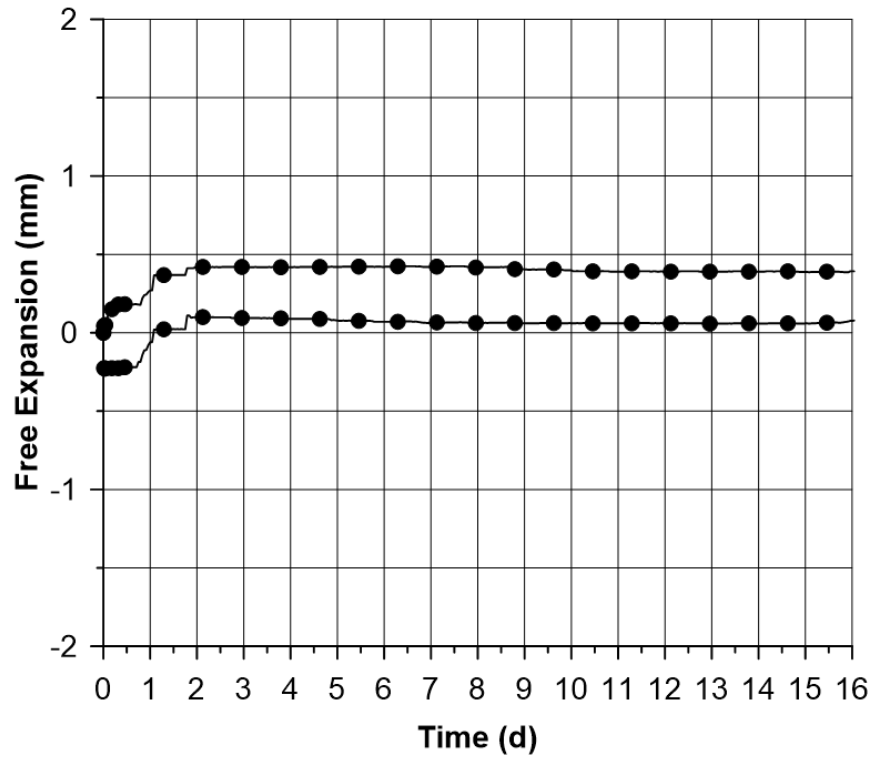


Figure 4-47: Free swell of M1 due to contamination with phosphoric acid of 56% concentration

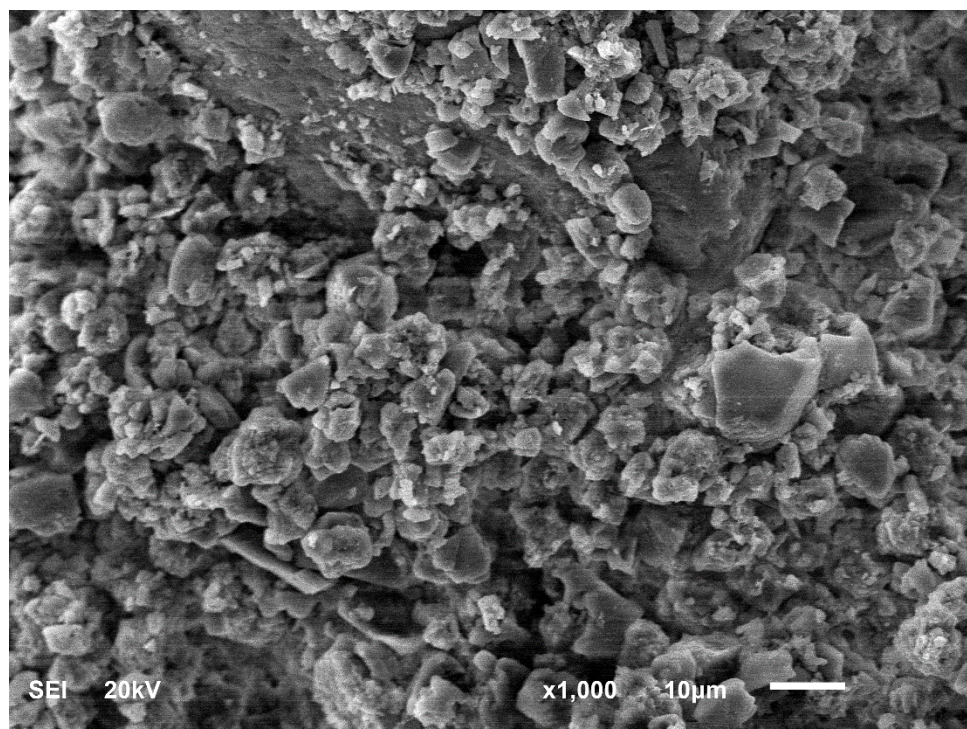


Figure 4-48: SEM picture for the top layer of M1 sample contaminated with 56% concentration phosphoric acid

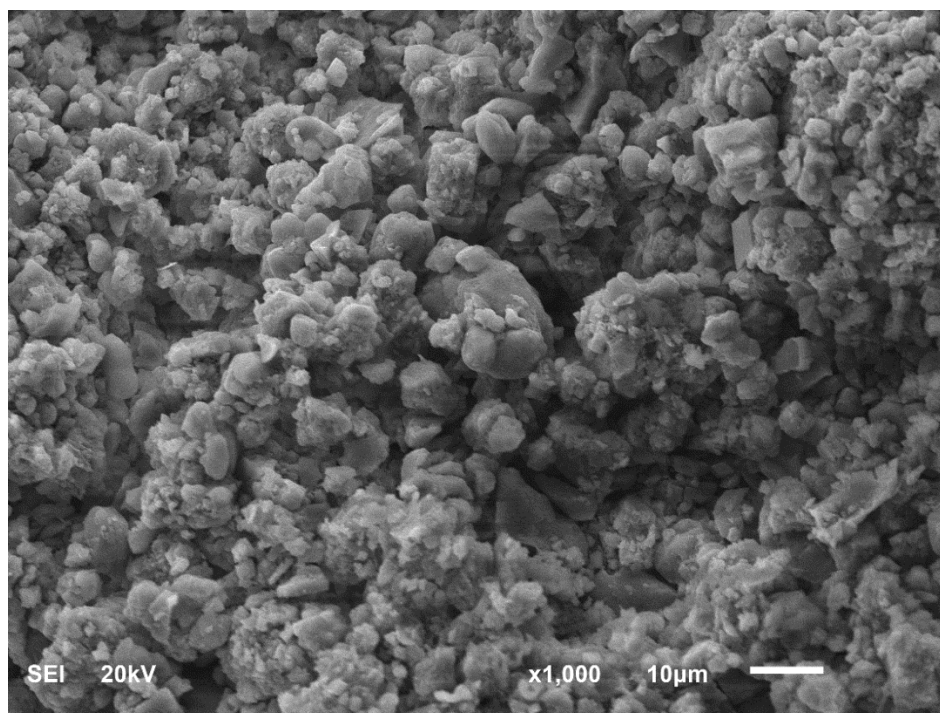


Figure 4-49: SEM picture for the middle layer of M1 sample contaminated with 56% concentration phosphoric acid

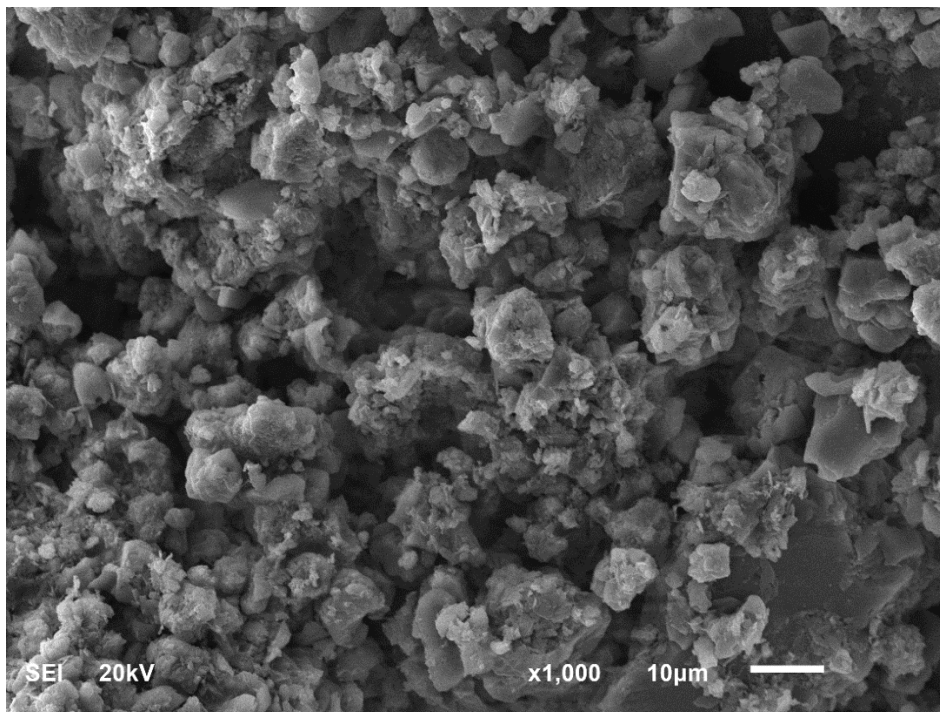


Figure 4-50: SEM picture for the bottom layer of M1 sample contaminated with 56% concentration phosphoric acid

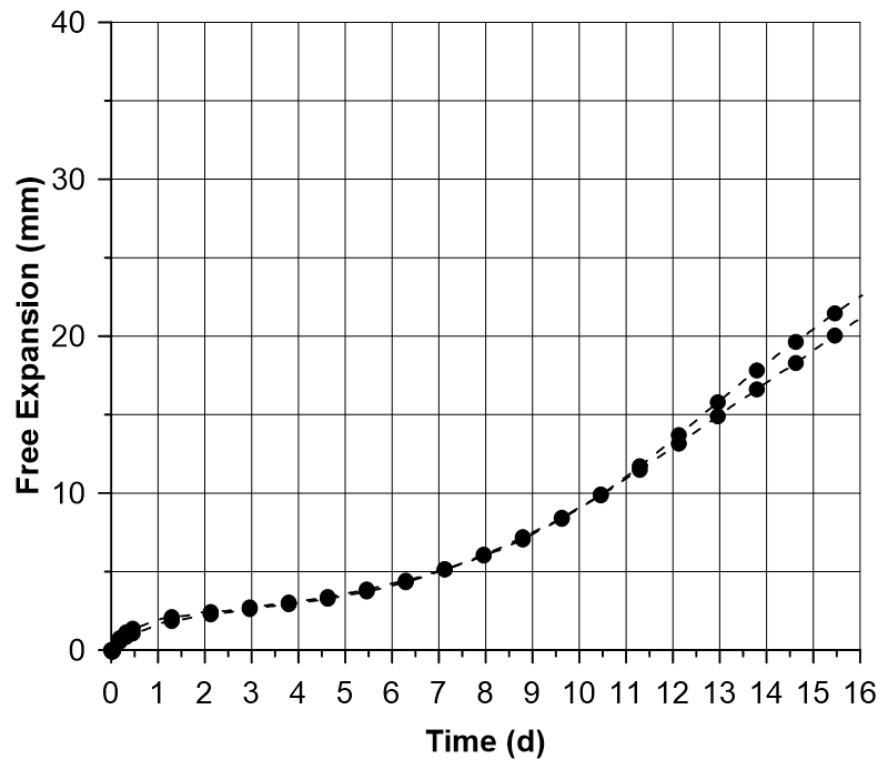


Figure 4-51: Free swell of M2 due to contamination with phosphoric acid of 56% concentration

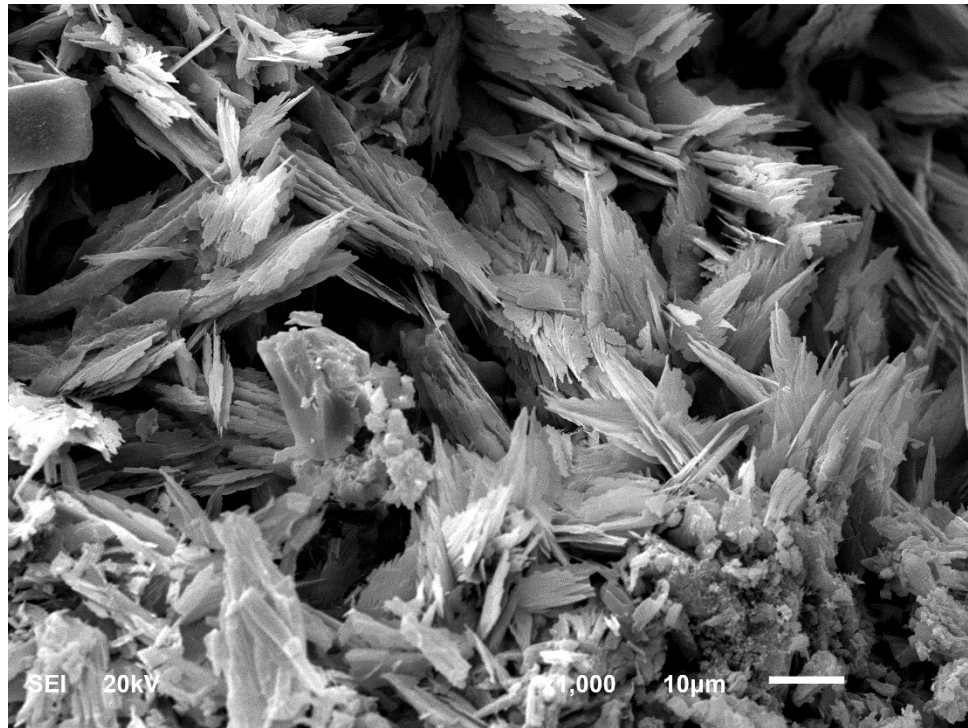


Figure 4-52: SEM picture for the top layer of M2 sample contaminated with 56% concentration phosphoric acid

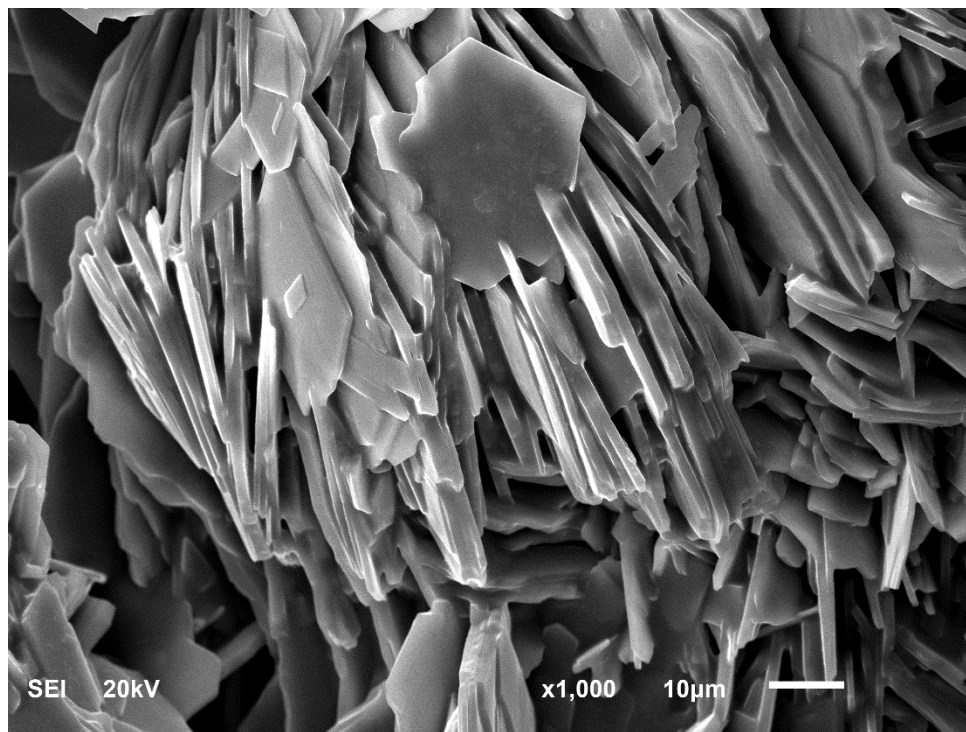


Figure 4-53: SEM picture for the middle layer of M2 sample contaminated with 56% concentration phosphoric acid

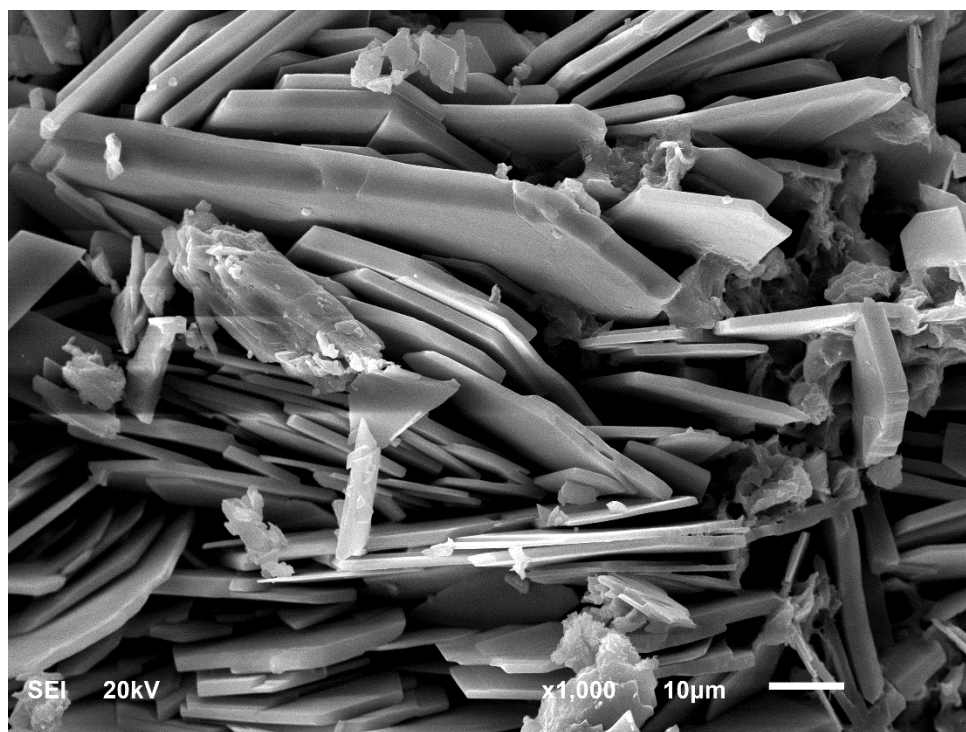


Figure 4-54: SEM picture for the bottom layer of M2 sample contaminated with 56% concentration phosphoric acid

4.2.7 Summary of Expansion Resulted Due to Sulfuric Acid

This section summarizes the expansion behavior of marl soils contaminated with sulfuric acid. Figure 4-55 present the average free swell percentage of M1 and M2 due to sulfuric acid contamination. The expansion of M1, which was caused by the sulfuric acid of 20% concentration, stabilized after two weeks with a value of 14%. However, 32% sulfuric acid produced a swelling of 16% and the swelling is continuing. Moreover, 70% sulfuric acid generated a minor expansion of 3.6%. This little swelling rate is ascribed to the crystallization in the bottom layer that stopped acid infiltration through the samples. M2 has an evident trend between swelling and acid concentration. From the figure, M2 with 20%, 32% and 70% concentration of sulfuric acid produced free swelling of 19%, 34% and 58%, respectively.

4.2.8 Summary of Expansion Resulted Due to Phosphoric Acid

This section summarizes the swelling results of marl soils polluted by phosphoric acid. Figure 4-56 presents the average free swell percentage of M1 and M2 due to phosphoric acid contamination. M1 with phosphoric acid did not show any expansion. This could be attributed to the impermeability of phosphoric acid to the samples. M2 samples have non-consistent expansion behavior in the first ten days. After that, the samples showed a consistent trend between swelling and acid concentration. At the end of acidification, M2 with 20%, 48% and 56% concentration of phosphoric acid exhibited expansion results of 16%, 20% and 29%, respectively. Additionally, M2 with 56% phosphoric acid showed significant expansion rate at the end of acidification period.

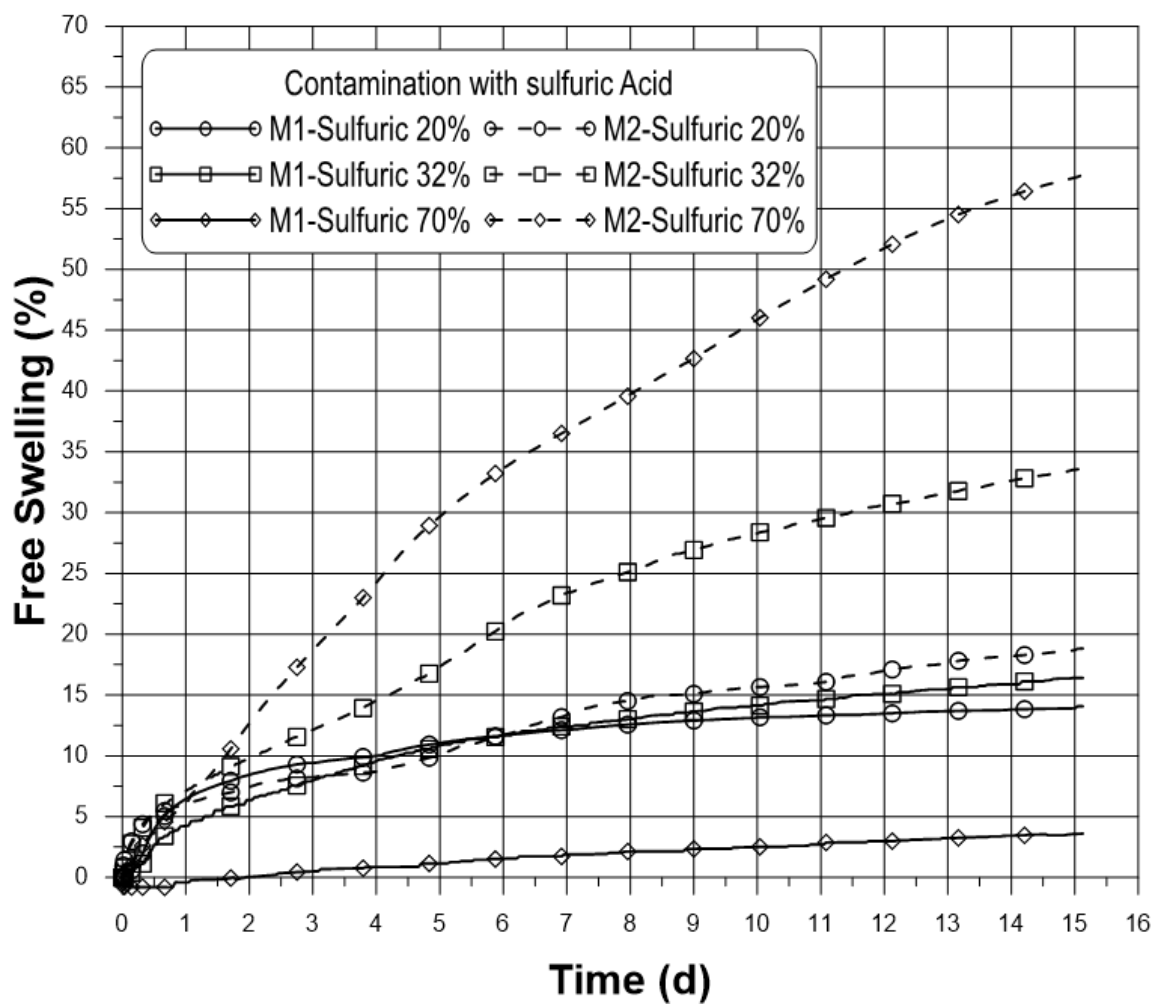


Figure 4-55: The average free swell percentage of M1 and M2 due to sulfuric acid contamination

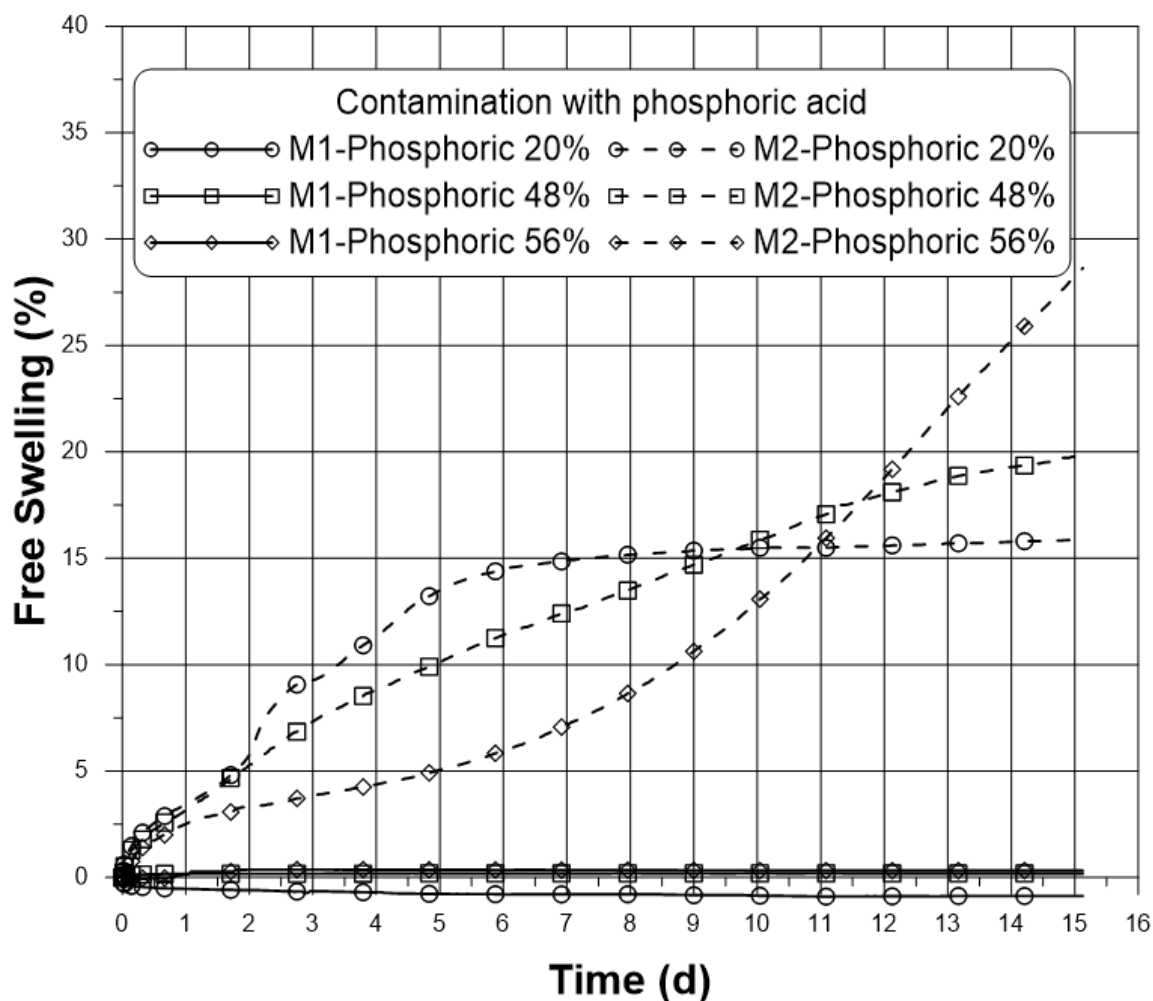


Figure 4-56: The average free swell percentage of M1 and M2 due to phosphoric acid contamination

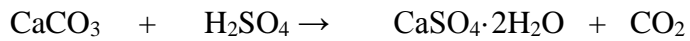
4.3 Soil Composition Alteration

Acid contamination of calcareous soils have led to volumetric and microstructural changes as stated in the previous section. However, this section is intended to show the compositional changes of marl soil due to acidification. XRD technology was utilized to investigate the middle layer of each contaminated sample. The outcome of XRD is presented in terms of semi-quantitative analysis. For that, the type and amount of mineralogical alteration of calcareous soil due to interaction with acids will be presented.

4.3.1 M1 Compositional Analysis

M1 sample has been initially analyzed before any contamination so as to be a reference for the analysis despite the fact that such small samples may not be representative of the actual soil composition. Table 4-2 shows the semi-quantitative analysis of uncontaminated and contaminated M1 with sulfuric acid. The carbonate materials (calcite and dolomite) content of uncontaminated M1 is in the range of 80%. Moreover, Figure 4-57 shows measurement profile of XRD for M1 contaminated with sulfuric acid of 20% concentration. Sulfuric acid of 20% concentration has a clear effect on M1 composition. Around 50% of the carbonate materials turned to gypsum ($\text{CaSO}_4 \cdot 2\text{H}_2\text{O}$), which is a product of the reaction of sulfuric acid with calcium carbonate. Gypsum was formed as a result of the reaction of dolomite and calcite with sulfuric acid, as shown in the following chemical reaction:

Calcite + sulfuric acid \rightarrow Gypsum + carbon dioxide



Dolomite + sulfuric acid \rightarrow Gypsum + magnesium + carbon dioxide



Furthermore, SEM results for the middle layer of M1 contaminated with 20% concentration sulfuric acid show monoclinic crystal system that represents the typical shape of gypsum crystal (Figure 4-9). In contrast, M1 with a higher concentration of sulfuric acid had shown no change in the composition because the acid could not reach the middle and top layers. Table 4-2 summarizes the semi-quantitative analysis for M1 contaminated with sulfuric acid of 32% and 70% concentration. Both of them consist of carbonate minerals with amounts close to that of the uncontaminated sample.

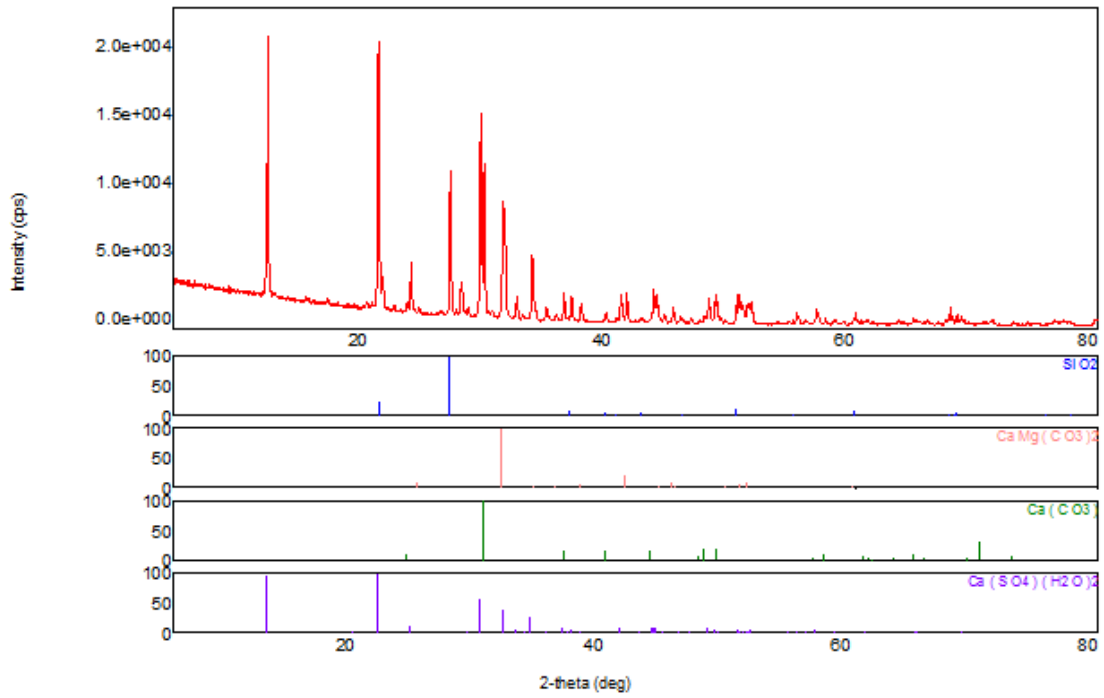


Figure 4-57: Measurement profile of XRD for M1 contaminated with 20% concentration sulfuric acid

Table 4-2: XRD semi-quantitative analysis for uncontaminated and contaminated M1 with sulfuric acid

Phase Name		Content (%)			
		Uncontaminated M1	Contaminated M1 with Sulfuric Acid of		
			20%	32%	70%
Carbonate	Dolomite	43.0	14.6	60	46.6
	Calcite	35.3	27.6	17.7	24.6
Quartz		21.6	11.6	22	28.7
Gypsum		-	46.2	-	-

The XRD results of the middle zone indicated that there is no significant reaction between the acid and the soil. This reveals that the acid did not penetrate into the middle zone. This observation can be supported by the formation of gypsum layer at the bottom zone (Figures 4-26 and 4-42) due to the strong reaction between the acid and both of dolomite and calcite. For that, the expansion of M1 with 32% sulfuric acid could be associated with the bottom layer only. Additionally, there is no obvious crystallization in the middle layer of M1 contaminated with sulfuric acid of a concentration of 32% or 70%, which are presented in Figures 4-25 and 4-41, respectively.

On the other hand, M1 did not show significant changes in mineralogy due to contamination with phosphoric acid. Table 4-3 presents the compositional analyses of uncontaminated and contaminated M1 with phosphoric acid of 20%, 48%, and 56% concentration. All of these results are approximately similar to the original uncontaminated sample of M1. These outcomes are in agreement with the expansion curves of the samples whereby no major swelling was observed.

Table 4-3: XRD semi-quantitative analysis for uncontaminated and contaminated M1 with phosphoric acid

Phase Name		Content (%)			
		Uncontaminated M1	Contaminated M1 with Phosphoric Acid of		
			20%	48%	56%
Carbonate	Dolomite	43.0	34.1	43.2	29.5
	Calcite	35.3	56.6	39.0	48.7
Quartz		21.6	9.2	17.8	10.2
Orthoclase		-	-	-	11.6
Calcium Phosphate		-	-	-	-

4.3.2 M2 Compositional Analysis

Similar to the preceding analysis of M1, an uncontaminated sample of M2 was analyzed and compared with the contaminated samples. Table 4-4 presents XRD semi-quantitative analysis for uncontaminated and contaminated M1 with sulfuric acid. Unlike M1, approximately 50% of M2 are carbonate minerals and the remaining part is quartz. Sulfuric acid of 20% concentration has an obvious effect on M2 composition. There is no trace for carbonate materials and a huge amount of gypsum was produced. Similarly, M2 with a higher concentration of sulfuric acid had shown a complete change of the carbonate minerals. In Table 4-4, the semi-quantitative analyses for M2 contaminated with 32% and 70% concentration sulfuric acid were presented. Both of them are composed of quartz and gypsum or anhydrous gypsum (anhydrite). Dolomite and calcite reacted completely with sulfuric acid to form gypsum. Quartz increased the permeability of M2 allowing the soil to infiltrate and react with carbonate minerals and transferred them to gypsum and anhydrite.

Table 4-4: XRD semi-quantitative analysis for uncontaminated and contaminated M2 with sulfuric acid

Phase Name		Content (%)			
		Uncontaminated M2	Contaminated M2 with Sulfuric Acid of		
			20%	32%	70%
Carbonate	Dolomite	41.6	-	-	-
	Calcite	7.2	-	-	-
Quartz		51.2	44.7	71	53.1
Gypsum		-	55.3	29.2	-
Anhydrite		-	-	-	47

Phosphoric acid caused much more and clear expansion with M2 in all concentrations. Furthermore, compositional analysis by XRD shows the product of reaction between phosphoric acid and carbonate minerals. Dolomite and calcite reacted with phosphoric acid to form calcium phosphate.

Calcite + phosphoric acid → Calcium phosphate + carbon dioxide



Dolomite + phosphoric acid → Calcium phosphate + magnesium + carbon dioxide



Table 4-5 presents the mineralogical analysis of M2 as a result of its reaction with phosphoric acid of 20%, 48%, and 56% concentration. As the concentration of phosphoric acid increased, the amount of reaction increased. For instance, M2 contaminated with phosphoric acid of 20% concentration showed a transformation of 19% of carbonate minerals to calcium phosphate. Moreover, phosphoric acid of 48% concentration had transformed 57% of carbonate minerals to calcium phosphate. Over and above, phosphoric acid of 56% concentration changed 87% of carbonate minerals to calcium phosphate.

Table 4-5: XRD semi-quantitative analysis for uncontaminated and contaminated M2 with sulfuric acid

Phase Name		Content (%)			
		Uncontaminated M2	Contaminated M2 with Phosphoric Acid of		
			20%	48%	56%
Carbonate	Dolomite	41.6	31.3	10	5.3
	Calcite	7.2	2.6	8.0	-
Quartz		51.2	58.0	58.0	61
Calcium Phosphate		-	8.1	23.8	34

4.4 Strength Variation Due to Acidification

Strength assessment procedure of the contaminated soil is mentioned in Chapter 3. The results of the strength assessment are in the form of stress versus penetration graphs. As the slope of the curve increased, the strength of the sample increased. Eventually, these results were compared with the referenced specimens of uncontaminated dry and soaked in water samples of both M1 and M2 soils.

4.4.1 Strength Alteration for the First Round

The first round of acidification was conducted by the sulfuric and phosphoric acid at 20% concentration. Table 4-6 shows the strength variation of all contaminated samples and it also presents the average swell percentage and crystallization zones. In addition, Figure 4-58 shows the strength curves for the first round plus the curves for the uncontaminated samples. It is clear from the graph that a large difference exists between soaked in water and unsoaked samples. The soaked samples have almost no strength of about 340 kPa for M1 and 170 kPa for M2. However, unsoaked samples exhibited a considerable strength of 4966 kPa for M1 and 4127 kPa for M2. M1 samples with 20% phosphoric acid have a strength of about 4933 kPa, which is close to the unsoaked sample and this outcome is consistent with the expansion curve and compositional analysis of M1 contaminated with phosphoric acid of 20% concentration. These samples did not show noticeable swelling and mineralogical variation. All the other contaminated samples in the first round were weak in strength measurement, which is similar to the soaked samples. Unlike, M2 sample with 20% phosphoric acid has little noticeable strength of about 1072 kPa. Moreover, M2 sample have visible expansion (Figure 4-56) and XRD analysis is Section 4.3 showed the effect of acids on these samples.

Table 4-6: Characteristics of all contaminated samples

Marl	Acid type	Acid concentration	Swelling %	Crystallization	Strength * (kPa)	Comment
M1	Sulfuric	20	14	Gets more towards acid source	133	Relative to the soaked sample **
		32	16	Bottom	449	Relative to the soaked sample
		70	3.6	Bottom	5411	Relative to unsoaked sample ***
	Phosphoric	20	<1	Non	4933	Relative to unsoaked sample
		48	<1	Non (only with acid interface)	6126	Relative to unsoaked sample
		56	<1	Non	5714	Relative to unsoaked sample
M2	Sulfuric	20	18.5	Gets more towards acid source	81	Relative to the soaked sample
		32	34	All layers	312	Relative to the soaked sample
		70	60	All layers	150	Relative to the soaked sample
	Phosphoric	20	15	All layers	1072	Quarter the unsoaked sample
		48	19.5	Gets more towards acid source	1983	Half the unsoaked sample
		56	30	Gets more towards acid source	482	Relative to the soaked samples

* The strength was measured when CBR plunger penetrated 12.5 mm in the sample.

** The strength of uncontaminated M1 is 340 kPa for soaked in water and 4966 kPa for unsoaked.

***The strength of uncontaminated M2 is 170 kPa for soaked in water and 4127 kPa for unsoaked.

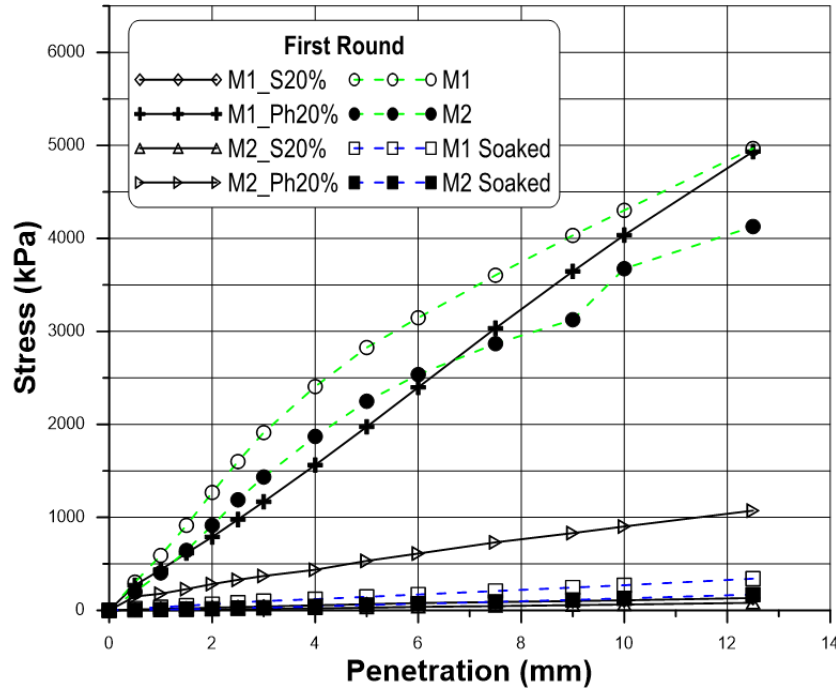


Figure 4-58: Strength curves for the first round

4.4.2 Strength Alteration for the Second Round

The second round of acid contamination was executed by sulfuric of 32% concentration and phosphoric acid of 48% concentration. Figure 4-59 presents the strength curves for the second round in addition to the curves of the uncontaminated samples for comparison. Similar to the first round, M1 sample with 48% phosphoric acid has a strength close to the unsoaked samples and this is in agreement with the expansion curves and compositional analysis of M1 contaminated with phosphoric acid of 48% concentration. This sample did not show expansion and compositional changes. Moreover, other contaminated samples in the second round have approximately similar strength to the soaked samples. Unlike, M2 with 48% phosphoric acid has remarkable strength of about 1983 kPa (Table 4-6). Moreover, in the expansion curve of M2 with 48% phosphoric acid (Figure 4-56), there is

apparent expansion and XRD analysis in Section 4.3 showed the effect of acids on these samples.

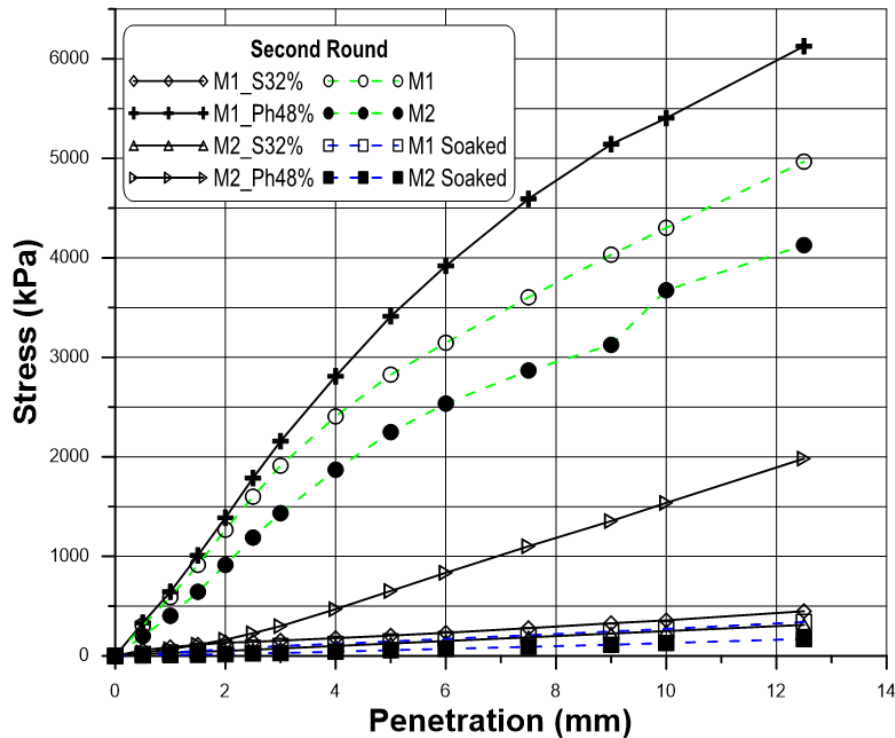


Figure 4-59: Strength curves for the second round

4.4.3 Strength Alteration for the Third Round

The third round of acid contamination was executed by sulfuric acid of 70% concentration and phosphoric acid of 56% concentration. Figure 4-60 demonstrates the strength curves for the third round in addition to the curves of the uncontaminated samples for comparison. Contaminated M1 sample showed a strength of 5411 kPa, which is relative to unsoaked sample (Table 4-6). This finding agreed with the swelling curves in Figures 4-55 and 4-56 and compositional analysis in Section 4.3 of M1 contaminated with 70% sulfuric and 56%

phosphoric acid. These samples did not show measurable volume and compositional changes. On the other hand, polluted M2 samples in the third round have approximately similar strength to the soaked samples (Table 4-6). These samples have obvious swelling and compositional alteration.

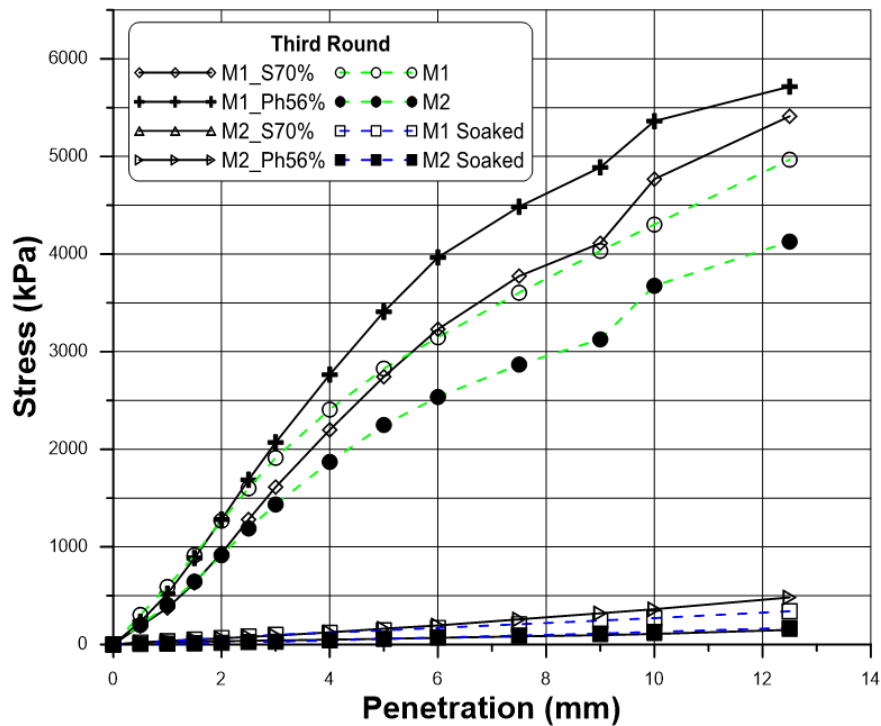


Figure 4-60: Strength curves for the third round

CHAPTER 5

CONCLUSIONS AND RECOMMENDATIONS

5.1 Summary

Calcareous sediments by definition are those soils that have considerable quantities of carbonate minerals like calcite and dolomite. These minerals have a basic nature because of carbonate minerals, hence, they are highly reactive with acids. Unfortunately, many petrochemical and fertilizer industries across the world are constructed on calcareous sediments. Leakage of acids from these industrial units is always expected. Then, the acid-calcareous reaction will cause volumetric changes to the subsoil and, consequently, the industrial installations might be damaged and stopped for maintenance. For that, assessing the effect of acid on calcareous soil became an important issue. Unlikely, there is shortage of published data about this subject. Only few publications from India and other places have been reported on studying the impact of acids on some soil types.

Quantifying the volumetric and compositional variation of calcareous soils contaminated with sulfuric and phosphoric acids was the main objective of this research. Two marl samples were procured from two different places in the Eastern Province of Saudi Arabia for this study. These marls were then contaminated with sulfuric and phosphoric acid at three different concentrations. The period of acid contamination was around two weeks. During this time, the volume change was continuously recorded. After that, the contaminated samples were subjected to microstructural and mineralogical analysis using

SEM and XRD. Moreover, the strength of polluted samples was tested in a modified way using CBR equipment.

5.2 Conclusions

Based on the outcomes of swelling, microstructural and mineralogical analyses of calcareous soils contaminated with sulfuric acid, the following conclusions could be drawn:

1. For non-plastic marl (M1), the expansion which was caused by the sulfuric acid of 20% in concentration almost ceased after two weeks with a value of 14% of expansion. However, 32% sulfuric acid produced a swelling of 16% and the swelling is still continuing. Moreover, 70% sulfuric acid generated a minor expansion of 3.6% with low swelling rate due to improper infiltration of acid.
2. SEM results indicated clear salt crystallization of M1 contaminated by 20% sulfuric acid and the size of crystals got increased toward the source of acid. In addition, sulfuric acid of 32% and 70% created crystallization at the bottom layer, which means the acid did not reach the whole samples.
3. XRD outcomes revealed a transformation of half the carbonate minerals to gypsum in the case of 20% sulfuric acid at the middle layer, whereas 32% and 70% sulfuric acid did not show any compositional change in the middle layer because the acid did not reach these locations.
4. There are two explanations for the unexpected behavior of expansion of M1 with sulfuric acid at different concentrations:
 - a. As the concentration of sulfuric acid increased, the amount of reaction increased. Consequently, the crystallization gets more with acid

concentration. For that, the permeability of bottom layer decreased with large crystals.

- b. The viscosity of sulfuric acid increased with the increase in concentration. For that, the movement of acid through porous media is affected by acid concentration.

5. The low plastic marl (M2) has an evident trend between swelling and acid concentration. From Figure 4-55, the expansion increased as the concentration of sulfuric acid increased.
6. XRD results of M2 contaminated with sulfuric acid agreed with the expansion curves where more acid concentration produced more swelling. In addition, higher acid concentration coincides with the higher amount of carbonate transformation to gypsum.
7. Strength curves have shown a degradation of strength along with the expansion caused by sulfuric acid.

Based on the finding of swelling, microstructural and mineralogical analyses of marl soils polluted with phosphoric acid, the following conclusions can be acquired:

- 1- M1 with phosphoric acid did not show any expansion. In addition, SEM and XRD analyses did not show any mineralogical variation on the samples as well. Moreover, strength curves displayed a strength similar to the unsoaked M1 sample. For that, all results indicated an impermeability of phosphoric acid to the samples.
- 2- M2 samples have unrelated expansion behavior in the first ten days. However, at the end of acidification, the samples presented an obvious trend between swelling and acid concentration where more acid concentration produced more swelling.

Additionally, M2 with 56% phosphoric acid showed expansion rate at the end of acidification period.

- 3- XRD results of M2 contaminated with phosphoric acid correspond to expansion curves where higher acid concentration coincides with the higher amount of carbonate transformation to calcium phosphate.

5.3 Recommendations for Future Studies

- 1- In industry, many types of acids are being used, therefore, it is required to investigate the effect of other acids in addition to sulfuric and phosphoric acids with calcareous soils.
- 2- Testing the effects of sulfuric and phosphoric acids on other types of soil will bring useful result.
- 3- Studying the permeability of acid in calcareous soil is helpful to interpret the expansion behavior. Moreover, the permeability will change with time due to chemical change.
- 4- The effect of acid will take more time in some cases. For that, it is recommended to increase the period of acidification.
- 5- The experimental program shall insure proper acid penetration through the sample height.

References

Aiban, S.A., Al-Abdul Wahhab HI, Al-Amoudi OSB. Identification, evaluation, and improvement of Eastern Saudi soils for construction purposes, final report. Riyadh, Saudi Arabia: King Abdulaziz City for Science and Technology (KACST AR-14-61); 1998a.

Aiban, S.A., Al-Amoudi OSB, Al-Abdul Wahhab HI, Ahmed HR. Characterization and properties of Eastern Saudi calcareous sediments. In: Proceedings of the second international conference on engineering for calcareous soils. Manama, Bahrain; 1998b. p. 371–81

Aiban, S.A. 1995. “Strength and Compressibility of Abqaiq Marl, Saudi Arabia.” *Engineering Geology*, 39 (3): 203–15.

Akili, W. 1980. “Some Properties of Remolded Carbonate Soils, Eastern Saudi Arabia soils.” Proc., 10th Int. Conf. on Soil Mechanics and Foundation Engineering, Stockholm, 4/4, 537–542.

Al-Amoudi, Omar Saeed Baghabra, Khaqan Khan, and Nasser Saban Al-Kahtani. 2010. “Stabilization of a Saudi Calcareous Marl Soil.” *Construction and Building Materials* 24 (10): 1848–54.

Assa’ad, Abdullah. 1998. “Differential Upheaval of Phosphoric Acid Storage Tanks in Aqaba, Jordan.” *Journal of Performance of Constructed Facilities*, 12 (2): 71–76.

Jozefaciuk, Grzegorz, and Grzegorz Bowanko. 2002. "Effect of Acid and Alkali Treatments on Surface Areas and Adsorption Energies of Selected Minerals." *Clays and Clay Minerals*, 50 (6): 771–83.

Komnitsas, K., A. Kontopoulos, I. Lazar, and M. Cambridge. 1998. "Risk Assessment and Proposed Remedial Actions in Coastal Tailings Disposal Sites in Romania." *Minerals Engineering*, 11 (12): 1179–90.

Pettijohn, F.J., 1975. *Sedimentary Rocks*, 3rd ed. Harper & Row, London.

H.N.Ramesh, S.D. Venkataraja Mohan, "Index Properties of Alkalies Treated Expansive and Non Expansive Soil Contaminated with Acids", IOSR Journal of Mechanical and Civil Engineering (IOSR-JMCE), Volume 6, Issue 5, pp 01-09, 2013

Ramesh, H.N., Venkatarajan, S.D. Mohan, and Abdul Bari. 2008. "Compaction and Strength Properties of Alkalies Treated Expansive Soil Contaminated with Acids." In *Proceedings of Indian Geotechnical Conference*, 2:466–69.

Rao SM, Rao KSS 1994. Ground heaving from caustic soda solution spillage—a case study. *Soil Found* (Japanese Society of Soil Mechanics and Foundation Engineering) 34(2):13–18

Singh, Sanjeev, and Arun Prasad. 2007. "Effects of Chemicals on Compacted Clay Liner." *Electronic Journal of Geotechnical Engineering* 12 (D): 1–15.

Sinha, U, A Sharma, S Bhargava, A Minocha, and P Kumar. 2003. "Effect of Seepage of Caustic Soda on Foundation and Remedial Measure in Alumina Plant." *Proc Geo-Tech Eng Infrastruct Dev I*, 229–234.

Sivapullaiah, P. V., Allam, M. M., & Sankara, G. 2004. "Structural Distortion Due to Heaving of Foundation Soil Induced by Alkali Contamination." In *International Conference on Structural and Foundation Failures* (pp. 2-4).

Sivapullaiah, P.V., Prasad, B.G. and Allam, M.M., 2008. "Volume Change Behavior of Calcitic Soil Influenced with Sulfuric Acid." In *GeoCongress 2008: Geotechnics of Waste Management and Remediation* (pp. 819-826). ASCE.

Sivapullaiah, P.V., Prasad, B.G., Allam, M.M., 2009. "Effect of Sulfuric Acid on Swelling Behavior of an Expansive Soil." *Soil & Sediment Contamination*, 18 (2): 121–35.

Sivapullaiah, Puvvadi Venkata. 2005. "Kaolinite–alkali Interaction and Effects on Basic Properties." *Geotechnical & Geological Engineering*, 23 (5): 601–14.

Sowers, G.B. and Sowers, G.F., 1951. Introductory Soil Mechanics and Foundations. *Soil Science*, 72(5), p.405.

Sridharan, A., Nagaraj, T.S. and Sivapullaiah, P.V., 1981, June. Heaving of soil due to acid contamination. In *Proceedings of the 10th International Conference on Soil Mechanics and Foundation Engineering, Stockholm* (Vol. 6, pp. 383-386).

Stephenson, R.W., Dempsey, B.A. and Heagler, J.B., 1989. Chemically induced foundation heave. In *Foundation Engineering: Current Principles and Practices* (pp. 1633-1642). ASCE.

Tyagi, B., Chudasama, C.D. and Jasra, R.V., 2006. Determination of structural modification in acid activated montmorillonite clay by FT-IR

spectroscopy. *Spectrochimica Acta Part A: Molecular and Biomolecular Spectroscopy*, 64(2), pp.273-278.

Umesha, T. S., S. V. Dinesh, and P. V. Sivapullaiah. 2012. "Effects of Acids on Geotechnical Properties of Black Cotton Soil." *International Journal of Geology*, 6 (3): 69–76.

Vitae

Name	:Ammar Mohammed Alshammari
Nationality	:Saudi
Date of Birth	:3/20/1990
Email	:amtqsh@gmail.com
Address	:A-Khozama, Hail, Saudi Arabia
Academic Background	:M.S. (Civil and Environmental Engineering-Geotechnical) January 2017 King Fahd University of Petroleum and Minerals Dhahran, Saudi Arabia B.S. (Civil and Environmental Engineering) May 2012 King Fahd University of Petroleum and Minerals Dhahran, Saudi Arabia